The Dissertation Committee for Yuki Watanabe
certifies that this is the approved version of the following dissertation:

Toward Understanding of the Complete Thermal History of the Universe: Probing the Early Universe by Gravitation

Committee:

Eiichiro Komatsu, Supervisor

Duane A. Dicus

Willy Fischler

Richard A. Matzner

Paul R. Shapiro

Toward Understanding of the Complete Thermal History of the Universe: Probing the Early Universe by Gravitation

by

Yuki Watanabe, B.Sc.

Dissertation

Presented to the Faculty of the Graduate School of

The University of Texas at Austin

in Partial Fulfillment

of the Requirements

for the Degree of

Doctor of Philosophy

The University of Texas at Austin

December 2009

To Grandfathers

Acknowledgments

I would like to thank my advisor, Eiichiro Komatsu, who gave me a chance and support to be a cosmologist and has led me to the right direction to do science. I would also like to thank my family who supported me over years. I thank to my friends in Austin, in Japan, and somewhere else. They always encouraged me to complete graduate studies. Finally, but not the last, I wish to thank my colleagues who shared the office: Joshua Adams, Donghui Jeong, Jun Koda, and Masatoshi Shoji.

Yuki Watanabe

The University of Texas at Austin

December 2009

Toward Understanding of the Complete Thermal History of the Universe: Probing the Early Universe by Gravitation

Publication No. ____________________

Yuki Watanabe, Ph.D.
The University of Texas at Austin, 2009

Supervisor: Eiichiro Komatsu

Gravitational waves are truly transparent to matter in the Universe and carry the information of the very early epoch. We show that the energy density spectrum of the primordial gravitational waves has characteristic features due to the successive changes in the relativistic degrees of freedom during the radiation era. Our calculations are solely based on the standard model of cosmology and particle physics, and therefore these features must exist. Our calculations significantly improve the previous ones which ignored these effects and predicted a smooth, featureless spectrum.

Going back in time to the beginning of the radiation era, reheating of the Universe must have taken place after inflation for primordial nucleosynthesis to begin. We show that reheating occurs spontaneously in a broad class of inflation models with $f(\phi)R$ gravity (ϕ is inflaton). The model does not require explicit couplings between ϕ and bosonic or fermionic matter fields. The couplings arise spontaneously when ϕ settles in the vacuum expectation value (vev) and oscillates. This mechanism allows inflaton quanta to decay into any fields which are not conformally invariant in $f(\phi)R$ gravity theories.

Applying the above method, we study implications of the large-N species solution to the hierarchy problem, proposed by G. Dvali, for reheating after inflation. We show that, in this scenario, the decay rates of inflaton fields through gravitational decay channels are enhanced by a factor of N, and thus they decay into N species of the quantum fields very efficiently. Without violating energy conservation, cosmological consideration places non-trivial constraints on Dvali's solution to the hierarchy problem.

Going back in time still further, we study the period just before the beginning of reheating, the era of coherent oscillation of scalar fields. We show that non-Gaussian primordial curvature perturbations appear temporarily in the coherent oscillation phase after multi-field inflation. We directly solve the evolution equation of non-Gaussianity on super-horizon scales caused by the non-linear influence of entropy perturbations on the curvature perturbations during this phase. We show that our approach precisely matches with the so-called "separate universe approach" or "δN formalism" by studying a simple quadratic two-field potential.

Contents

List of Tables

List of Figures

Chapter 1

Introduction

My research interest lies in the physics of the early universe and cosmology. The focus of my dissertation project is to understand the complete thermal history of the universe by filling the gap between theoretical physics and the observed universe.

Inflation is an indispensable building block of the standard model of cosmology. Currently there are more than one hundred models of inflation in the literature. Since different models are motivated by different theories of fundamental physics at ultra-high energies, one can hope to learn a great deal about fundamental physics by ruling out inflation models observationally. It is well known that the shape of the power spectrum of primordial density fluctuations and the amplitude of primordial gravitational waves (GWs) are powerful probes of the physics of inflation. One can constrain inflation models by using the observed anisotropy of the cosmic microwave background (CMB) radiation and its polarization.

Are there other ways of testing inflation? In my dissertation work, I have studied gravitational waves, reheating, and non-Gaussianity of primordial fluctuations as a probe of the physics of inflation.

Observed shape of the primordial GW spectrum. If one could directly measure the *shape* of the power spectrum of primordial GWs over a wide range of frequencies, it provides a way to probe *both* the physics of inflation *and* the entire thermal history after inflation since GWs are truly transparent to matter contents of the universe. In chapter 2, we calculate the primordial GW spectrum, fully taking into account the evolution of the relativistic degrees of freedom and anisotropic stress from neutrino free-streaming, and find characteristic features on the spectrum due to various annihilation thresholds of elementary particles in the standard model and its minimal supersymmetric extension [1]. Our work provides the most precise calculation of the observed GW spectrum to date.

Reheating after inflation due to gravitational inflaton decay. To start a hot Big Bang universe, reheating must have taken place after inflation. Yet, the mechanism for reheating is not understood very well. In chapter 3 we show that reheating of the universe occurs spontaneously in a broad class of inflation models with $f(\phi)R$ gravity, where ϕ is the inflaton and R is the Ricci scalar [2]. The model does not require explicit couplings between ϕ and bosonic or fermionic matter fields, and hence quite generic. The couplings arise spontaneously when ϕ settles in the vacuum expectation value (vev) and oscillates, with coupling constants given by derivatives of $f(\phi)$ at the vev and the mass of resulting bosonic or fermionic fields. This mechanism allows inflaton quanta to decay into any light fields which are not conformally invariant in theories with $f(\phi)R$ term. Non-minimal gravitational coupling term, $f(\phi)R$, shows up in any candidate theories of fundamental physics which involve compactification of extra dimensions with the form of $f(\phi)$ depending on models.

We calculate rates of decay processes and the resulting lower bound on the reheating temperature from this mechanism. We argue that one must always check that the reheating temperature in any inflation models with $f(\phi)R$ term is reasonable, e.g., the reheating temperature does not exceed the critical temperature above which too many gravitinos would be produced thermally. This mechanism also allows ϕ to decay into gravitinos through supergravity effects [3]. Both of these effects should provide non-trivial constraints on $f(\phi)$, which are totally independent of conventional constraints from the shape of the power spectrum of primordial density fluctuations and the amplitude of primordial GWs. Indeed, we have shown that a class of models with the large-N species (proposed by G. Dvali [4]) is significantly constrained by this argument [5] (chapter 4).

Non-Gaussian correlations from multi-field inflation and coherent oscillation phase. Non-Gaussianity (NG) of primordial fluctuations is a very hot and active field of research in cosmology and particle physics today. While many mechanisms for generating NG have been studied, NG from reheating after inflation has been studied to much lesser extent. Very efficient and fast reheating, so-called *preheating*, can happen during the coherent oscillation of the inflaton [6, 7]. Preheating models require at least two interacting scalar fields, including inflaton, and thus have two directions of perturbations. The perturbations parallel to the background trajectory are adiabatic modes, while those orthogonal are entropy modes. It can be shown that entropy perturbations imprinted on a large scale can generate adiabatic perturbations on the same scale.

Those generated adiabatic modes are non-Gaussian due to mode couplings if non-linearity is important [8]. The previous work on NG from preheating used the so-called δN formalism, coupled with the lattice simulation [9, 10]. They reported considerably large NG. However, the validity of δN formalism has not been verified for preheating. To clarify the situation, in chapter 5, we study the generation mechanism of NG during the coherent oscillation phase. We find that temporarily large NG is possible even without resonant interaction between scalar fields if the coherent oscillation of the fields simply lasts long, although the net effect turns out to be too small to observe due to various cancellations. We also clarify the issue by comparing the δN formalism with directly solving the evolution equation of NG on super-horizon scales in a simple two-field system. This shows that one can use the δN formalism or the covariant and non-linear perturbation equations to study NG from multi-field inflation, and possibly also from preheating.

In summary, through my Ph.D. dissertation, I have conducted theoretical studies of inflationary cosmology, using GWs, gravitational decay of inflaton, and NG. This provides us with novel ways to search for the physics of inflation.

Chapter 2

Gravitational Wave Background Spectrum in the Standard Model

2.1 Introduction

Detection of the stochastic background of primordial gravitational waves has profound implications for the physics of the early universe and the high energy physics that is not accessible by particle accelerators [11, 12, 13, 14, 15, 16, 17, 18, 19, 20, 21, 22, 23, 24]. The basic reason why relic gravitational waves carry information about the very early universe is that particles which decoupled from the primordial plasma at a certain time, $t \sim t_{\rm dec}$, when the universe had a temperature of $T \sim T_{\rm dec}$, memorize the physical state of the universe at and below $T_{\rm dec}$. Since gravitons decoupled below the Plank energy scale, the relic gravitons memorize all the expansion history of the universe after they decoupled and thus would probe deeper into the very early universe. Gravitational waves act therefore as the *time machine* that allows us to see through the entire history of the universe. Another example of relic species is the cosmic microwave background (CMB) photons, which decoupled from matter at $T \sim 0.3$ eV and can trace the physical state of the universe back to 0.3 eV. On the other hand, the primordial gravitational waves carry information on the state of the much earlier universe than the CMB photons do.

The purpose of this chapter is to study the evolution of primordial gravitational waves through changes in the physical conditions in the universe within the Standard Model of elementary particles and beyond. For instance, the quark gluon plasma (QGP) phase to hadron gas phase transition causes a sharp feature in the gravitational wave spectrum. The change of the number of relativistic degrees of freedom affects the Hubble rate by reducing the growth rate of the Hubble radius during the transition. Thus, the rate at which modes re-enter the horizon is changed during the transition and a step in the spectrum appears at frequencies on the order of the Hubble rate at the transition. For the QGP phase transition this frequency is $\sim 10^{-7}$ Hz today and the correction is about 30% [25, 26]. Other large drops in the number of relativistic degrees of freedom occur at electron positron annihilation and possibly at the supersymmetry (SUSY) breaking. Since the gravitational wave spectrum is sensitive to the number of relativistic degrees of freedom, one can search for evidence of supersymmetry in the very beginning of the universe by looking at the relevant frequency region ($\sim 10^{-3}$ Hz). For energy scales lower than neutrino decoupling (~ 2 MeV [27]) we shall also account for the damping effect from neutrino free-streaming [28, 29, 30]. We show that a combination of these two effects gives rise to a highly nontrivial shape of the gravitational wave spectrum.

The primordial gravitational wave spectrum will also provide us with information about inflation. The energy scale of inflation is directly related to the amplitude of the spectrum. The modes which re-entered the horizon during the radiation dominated epoch show a nearly scale invariant spectrum if we do not consider the change of the effective number of degrees of freedom. Typically the amplitude of the spectrum is of order 10^{-15} for 10^{16} GeV inflation energy scale in such a frequency region. Inflation ends when the inflaton decays into radiation and reheats the universe [31, 32, 33]. The energy scale of reheating could be seen from the highest frequency end ($\sim k_{\rm rh}$) of a nearly scale invariant energy density spectrum of the primordial gravitational waves. The lowest frequency mode observable today corresponds to the horizon size today, and the interval between the lowest frequency and $k_{\rm rh}$ would give the number of e-holdings, which tells us the duration of inflation between the end of inflation and the time at which fluctuations having the wavelength of the current horizon size left the horizon during inflation. The slope of the spectrum provides the power-law index of the tensor perturbation, n_T [22, 21, 23]. $n_T = 0$ corresponds to a scale invariant power spectrum from de Sitter inflation. In a large class of inflationary models $|n_T|$ is not zero but much smaller than unity, and its determination constrains the inflationary models. As the effect of n_T has been investigated by many authors, e.g. [20, 21, 22, 23, 34, 35], and is easy to include, we shall assume de Sitter inflation ($n_T = 0$) throughout this chapter. Our result is general and easily applicable to any kind of models which produce primordial tensor perturbations. (e.g. Ekpyrotic models [36]).

The primordial gravitational waves not only test and probe the physics of inflation and reheating, but also can provide the tomography of the standard model of particle physics and models beyond. The study of its spectrum enables us to probe the very early universe in a truly transparent way. The goal of this chapter is to show how the constituents in the early and very early universe would affect the primordial gravitational wave spectrum, which is observable in principle and may be observable in the future by the next generation observational projects, such as the Big Bang Observer (BBO) proposed to NASA [37] and the DECIGO proposed in Japan [38]. We present a new, rigorous computation of the primordial gravitational wave spectrum from de Sitter inflation with the Standard Model of particle physics.

It is easy to extend our results to non-de Sitter (e.g., slow-roll) inflation models.

The outline of this chapter is as follows. In Sec. 2.2, basics about the primordial gravitational waves from inflation are reviewed. In subsection 2.2.1 we give analytical solutions of gravitational waves in some limiting cases. We define energy density of gravitational waves in subsection 2.2.2. The effect of neutrino free-streaming on the spectrum is formulated and explained in subsection 2.2.3. The numerical solution to the integro-differential equation is also presented. In Sec. 2.3, a crucial quantity during radiation domination, the effective relativistic degrees of freedom, g_*, is introduced and related to the primordial gravitational wave spectrum in heuristic and intuitive manners to illustrate the underlying physics. In Sec. 2.4, we give an improved calculation of the primordial gravitational wave spectrum in the Standard Model, employing de Sitter inflation. In subsection 2.4.1 we give more detailed analytical accounts of numerical solutions of gravitational waves when the effective number of relativistic species changes. Our final results are summarized in Figs. 2.7 and 2.8. In Appendix B.1 we give useful formulae for the Bessel type functions.

Units are chosen as $c = \hbar = k_B = 1$ and $\sqrt{8\pi G}$ is retained. Indices λ, μ, $\nu, \dots$ run from 0 to 3, and i, j, $k, \dots$ run from 1 to 3. Over-dots are used for derivatives with respect to time throughout the chapter. Primes are mainly used for derivatives with respect to conformal time, but sometimes with respect to arguments we are focusing on. Barred quantities are unperturbed parts of variables.

2.2 Wave equation, power spectrum, and energy density

In this section we define the power spectrum, $\Delta_h^2(k)$, and relative spectral energy density, $\Omega_h(k)$, of the gravitational wave background. We do this because some authors use different conventions in the literature. For tensor perturbations on an isotropic, uniform and flat background spacetime, the metric is given by

$$ds^2 = a^2(\tau)[-d\tau^2 + (\delta_{ij} + h_{ij})dx^i dx^j], \tag{2.1}$$

$$g_{\mu\nu} = a^2(\tau)(\eta_{\mu\nu} + h_{\mu\nu}), \tag{2.2}$$

where

$$\eta_{\mu\nu} = \mathrm{diag}(-1, 1, 1, 1), \quad h_{00} = h_{0i} = 0, \quad |h_{ij}| \ll 1. \tag{2.3}$$

Here and after we shall work in the transverse traceless (TT) gauge, which leaves only the tensor modes in perturbations, i.e. $h_{ij,j} = 0$ and $h^i{}_i = 0$. In the linear perturbation theory the TT metric fluctuations are gauge invariant [1]. We shall denote the two independent polarization states of the perturbation as $\lambda = +, \times$ and sometimes suppress them when causing no confusion. We decompose h_{ij} into plane waves with the comoving wave number, $|\mathbf{k}| \equiv k$, as

$$h_{ij}(\tau, \mathbf{x}) = \sum_\lambda \int \frac{d^3k}{(2\pi)^3} h_\lambda(\tau; \mathbf{k}) e^{i\mathbf{k}\cdot\mathbf{x}} \epsilon^\lambda_{ij}, \tag{2.4}$$

where ϵ^λ_{ij} is the polarization tensor and $\lambda = +, \times$. The equation for the wave amplitude, $h_\lambda(\tau; \mathbf{k}) \equiv h_{\lambda,\mathbf{k}}$, is obtained by requiring the perturbed metric [Eq. (2.2)] to satisfy the Einstein equation to $\mathcal{O}(h)$. One finds that $\delta G_{ij} = 8\pi G \delta T_{ij}$ in the linear order [41] yields

$$-\frac{1}{2} h_{ij;\nu}{}^{;\nu} = 8\pi G \Pi_{ij}, \tag{2.5}$$

[1] In classic references [39, 40], $h_{ij} = 2H_{Tij}$ and $\Pi_{ij} = \bar{p}\pi_{Tij}$ for tensor perturbations, which are automatically gauge-invariant.

where $\Pi_{ij}(t, \mathbf{x})$ is the anisotropic part of the stress tensor, defined by writing the spatial part of the perturbed energy-momentum tensor as

$$T_{ij} = pg_{ij} + a^2\Pi_{ij}, \tag{2.6}$$

where p is pressure. For a perfect fluid $\Pi_{ij} = 0$, but this would not be true in general. In the cosmological context, the amplitude of gravitational waves is affected by anisotropic stress when neutrinos are freely streaming (less than $\sim 10^{10}$K) [28, 42, 43, 29, 30, 44, 45, 46]. As we only deal with tensor perturbations, h_{ij}, we may treat each component as a scalar quantity under general coordinate transformation, which means e.g. $h_{ij;\mu} = h_{ij,\mu}$. The left-hand side of Eq. (2.5) becomes

$$\begin{aligned} h_{ij;\nu}{}^{;\nu} &= \bar{g}^{\mu\nu}(h_{ij,\mu\nu} - \Gamma^{\alpha}_{\mu\nu}h_{ij,\alpha}), \\ &= -\ddot{h}_{ij} + \left(\frac{\nabla^2}{a^2}\right)h_{ij} - \left(\frac{3\dot{a}}{a}\right)\dot{h}_{ij}, \end{aligned} \tag{2.7}$$

where $\Gamma^0_{0\nu} = \Gamma^0_{\mu 0} = 0$, $\Gamma^0_{ij} = \delta_{ij}\dot{a}a$, and $\bar{g}^{ij} = a^{-2}\delta_{ij}$ have been used. Commas denote partial derivatives, while semicolons denote covariant derivatives in Eqs. (2.5) and (2.7). Transforming this equation into Fourier space, one obtains

$$\ddot{h}_{\lambda,\mathbf{k}} + \left(\frac{3\dot{a}}{a}\right)\dot{h}_{\lambda,\mathbf{k}} + \left(\frac{k^2}{a^2}\right)h_{\lambda,\mathbf{k}} = 16\pi G\Pi_{\lambda,\mathbf{k}}, \tag{2.8}$$

where the Laplacian ∇^2 in the second term of (2.5) has been replaced by $-k^2$ in the third term of (2.8). The second term represents the effect of the expansion of the universe. Using conformal time derivatives ($' \equiv \frac{\partial}{\partial\tau}$), we may obtain

$$h''_{\lambda,\mathbf{k}} + \left(\frac{2a'}{a}\right)h'_{\lambda,\mathbf{k}} + k^2h_{\lambda,\mathbf{k}} = 16\pi Ga^2\Pi_{\lambda,\mathbf{k}}. \tag{2.9}$$

This is just the massless Klein-Gordon equation for a plane wave in an expanding space with a source term. Thus, each polarization state of the wave behaves as a massless, minimally coupled, real scalar field, with a normalization factor of $\sqrt{16\pi G}$ relating the two.

Next, let us consider the time evolution of the spectrum. After the fluctuations left the horizon, $k \ll aH$, equation (2.9) would become

$$\frac{h''_{\lambda,\mathbf{k}}}{h'_{\lambda,\mathbf{k}}} \approx -\frac{2a'}{a}, \tag{2.10}$$

whose solution is

$$h_{\lambda,\mathbf{k}}(\tau) = A + B\int^{\tau} \frac{d\tau'}{a^2(\tau')}, \tag{2.11}$$

where A and B are integration constants. Ignoring the second term that is a decaying mode, one finds that $h_{\lambda,\mathbf{k}}$ remains constant outside the horizon. Note that we have ignored the effect of anisotropic stress outside the horizon, as this term is usually given by causal mechanism which must vanish outside the horizon. Therefore, one may write a general solution of $h_{\lambda,\mathbf{k}}$ at any time as

$$h_{\lambda,\mathbf{k}}(\tau) \quad \equiv \quad h^{prim}_{\lambda,\mathbf{k}}\mathcal{T}(\tau,k), \tag{2.12}$$

where $h^{prim}_{\lambda,\mathbf{k}}$ is the primordial gravitational wave mode that left the horizon during inflation. The transfer function, $\mathcal{T}(\tau,k)$, then describes the sub-horizon evolution of gravitational wave modes after the modes entered the horizon. The transfer function is normalized such that $\mathcal{T}(\tau,k) \to 1$ as $k \to 0$. The power spectrum of gravitational waves, $\Delta_h^2(k)$, may be defined as

$$\langle h_{ij}(\tau,\mathbf{x})h^{ij}(\tau,\mathbf{x})\rangle = \int \frac{dk}{k}\Delta_h^2(\tau,k), \tag{2.13}$$

which implies

$$\Delta_h^2(\tau,k) = \frac{2k^3}{2\pi^2}\sum_{\lambda}\langle|h_{\lambda,\mathbf{k}}(\tau)|^2\rangle. \tag{2.14}$$

Using equation (2.12), one may write the time evolution of the power spectrum as

$$\Delta_h^2(\tau,k) \equiv \Delta_{h,prim}^2 \left[\mathcal{T}(\tau,k)\right]^2, \tag{2.15}$$

where

$$\Delta_{h,prim}^2 = \frac{2k^3}{2\pi^2}\sum_\lambda \langle|h_{\lambda,\mathbf{k}}^{prim}|^2\rangle = \frac{16}{\pi}\left(\frac{H_{\rm inf}}{m_{Pl}}\right)^2. \tag{2.16}$$

We have used the prediction for the amplitude of gravitational waves from de-Sitter inflation at the last equality, and $H_{\rm inf}$ is the Hubble constant during inflation. One may easily extend this result to slow-roll inflation models.

The energy density of gravitational waves is given by the 0-0 component of stress-energy tensor of gravitational waves:

$$\rho_h(\tau) = \frac{\langle h'_{ij}(\tau,\mathbf{x})h^{ij\prime}(\tau,\mathbf{x})\rangle}{32\pi G a^2(\tau)}. \tag{2.17}$$

The relative spectral energy density, $\Omega_h(\tau,k)$, is then given by the Fourier transform of energy density, $\tilde{\rho}_h(\tau) \equiv \frac{d\rho_h}{d\ln k}$, divided by the critical density of the universe, $\rho_{\rm cr}(\tau)$ (see subsection 2.2.2 for full derivation):

$$\Omega_h(\tau,k) \quad \equiv \quad \frac{\tilde{\rho}_h(\tau,k)}{\rho_{\rm cr}(\tau)} = \frac{\Delta_{h,prim}^2}{12a^2(\tau)H^2(\tau)}\left[\mathcal{T}'(\tau,k)\right]^2. \tag{2.18}$$

Note that $\Omega_h(k)$ is often defined as $\Omega_h(\tau,k) = \frac{\Delta_{h,prim}^2}{12a^2(\tau)H^2(\tau)}k^2\left[\mathcal{T}(\tau,k)\right]^2 = \frac{k^2}{12a^2(\tau)H^2(\tau)}\Delta_h^2(\tau,k)$ in the literature [22, 23, 34, 47]. This definition is not compatible with the 0-0 component of stress energy tensor; however, it is a good approximation when the modes are deep inside the horizon, $k \gg aH$. Let us briefly explain a relation between these two definitions. The transfer function is usually given by Bessel type functions, $\mathcal{T}(x) = \frac{1}{x^n}[Aj_n(x) + By_n(x)]$. The conformal time derivative of the transfer function is thus given by $\frac{d}{d\tau}\mathcal{T}(x) = -\frac{k}{x^n}\left[Aj_{n+1}(x) + By_{n+1}(x)\right]$, where $x \equiv k\tau$. Therefore, in the limit that the modes are deep inside the horizon, $k \gg aH$, one ob-

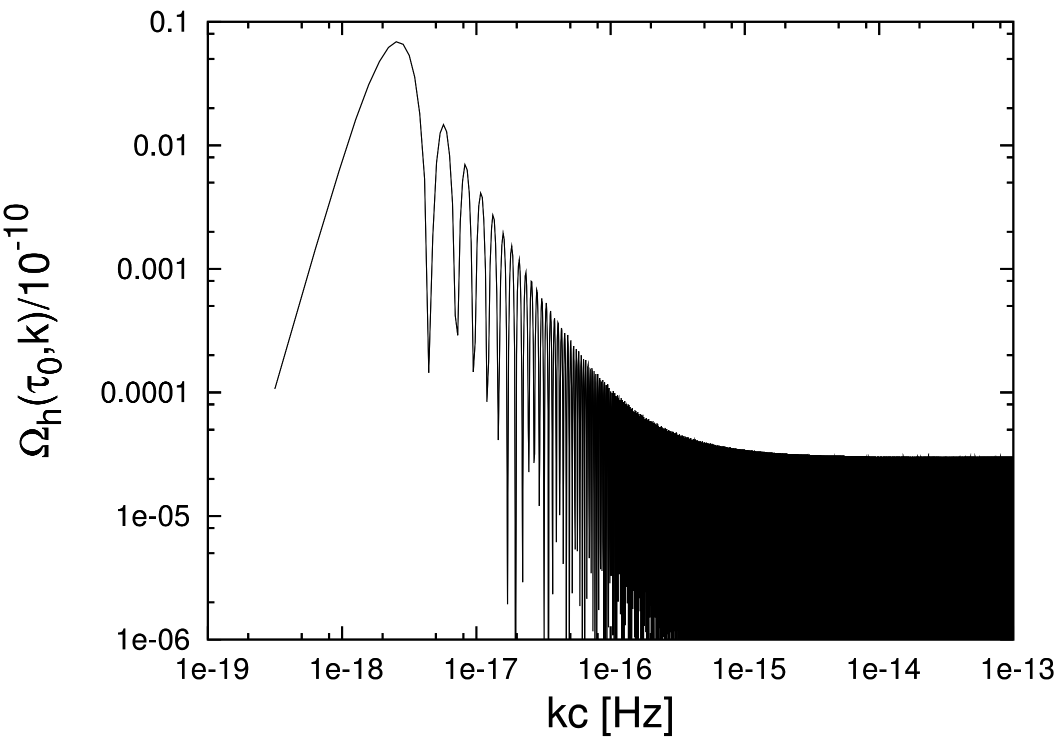

Figure 2.1: The primordial gravitational wave spectrum at present, $\tau = \tau_0$, as a function of the comoving wavenumber, k (or kc in units of Hertz). The frequency of gravitational waves observed today is related to k by $f_0 = kc/2\pi$. The spectrum at large wavenumber is exactly scale-invariant as we have assumed de-Sitter inflation. In this figure we have not taken into account the effects of the change in effective relativistic degrees of freedom or neutrino free-streaming.

tains $\Omega_h(k) = \frac{\Delta^2_{h,prim}}{12a^2(\tau)H^2(\tau)} \left[\mathcal{T}'(\tau,k)\right]^2 \approx \frac{\Delta^2_{h,prim}}{12a^2(\tau)H^2(\tau)} k^2 \left[\mathcal{T}(\tau,k)\right]^2$, which agrees with the definition of $\Omega_h(k)$ in [22, 23, 34, 47]. The difference between Ω_h and $k^2\Delta^2_h$ would affect the prediction only at the largest scales, where both the overall amplitude and phases are different. (The phases are shifted by $\pi/2$.)

Figure 2.1 shows a numerical calculation of equation (2.18) for $\Omega_m = 1 - \Omega_r$, $\Omega_r h^2 = 4.15 \times 10^{-5}$, and $h = 0.7$. We ignored the contribution from dark energy, which is only important at the lowest frequency regime that we are not interested in in this chapter. One may understand the basic features in this numerical result as follows. Energy density of gravitational waves evolves just like that of radiation inside the horizon, $\tilde{\rho}_h(\tau, k) \propto a^{-4}$, for $k \gg aH$. This implies that the relative spectral energy density, $\Omega_h(\tau, k)$, inside the horizon remains independent of time during the radiation era while it decreases as $\Omega_h(\tau, k) \propto a^{-1}$ during the matter era. Therefore, the modes that entered the horizon during the matter era *later* would decay *less*. As the low frequency modes represent the modes that entered the horizon at late times, $\Omega_h(\tau, k)$ rises toward lower frequencies. On the other hand, $\Omega_h(\tau, k)$ at $k \gtrsim 10^{-15}$ Hz is independent of k. These are the modes that entered the horizon during the radiation era for which $\Omega_h(\tau, k)$ was independent of time. After the matter-radiation equality all of these modes suffered the same amount of redshift, and thus the shape of $\Omega_h(\tau, k)$ still remains scale-invariant at $k \gtrsim 10^{-15}$ Hz.

These qualitative arguments may be made more quantitative by using the following analytical solutions of $\Omega_h(\tau, k)$ for three different regimes (see subsection 2.2.1 for derivation):

$$\Omega_h(\tau < \tau_{\rm eq}, k > k_{\rm eq}) = \frac{\Delta^2_{h,prim} a^2}{12 H^2_{\rm eq} a^4_{\rm eq}} k^2 \left[j_1(k\tau)\right]^2 , \tag{2.19}$$

$$\Omega_h(\tau > \tau_{\rm eq}, k > k_{\rm eq}) = \frac{\Delta^2_{h,prim} a}{12 H^2_0 a^3_0} k^2 \frac{\tau^2_{eq}}{\tau^2} \left[A(k) j_2(k\tau) + B(k) y_2(k\tau)\right]^2 , \tag{2.20}$$

$$\Omega_h(\tau > \tau_{\rm eq}, k < k_{\rm eq}) = \frac{\Delta^2_{h,prim} a}{12 H^2_0 a^3_0} k^2 \left[\frac{3 j_2(k\tau)}{k\tau}\right]^2 , \tag{2.21}$$

where $\tau_{\rm eq}$ is the conformal time at the matter-radiation equality, $k_{\rm eq}$ is the comoving wavenumber of the modes that entered the horizon at equality, and $j_0'(x) = -j_1(x)$ and $\left[\frac{j_1(x)}{x}\right]' = -\frac{j_2(x)}{x}$ have been used to compute $\mathcal{T}'(\tau, k)$. (Spherical Bessel functions are given in Appendix B.1.) The first solution [Eq. (2.19)] describes $\Omega_h(\tau, k)$ during radiation era for the modes that entered the horizon before $\tau_{\rm eq}$. This solution is of course not relevant to what we observe today. (We do not live in the radiation era.) The second [Eq. (2.20)] and third [Eq. (2.21)] solutions describe $\Omega_h(\tau, k)$ during matter era for the modes that entered the horizon before and after $\tau_{\rm eq}$, respectively. The k-dependent coefficients $A(k)$ and $B(k)$ are given in equation (2.30) and (2.31), respectively. While the expression is slightly complicated, one can find that the second solution is independent of k when the oscillatory part is averaged out, which explains a scale-invariant spectrum at high frequencies, $k > k_{\rm eq} \sim 10^{-15}$ Hz. On the other hand, the third solution gives $\Omega_h(\tau, k) \propto k^{-2}$, which explains the low frequency spectrum.

Figure 2.1 (and its extension to slow-roll inflation which yields a small tilt in the overall shape of the spectrum) has been widely referred to as the prediction from the standard model of cosmology. However, as we shall show in the subsequent sections, the standard model of cosmology actually yields much richer gravitational wave spectrum with more characteristic features in it.

2.2.1 Analytical solutions of wave equation

In this subsection we shall discuss solutions of the equation of motion [Eq. (2.9)]. While we assume $\Pi_{ij} = 0$ in this subsection, we shall treat $\Pi_{ij} \neq 0$ in subsection 2.2.3. Imposing appropriate boundary conditions [48], one obtains simple analytical solutions for tensor modes of fluctuations in the inflationary (de Sitter), radiation dominated (RD) and matter dominated (MD) universe, as

$$\begin{aligned} h_{\mathbf{k}}(\tau) &= \frac{\sqrt{16\pi G}}{\sqrt{2k}a}\left(1 - \frac{i}{k\tau}\right)e^{-ik\tau}\alpha(\mathbf{k}), \\ &= -\frac{\tau}{a}\sqrt{8\pi Gk}h_1^{(2)}(k\tau)\alpha(\mathbf{k}) \qquad \text{inflation}, \qquad (2.22) \\ h_{\mathbf{k}}(\tau) &= \left[j_0(k\tau)\right] h_{\mathbf{k}}^{prim} \qquad \text{RD}, \qquad (2.23) \\ h_{\mathbf{k}}(\tau) &= \left[\frac{3j_1(k\tau)}{k\tau}\right] h_{\mathbf{k}}^{prim} \qquad \text{MD}, \qquad (2.24) \end{aligned}$$

where $\alpha(\mathbf{k})$ is a stochastic variable satisfying $\langle\alpha(\mathbf{k})\alpha^*(\mathbf{k}')\rangle = \delta^3(\mathbf{k}-\mathbf{k}')$, and spherical Bessel-type functions are given in Appendix B.1. We classify wave modes by their horizon crossing time, $\tau_{\rm hc}$;

$$| \mathbf{k} |= k \begin{cases} > k_{\rm eq} & \text{the modes that entered the horizon during RD: } \tau_{\rm hc} < \tau_{\rm eq} \\ < k_{\rm eq} & \text{the modes that entered the horizon during MD: } \tau_{\rm hc} > \tau_{\rm eq} \end{cases} \quad (2.25)$$

where $\tau_{\rm eq}$ denotes the time at the matter-radiation equality, and $\tau_{\rm hc}$ denotes the time when fluctuation modes crossed the horizon, $k\tau_{\rm hc} = 1$. Notice that $|h_k(\tau)|^2$ for each solution (2.22) - (2.24) does not depend on time ($\equiv |h_k^{prim}|^2$) at the super-horizon scale, $|k\tau| \ll 1$.

The tensor mode fluctuations from the inflationary universe left the horizon and *froze out*. Its dimensionless spectrum is given from Eq. (2.22) as

$$\begin{aligned} \Delta_h^2(k) \quad &\equiv \quad 4k^3 \frac{|h_k^{\rm inf}|^2}{2\pi^2} = 64\pi G \left(\frac{H_{\rm inf} k\tau}{2\pi}\right)^2 \left(1 + \frac{1}{k^2\tau^2}\right) \\ &\simeq \quad \frac{16}{\pi}\left(\frac{H_{\rm inf}}{m_{\rm Pl}}\right)^2 \equiv 4k^3 \frac{|h_k^{prim}|^2}{2\pi^2} \qquad (|k\tau| \ll 1), \end{aligned} \quad (2.26)$$

where $H_{\rm inf}$ is the Hubble parameter during inflation and $\tau = -1/(aH_{\rm inf})$ is used in the second equality. Note that the conventional factor 4 is from $\int \frac{dk}{k}\Delta_h^2(k) \equiv \langle h_{ij}h^{ij}\rangle = 2[\langle|h_+|^2\rangle + \langle|h_\times|^2\rangle] = 4|h|^2$, where $|h_{+,k}| = |h_{\times,k}| \equiv |h|$ is assumed [49]. From the Friedman equation during inflation, one obtains $H_{\rm inf}^2 \approx \frac{8\pi}{3m_{\rm Pl}^2}V(\phi)$, which gives $\Delta^2_{h,prim} \approx 10V(\phi)/m_{\rm Pl}^4$; thus $\Delta^2_{h,prim}$ is sensitive to the shape of inflaton potential [22, 21, 23]. The dimensionless spectrum (2.26) is nearly independent k. This is the famous prediction of the inflationary scenario known as a nearly scale invariant spectrum. As long as we consider de Sitter inflation, the spectrum is exactly scale invariant, i.e. $\propto k^0$ as ϕ is at rest.

Using the transfer function [Eq. (2.12)], we obtain the time evolution of the amplitude of gravitational waves as

$$\mathcal{T}(\tau < \tau_{\rm eq}, k > k_{\rm eq}) = j_0(k\tau), \tag{2.27}$$

$$\mathcal{T}(\tau > \tau_{\rm eq}, k > k_{\rm eq}) = \frac{\tau_{eq}}{\tau}\left[A(k)j_1(k\tau) + B(k)y_1(k\tau)\right], \tag{2.28}$$

$$\mathcal{T}(\tau, k < k_{\rm eq}) = \frac{3j_1(k\tau)}{k\tau}, \tag{2.29}$$

where

$$A(k) = \frac{3}{2k\tau_{\rm eq}} - \frac{\cos 2k\tau_{\rm eq}}{2k\tau_{\rm eq}} + \frac{\sin 2k\tau_{\rm eq}}{(k\tau_{\rm eq})^2}, \tag{2.30}$$

$$B(k) = -1 + \frac{1}{(k\tau_{\rm eq})^2} - \frac{\cos 2k\tau_{\rm eq}}{(k\tau_{\rm eq})^2} - \frac{\sin 2k\tau_{\rm eq}}{2k\tau_{\rm eq}}. \tag{2.31}$$

Their conformal time derivatives are given as

$$\mathcal{T}'(\tau < \tau_{\rm eq}, k > k_{\rm eq}) = -kj_1(k\tau), \tag{2.32}$$

$$\mathcal{T}'(\tau > \tau_{\rm eq}, k > k_{\rm eq}) = -\frac{k\tau_{eq}}{\tau}\left[A(k)j_2(k\tau) + B(k)y_2(k\tau)\right], \tag{2.33}$$

$$\mathcal{T}'(\tau, k < k_{\rm eq}) = -\frac{3j_2(k\tau)}{\tau}. \tag{2.34}$$

Eqs. (2.27) and (2.28) are the evolution of modes which entered the horizon during the radiation era, while Eq. (2.29) is the evolution of modes which entered the horizon during the matter era. Coefficients $A(k)$ and $B(k)$ are obtained by equating a solution (2.27) with (2.28) and their first derivatives [(2.32) and (2.33)] at the matter-radiation equality. The transfer function for the intermediate regime, Eq. (2.28), can be calculated numerically so that the two other limiting solutions match smoothly (See Fig. 2.1). If the wavelength of the gravitational waves is much shorter than the duration of the cosmological transition, a WKB approximation may be appropriate [44, 50, 51]. Here we just assumed the instantaneous transition to illustrate the main point. The analytical solutions as well as numerical solutions are presented and compared in Fig. 2.2 and 2.3. The higher k-modes enter the horizon earlier, and their amplitudes are damped more by the cosmological redshift.

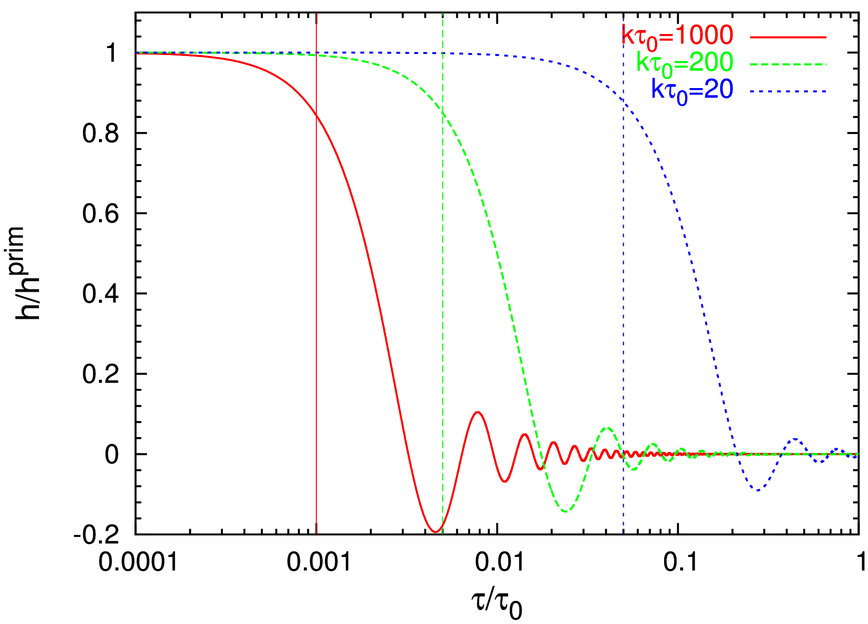

Figure 2.2: Numerical solutions of tensor perturbations. The solid, dashed, and short-dashed lines show the high, medium, and low frequency modes, respectively. The higher k-modes enter the horizon earlier, and are damped more by the cosmological redshift. Vertical lines define the horizon crossing time for each k-mode.

2.2.2 The relative spectral density: $\Omega_h(k)$

Here we shall define the energy momentum tensor of gravitational waves following the argument and the definition in §35.7 and §35.13 of [52]. The Ricci tensor for the metric of the form given in Eq. (2.1) may be expanded in metric perturbations, h:

$$R_{\mu\nu} = \bar{R}_{\mu\nu} + R^{(1)}_{\mu\nu} + R^{(2)}_{\mu\nu} + \mathcal{O}(h^3), \tag{2.35}$$

where $R^{(1)}_{\mu\nu} \sim \mathcal{O}(h)$ and $R^{(2)}_{\mu\nu} \sim \mathcal{O}(h^2)$.

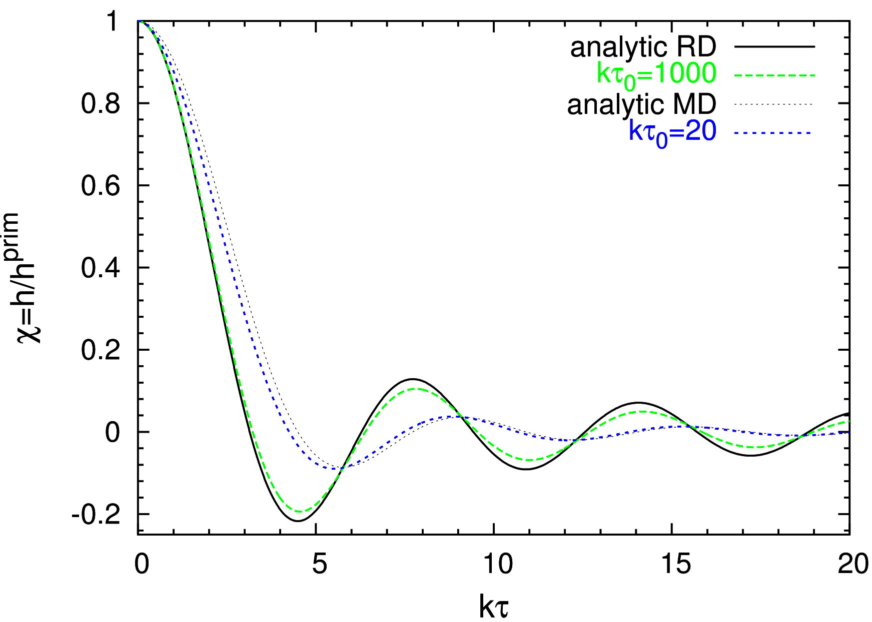

Figure 2.3: Comparison between numerical solutions and analytical solutions of tensor perturbations. The dashed and short-dashed lines show numerical solutions of the high and low frequency modes, respectively. The higher k-modes enter the horizon earlier, and thus the numerical solution is well approximated by the analytical solution during the radiation era, $\chi(k\tau) = j_0(k\tau)$ (solid line). On the other hand, the lower k-modes enter the horizon much later, and thus the numerical solution is close to the analytical solution during the matter era, $\chi(k\tau) = 3j_1(k\tau)/k\tau$ (dotted line).

For the vacuum field equation, $R_{\mu\nu} = 0$. As the Einstein equation is nonlinear, $\bar{R}_{\mu\nu}$ is in general not linear in $h_{\mu\nu}$. The linear term in Eq. (2.35) must obey the vacuum equation,

$$R^{(1)}_{\mu\nu} = 0. \tag{2.36}$$

This is an equation for the propagation of the gravitational waves, which corresponds to Eq. (2.9) or more generally to Eq. (2.74) in the FRW universe. The remaining part of $R_{\mu\nu}$ may be divided into a smooth part which varies only on scales larger than some coarse-graining scales,

$$\bar{R}_{\mu\nu} + \langle R^{(2)}_{\mu\nu} \rangle = 0, \tag{2.37}$$

and a fluctuating part which varies on smaller scales

$$R^{(1)\text{nonlinear}}_{\mu\nu} + R^{(2)}_{\mu\nu} - \langle R^{(2)}_{\mu\nu} \rangle = 0, \tag{2.38}$$

up to the second order in $h_{\mu\nu}$. Here, $R^{(1)\text{nonlinear}}_{\mu\nu}$ is defined by Eq. (2.38) and represents the nonlinear correction to the propagation of $h_{\mu\nu}$, Eq. (2.36), which gives $h_{\mu\nu} \to h_{\mu\nu} + j_{\mu\nu}$, where $j_{\mu\nu} \sim \mathcal{O}(h^2)$ [52]. Eq. (2.37) represents how the stress energy in the gravitational waves creates the background curvature. The Einstein equation in vacuum is then

$$\bar{G}_{\mu\nu} = \bar{R}_{\mu\nu} - \frac{1}{2}\bar{R}\bar{g}_{\mu\nu} = 8\pi G T^{(GW)}_{\mu\nu}, \tag{2.39}$$

$$T^{(GW)}_{\mu\nu} \equiv -\frac{1}{8\pi G}\left(\langle R^{(2)}_{\mu\nu} \rangle - \frac{1}{2}\bar{g}_{\mu\nu}\langle R^{(2)} \rangle \right), \tag{2.40}$$

where $T^{(GW)}_{\mu\nu}$ is a definition of the energy momentum tensor for the gravitational waves and $\langle \quad \rangle$ denotes an average over several wavelengths. The importance of the effective energy momentum tensor is that it tells us how *backreaction* from energy density of gravitational waves would affect the expansion law of the background universe. Note that the *effective* energy momentum tensor defined by Eq. (2.40) is different from that defined by the Neother current of the Lagrangian density, $T_{\mu\nu}^{\text{Neother}} \equiv \frac{2}{\sqrt{-g}}\frac{\delta S^{(2)}}{\delta g^{\mu\nu}}$, where $S^{(2)}$ is the second order perturbation in the Einstein-Hilbert action. These definitions coincide only deep inside the horizon. Note also that in the notation of [52], $G = 1$, but in our notation, $\hbar = c = 1$, $G = m_{\text{Pl}}^{-2}$,where m_{Pl} is the Plank mass. Since $\langle R^{(2)} \rangle = 0$ [52],

$$T_{\mu\nu}^{(GW)} = \frac{1}{32\pi G}\langle h_{\alpha\beta|\mu}h^{\alpha\beta}{}_{|\nu}\rangle = \frac{1}{32\pi G}\langle h_{\alpha\beta,\mu}h^{\alpha\beta}{}_{,\nu}\rangle + \mathcal{O}(h^3), \tag{2.41}$$

where $|$ is the covariant derivative with respective to background metric, $\bar{g}_{\mu\nu}$. Note that we have employed the transverse-traceless (TT) gauge. In linear theory we neglect higher order terms in the energy momentum tensor.

The energy density of gravitational waves, ρ_h, is defined by the 0-0 component of the energy momentum tensor.

$$\rho_h(\tau) \equiv T_{00}^{(GW)} = \frac{1}{32\pi G}\langle \dot{h}_{ij}\dot{h}^{ij}\rangle, \tag{2.42}$$

where h_{ij} is in the TT gauge. There are only two independent modes for gravitational waves;

$$h_{ij} = \begin{pmatrix} h_+ & h_\times & 0 \\ h_\times & -h_+ & 0 \\ 0 & 0 & 0 \end{pmatrix}, \tag{2.43}$$

where $+$ and $\times$ denote two independent polarization modes and their propagation direction is taken in $\hat{z}$ direction. Hence,

$$
\begin{aligned}
\rho_h(\tau) &= \frac{2}{32\pi G}\langle \dot{h}_+^2 + \dot{h}_\times^2 \rangle \\
&= \frac{1}{16\pi G a^2}\langle {h'}_+^2 + {h'}_\times^2 \rangle \\
&= \frac{1}{16\pi G a^2}\int \frac{d^3k}{(2\pi)^3}\int \frac{d^3k'}{(2\pi)^3}\langle \left({h'}_{+,\mathbf{k}}{h'}_{+,\mathbf{k'}} + {h'}_{\times,\mathbf{k}}{h'}_{\times,\mathbf{k'}}\right) e^{i(\mathbf{k}+\mathbf{k'})\cdot\mathbf{x}}\rangle,
\end{aligned} \tag{2.44}
$$

where Fourier transformation was done and ${h^*}_{\lambda,\mathbf{k}} = h_{\lambda,-\mathbf{k}}$ in the last step. For stochastic modes, the spatial average over several wavelengths, $\langle \quad \rangle$, is equivalent to the ensemble average in k space;

$$
\langle {h'}_{\lambda,\mathbf{k}}{h'}_{\lambda',\mathbf{k'}} \rangle = (2\pi)^3 \delta_{\lambda,\lambda'}\delta^{(3)}(\mathbf{k}+\mathbf{k'})|h'_{\lambda,k}|^2, \tag{2.45}
$$

where $\lambda = +, \times$. Using (2.44) and (2.45), we obtain

$$
\rho_h(\tau) = \frac{1}{16\pi G a^2}\int \frac{d^3k}{(2\pi)^3}\left[|{h'}_{+,k}(\tau)|^2 + |{h'}_{\times,k}(\tau)|^2\right]. \tag{2.46}
$$

It is reasonable to assume that the primordial gravitational waves are unpolarized, i.e. $|h_{+,k}|^2 = |h_{\times,k}|^2$. Whenever we express the time evolution of some quantities, it is convenient to express them in terms of the transfer function,$\mathcal{T}(k\tau)$, and the primordial amplitude,$\Delta^2_{h,prim}$, defined as (2.12);

$$
\rho_h(\tau) = \frac{1}{32\pi G a^2}\int d\ln k \Delta^2_{h,prim}\left[\mathcal{T}'(k\tau)\right]^2, \tag{2.47}
$$

where

$$
\Delta^2_{h,prim} \equiv 4\frac{k^3}{2\pi^2}|h_k^{prim}|^2 = \frac{16}{\pi}\left(\frac{H_{\rm inf}}{m_{Pl}}\right)^2. \tag{2.48}
$$

Here, $|h_k^{prim}|^2$ is the amplitude of gravitational waves outside the horizon, $|\, k\tau \,| \ll 1$, during inflation. Well inside the horizon averaging over several periods, the leading term of $\overline{[\mathcal{T}'(k\tau)]^2}$ is proportional to $\tau^{-2} \propto a^{-2}$ during the radiation era and $\propto \tau^{-4} \propto a^{-2}$ during the matter era. Thus $\rho_h \propto a^{-4}$, which is consistent with the fact that graviton is massless and thus relativistic.

It is common to define the relative spectral density as the normalized energy density per logarithmic scale.

$$\begin{aligned} \Omega_h(\tau, k) &\equiv \frac{\tilde{\rho}_h(\tau, k)}{\rho_{\rm cr}(\tau)}, \\ \tilde{\rho}_h(\tau, k) &\equiv \frac{d\rho_h(\tau)}{d\ln k}, \end{aligned} \tag{2.49}$$

where $\rho_{\rm cr}(\tau)$ is critical density of the universe, and $\tilde{\rho}_h(\tau, k)$ denotes energy density of the gravitational waves per logarithmic scale. Inserting (2.47) into (2.49), we obtain

$$\Omega_h(\tau, k) = \frac{\Delta^2_{h,prim}}{32\pi G a^2 \rho_c(\tau)} \left[\mathcal{T}'(\tau, k)\right]^2. \tag{2.50}$$

Recalling Friedman equation, $H^2 = 8\pi G\rho_c/3$, (2.50) becomes

$$\Omega_h(\tau, k) = \frac{\Delta^2_{h,prim}}{12 H^2(\tau) a^2} \left[\mathcal{T}'(\tau, k)\right]^2. \tag{2.51}$$

In this chapter, we shall evaluate this quantity exactly within the Standard Model of elementary particles. For an analytical model, $\mathcal{T}'(\tau, k)$ is given by Eqs. (2.32) – (2.34).

2.2.3 Collisionless damping due to neutrino free-streaming

In this subsection, we review the effect of collisionless particles on gravitational waves. Treating relativistic neutrino gas by classical kinetic theory, the linearized Einstein-Boltzmann equation (2.5) can be written as an integro-differential equation (2.74). The derivation of this integro-differential equation is given in the literature, for instance [28, 43, 29, 30] for both scalar and tensor modes, [42] for scalar modes, and will be reviewed briefly in this subsection.

At the temperature of ~ 2 MeV, where neutrinos decoupled and became out of equilibrium with photons, electrons, or positrons, the number of effective relativistic species is $g_*(\sim 2MeV) = 10.75$.[2] The free-streaming neutrino gas after their decoupling satisfies the collisionless Boltzmann equation, i.e. the Vlasov equation,

$$\frac{dF(x,P)}{dt} = 0, \tag{2.52}$$

where $F(x,P) = \bar{F}(P) + \delta F(x,P)$ is a distribution function. The distribution function of relativistic neutrinos is given by

$$\bar{F}(P^0) = \frac{g_\nu}{e^{P^0/T}+1}, \tag{2.53}$$

where g_ν denotes the number of helicity states for neutrinos and anti-neutrinos. Here, $P^\mu \equiv \frac{dx^\mu}{d\lambda}$ and $P^0 = \sqrt{g_{ij}P^iP^j}$, which is implied by the constraint for relativistic particles;

$$g_{\mu\nu}P^\mu P^\nu = 0. \tag{2.54}$$

Therefore, there are only three independent components of the momentum vector. One can also relate P^i with $P_0 = -P^0$ as

$$P^i = \pm\frac{\gamma^i P_0}{a}\left(1 - \frac{1}{2}h_{jk}\gamma^j\gamma^k\right), \tag{2.55}$$

where $\gamma^i = \gamma_i$'s are directional cosines and P^0 is the energy of neutrinos. We chose positive sign convention for $P^0 \equiv \frac{dt}{d\lambda}$. Note that $\delta_{ij}\gamma^i\gamma^j = 1$, and $P^i \equiv C\gamma^i P_0$, where

[2] We have assumed instantaneous decoupling of neutrinos, but this is not true in general.

the coefficient, C, is obtained from Eq. (2.54);

$$\begin{aligned} 0 &= P_0P^0 + a^2P^jP^j + a^2h_{ij}P^iP^j, \\ 0 &= -(P_0)^2 + a^2C^2P_0^2 + a^2h_{ij}\gamma^i\gamma^jC^2P_0^2, \\ 1 &= a^2C^2(1 + h_{ij}\gamma^i\gamma^j). \end{aligned}$$

We consider tensor perturbations. Eq. (2.52) can be expressed as

$$\frac{dF(t, x^i, \gamma^i, P^0)}{dt} = \frac{\partial F}{\partial t} + \frac{dx^i}{dt}\frac{\partial F}{\partial x^i} + \frac{dP^0}{dt}\frac{\partial F}{\partial P^0} + \frac{d\gamma^i}{dt}\frac{\partial F}{\partial \gamma^i} = 0. \tag{2.56}$$

The last term is negligible in the linear perturbation theory, as $\frac{\partial F}{\partial \gamma^i}$ is of the first order in perturbations and $\dot{\gamma}^i = -\frac{1}{2a}h_{jk,i}\gamma^j\gamma^k$.

For the second term $\frac{\partial F}{\partial x^i}$ is of the first order in perturbations and

$$\frac{dx^i}{dt} = \frac{dx^i}{d\lambda}\frac{d\lambda}{dt} = \frac{P^i}{P^0}. \tag{2.57}$$

Using Eq. (2.55), one obtains

$$\frac{dx^i}{dt}\frac{\partial F}{\partial x^i} = \frac{\gamma^i}{a}\frac{\partial F}{\partial x^i} \tag{2.58}$$

in the leading order, as $\bar{F}$ does not depend on x^i; thus, $\frac{\partial F}{\partial x^i}$ is a perturbation.

For the third term we use the geodesic equation,

$$\begin{aligned} \frac{dP^\mu}{d\lambda} &= -\Gamma^\mu{}_{\alpha\beta}P^\alpha P^\beta, && (2.59) \\ \Gamma^\mu{}_{\alpha\beta} &= \frac{g^{\mu\nu}}{2}\left[\frac{\partial g_{\alpha\nu}}{\partial x^\beta} + \frac{\partial g_{\beta\nu}}{\partial x^\alpha} - \frac{\partial g_{\alpha\beta}}{\partial x^\nu}\right]. && (2.60) \end{aligned}$$

The time component of the geodesic equation is

$$
\begin{aligned}
\frac{dt}{d\lambda}\frac{dP^0}{dt} &= -\Gamma^0{}_{\alpha\beta}P^\alpha P^\beta, \\
&= -\frac{g^{0\nu}}{2}\left[2\frac{\partial g_{\alpha\nu}}{\partial x^\beta} - \frac{\partial g_{\alpha\beta}}{\partial x^\nu}\right]P^\alpha P^\beta, \\
&= -\frac{\dot{a}}{a}(P^0)^2 - \frac{1}{2}a^2\frac{\partial h_{ij}}{\partial t}P^iP^j, \qquad (2.61)
\end{aligned}
$$

where $g_{00} = -1,\ g_{0i} = 0$ were used from the second line to the last line. Up to the first order in perturbations

$$
\frac{1}{P^0}\frac{dP^0}{dt} = -\frac{\dot{a}}{a} - \frac{1}{2}\frac{\partial h_{ij}}{\partial t}\gamma^i\gamma^j, \qquad (2.62)
$$

where we have used Eq. (2.55) and neglected higher order terms. This equation describes the change in the neutrino energy as it propagates in a FRW universe with gravitational waves. The first term accounts for the redshift of energy due to an isotropic expansion. The second term tells us that neutrinos lose energy if $\frac{\partial h_{ij}}{\partial t} > 0$, or gain energy if $\frac{\partial h_{ij}}{\partial t} < 0$ from gravitational waves. This energy flow from neutrinos to gravitational waves causes collisionless damping (Fig. 2.4) and amplification of gravitational waves. When integrated, the damping effect always overcome the amplification effect.

Finally, by combining Eqs. (2.56), (2.58), and (2.62), the Vlasov equation for the first order perturbations is obtained as

$$
\left(\frac{dF}{dt}\right)_{\text{first order}} = \frac{\partial\delta F}{\partial t} + \frac{\gamma^i}{a}\frac{\partial\delta F}{\partial x^i} - P^0\frac{\partial\delta F}{\partial P^0}\frac{\dot{a}}{a} - P^0\frac{\partial\bar{F}}{\partial P^0}\frac{1}{2}\frac{\partial h_{ij}}{\partial t}\gamma^i\gamma^j = 0, \qquad (2.63)
$$

where $F = \bar{F} + \delta F(t, x^i, \gamma^i, P^0)$ and δF is a tensor type perturbation in a distribution function of neutrinos. The zeroth order Vlasov equation merely gives cosmological redshift, $P^0 \propto a^{-1}$, as explained above. Defining $\mu \equiv \gamma^i k_i/k$ and Fourier transforming Eq. (2.63), the first order Vlasov equation in the momentum space is given as

$$\frac{\partial f_k}{\partial t} - \frac{\dot{a}}{a} P^0 \frac{\partial f_k}{\partial P^0} + \frac{ik\mu}{a} f_k = P^0 \frac{\partial \bar{F}}{\partial P^0} \frac{1}{2} \frac{\partial h_k}{\partial t}, \tag{2.64}$$

where we have used

$$h_{ij}(t, \mathbf{x}) = \sum_{\lambda=+,\times} \int \frac{d^3k}{(2\pi)^3} h_{\lambda,k}(t) Q^{\lambda}_{ij}(\mathbf{x}), \tag{2.65}$$

$$\delta F = \sum_{\lambda=+,\times} \int \frac{d^3k}{(2\pi)^3} f_{\lambda,k}(t, P^0, \mu) \gamma^i \gamma^j Q^{\lambda}_{ij}(\mathbf{x}). \tag{2.66}$$

Here, tensor harmonics $Q^{\lambda}_{ij}(\mathbf{x})$ are solutions of the tensor Helmholtz equation; ${Q^{\lambda}_{ij|a}}^{|a}(\mathbf{x}) + k^2 Q^{\lambda}_{ij}(\mathbf{x}) = 0$, $\partial_l Q^{\lambda}_{ij} = ik_l Q^{\lambda}_{ij}$. They are symmetric, traceless, and divergenceless; $Q^{\lambda}_{ij} = Q^{\lambda}_{ji}$, $\gamma^{ij} Q^{\lambda}_{ij} = {Q^{\lambda}_{ij}}^{|j} = 0$, where $\gamma^{ij} \equiv a^2 \bar{g}^{ij}$ and $|$ denotes the covariant derivative with respect to the spatial metric γ^{ij}. Note that Fourier transformation here is the generalization of Eq. (2.4) for arbitrary spatial geometry of the universe. One can treat $Q^{\lambda}_{ij}(\mathbf{x})$ as a plane wave in a flat geometry case.

Due to the existence of the second term on the left-hand side of Eq. (2.64), we cannot solve this equation. Thus following [42], we introduce the comoving momentum, $q^\mu \equiv aP^\mu$. Regarding F as a function of comoving energy, $q \equiv q^0$, and conformal time, τ, the third term in Eq. (2.56) may be replaced by $\frac{dq}{d\tau}\frac{\partial F}{\partial q} = -\frac{1}{2} q h'_{ij} \gamma^i \gamma^j \frac{\partial \bar{F}}{\partial q}$ up to the linear order. Then the linearized Vlasov equation, $\frac{d}{d\tau} F(\tau, x^i, \gamma^i, q) = 0$, becomes

$$\frac{\partial f_k}{\partial \tau} + ik\mu f_k = q \frac{\partial \bar{F}}{\partial q} \frac{1}{2} \frac{\partial h_k}{\partial \tau}, \tag{2.67}$$

where $f_k = f_k(\tau, q, \mu)$. One finds the solution of Eq. (2.67) as

$$f_k(\tau, q, \mu) = e^{-i\mu k(\tau - \tau_{\nu\,\mathrm{dec}})} f_k(\tau_{\nu \mathrm{dec}}, q, \mu) + \frac{q}{2} \frac{\partial \bar{F}}{\partial q} \int_{\tau_{\nu\,\mathrm{dec}}}^{\tau} d\tau' h'_k(\tau') e^{-i\mu k(\tau - \tau')}, \tag{2.68}$$

where the prime on $h_k(\tau)$ denotes the derivative with respect to the conformal time. As there is no primordial tensor perturbations in the neutrino distribution function before neutrino decoupling, $f_k(\tau_{\nu\mathrm{dec}}, q, \mu) = 0$.

The right-hand side of the linearized Einstein equation includes anisotropic stress as in Eq. (2.5);

$$\delta T_{ij}^{(\nu)} = a^2 \sum_{\lambda=+,\times} \int \frac{d^3k}{(2\pi)^3} \Pi_{\lambda,k} Q_{ij}^{\lambda}(\mathbf{x}), \tag{2.69}$$

where $T_{ij}^{(\nu)}$ denotes the stress energy tensor of neutrinos. Since $T_{ij}^{(\nu)} = \frac{1}{\sqrt{-g}} \int \frac{d^3q}{q^0} q_i q_j F(q)$, its perturbation can be expressed as

$$\begin{aligned} \delta T_{ij}^{(\nu)} &= a^{-4} \int \frac{d^3q}{q^0} \left[\bar{q}_i \bar{q}_j \delta F + (\delta q_i \bar{q}_j + \bar{q}_i \delta q_j) \bar{F} \right], \\ \delta F &= \sum_{\lambda=+,\times} \int \frac{d^3k}{(2\pi)^3} f_{\lambda,k}(\tau, q, \mu) \gamma^l \gamma^m Q_{lm}^{\lambda}(\mathbf{x}). \end{aligned} \tag{2.70}$$

The second and the third terms of (2.70) cancel out in linear perturbation theory. Thus

$$\Pi_{\lambda,k} Q_{ij}^{\lambda}(\mathbf{x}) = a^{-4} \int \frac{d^3q}{q^0} q^2 \gamma^i \gamma^j \gamma^l \gamma^m f_{\lambda,k} Q_{lm}^{\lambda}(\mathbf{x}). \tag{2.71}$$

Inserting solution of the Vlasov equation (2.68) into Eq. (2.71) and using equality $\int d\Omega_q \gamma^i \gamma^j \gamma^l \gamma^m e^{-i\hat{\gamma}\cdot\hat{k}u} Q_{lm}^{\lambda} = \frac{1}{8}(\delta^{il}\delta^{jm} + \delta^{im}\delta^{jl}) \int d\Omega_q e^{-i\mu u}(1 - 2\mu^2 + \mu^4) Q_{lm}^{\lambda}$, one obtains

$$\begin{aligned} \Pi_k &= \frac{1}{4a^4} \int d^3q q (1 - 2\mu^2 + \mu^4) f_k, \\ &= -4\bar{\rho}_\nu(\tau) \int_{\tau_{\nu\,\mathrm{dec}}}^{\tau} d\tau' \left(\frac{j_2[k(\tau - \tau')]}{k^2(\tau - \tau')^2} \right) h_k'(\tau'). \end{aligned} \tag{2.72}$$

Here, $\bar{q}_i = aq\gamma^i$ and $\bar{q}^i = a^{-1} q \gamma^i$, and $\bar{\rho}_\nu(\tau) = a^{-4} \int d^3q q \bar{F}(q)$ is the unperturbed neutrino energy density, and a negative sign appears on the right-hand side of Eq. (2.72) because integration by parts has been done. Also, we have used the identity

$$\frac{1}{16}\int_{-1}^{1} d\mu (1-2\mu^2+\mu^4)e^{-i\mu u} = \frac{j_2(u)}{u^2}. \tag{2.73}$$

Note that $\frac{j_2(-u)}{(-u)^2} = \frac{j_2(u)}{u^2}$, $\int_{-\infty}^{\infty} \frac{j_2(u)}{u^2} du = \frac{\pi}{8}$, and $\lim_{u\to 0}\frac{j_2(u)}{u^2} = \frac{1}{15}$.[3]

Then the Einstein-Vlasov equation takes a form of an integro-differential equation;

$$\begin{aligned} h_k''(\tau) + & \left[\frac{2a'(\tau)}{a(\tau)}\right] h_k'(\tau) + k^2 h_k(\tau) \\ & = -24 f_\nu(\tau)\left[\frac{a'(\tau)}{a(\tau)}\right]^2 \int_{\tau_{\nu\ \mathrm{dec}}}^{\tau} d\tau' \left[\frac{j_2[k(\tau-\tau')]}{k^2(\tau-\tau')^2}\right] h_k'(\tau'), \end{aligned} \tag{2.74}$$

and the fraction of the total energy density in neutrinos is

$$\begin{aligned} f_\nu(\tau) & \equiv \frac{\bar\rho_\nu(\tau)}{\bar\rho(\tau)} \\ & = \frac{\Omega_\nu (a_0/a)^4}{\Omega_M (a_0/a)^3 + (\Omega_\gamma+\Omega_\nu)(a_0/a)^4} = \frac{f_\nu(0)}{1+a(\tau)/a_{EQ}}, \end{aligned} \tag{2.75}$$

where

$$f_\nu(0) = \frac{\Omega_\nu}{\Omega_\gamma + \Omega_\nu} = 0.40523. \tag{2.76}$$

The integro-differential equation (2.74) was studied in [30, 44, 45, 46] in the cosmological context. Here we shall solve this equation numerically with all the Standard Model particles participating in the cosmic thermal plasma. Anisotropic stress, Π_k, vanishes during the matter era, as $f_\nu \to 0$. Therefore, the damping effect is unimportant during the matter era.

[3] In the references [30, 45], $K[u] \equiv -\frac{\sin u}{u^3} - \frac{3\cos u}{u^4} + \frac{3\sin u}{u^5} = \frac{1}{15}\left(j_0(u) + \frac{10}{7}j_2(u) + \frac{3}{7}j_4(u)\right)$, which is the same function as our kernel, i.e. $K[u] = \frac{j_2(u)}{u^2}$.

Following [30], we write

$$h_\lambda(u) \equiv h_\lambda(0)\chi(u), \tag{2.77}$$

which gives

$$\chi''(u) + \left[\frac{2a'(u)}{a}\right]\chi'(u) + \chi(u) = -24 f_\nu(u)\left[\frac{a'(u)}{a}\right]^2 \int_{u_{\nu\ \mathrm{dec}}}^{u} dU \left[\frac{j_2(u-U)}{(u-U)^2}\right]\chi'(U), \tag{2.78}$$

where $u \equiv k\tau$, and derivatives are taken with respect to u. After the end of inflation,τ_{end}, the amplitude of cosmological fluctuations is conserved until the mode re-enter the horizon, $h_\lambda(0) = h_{\lambda,\mathbf{k}}(\tau_{\mathrm{end}})$. Note that the right hand side of Eq.(2.78) disappears on the super horizon scales — neutrino free-streaming affects the tensor metric perturbation only inside the horizon. The initial conditions are taken to be

$$\chi(0) = 1, \quad \chi'(0) = 0. \tag{2.79}$$

We solve Eq. (2.78) numerically by two steps; (i) we obtain $a(\tau)$ and $a'(\tau)$ from the Friedman equation (2.85) with $g_*(\tau)$ in Sec. 2.3 [Fig. 2.6], and (ii) we solve Eq. (2.78) with the scale factor that we obtained in the step (i) The numerical solutions as well as analytical solutions are presented and compared in Fig. 2.4. The higher Fourier modes enter the horizon during the radiation era, but after neutrino decoupling. Thus they are damped due to the presence of the right-hand side of Eq. (2.78).

In order to estimate the damping effect, let us consider the radiation era after neutrino decoupling. During the radiation era, $a'(u)/a = 1/u$, the analytical solution is given by $\chi(u) = j_0(u)$ in the absence of neutrino free-streaming in Eq. (2.78). In the presence of neutrino free-streaming, the solution becomes asymptotically ($u \gg 1$)

$$\chi(u) \to A\frac{\sin(u+\delta)}{u}, \tag{2.80}$$

where $A = 0.80313$ and $\delta = 0$ are obtained from our numerical calculations. This asymptotic solution is valid only for rather long wavelength modes which entered the horizon well after the neutrino decoupling. The suppression factor $A^2 = 0.64502$ applies to the gravitational wave spectrum of the modes that entered the horizon after neutrino decoupling but before matter domination.

In order to understand the shape of the spectrum, Figs. 2.7 and 2.8, we need to consider shorter wavelength modes as well. This may be understood as follows. As we saw in Eq. (2.62), if the time derivative of the mode is negative (positive), the mode is damped (amplified). Integrating the amplitude of gravitational waves over time, the net effect of neutrino free-streaming almost always damps gravitational waves. This is because the contribution is mainly from the first period of $\chi'(u)$, where the first trough is larger than the first peak. Therefore, neutrino free-streaming always makes gravitational waves damp regardless of their frequencies. Note that this feature is generic to any kinds of free-streaming particles, but not realistic for neutrinos as we mentioned in Sec. 2.4.

For extremely short wavelength modes which have already been inside the horizon before neutrino decoupling, $k\tau_{\nu\mathrm{dec}} \gg 1$ or $k > 10^{-9}$ Hz, the suppression becomes negligibly small; $A \to 1$, but the phase delay, δ, is non-zero. These modes are undamped as positive and negative contributions of χ' to the gravitational wave energy cancel out each other after several periods of χ'. No net energy conversion from gravitational waves to free-streaming neutrinos would occur.

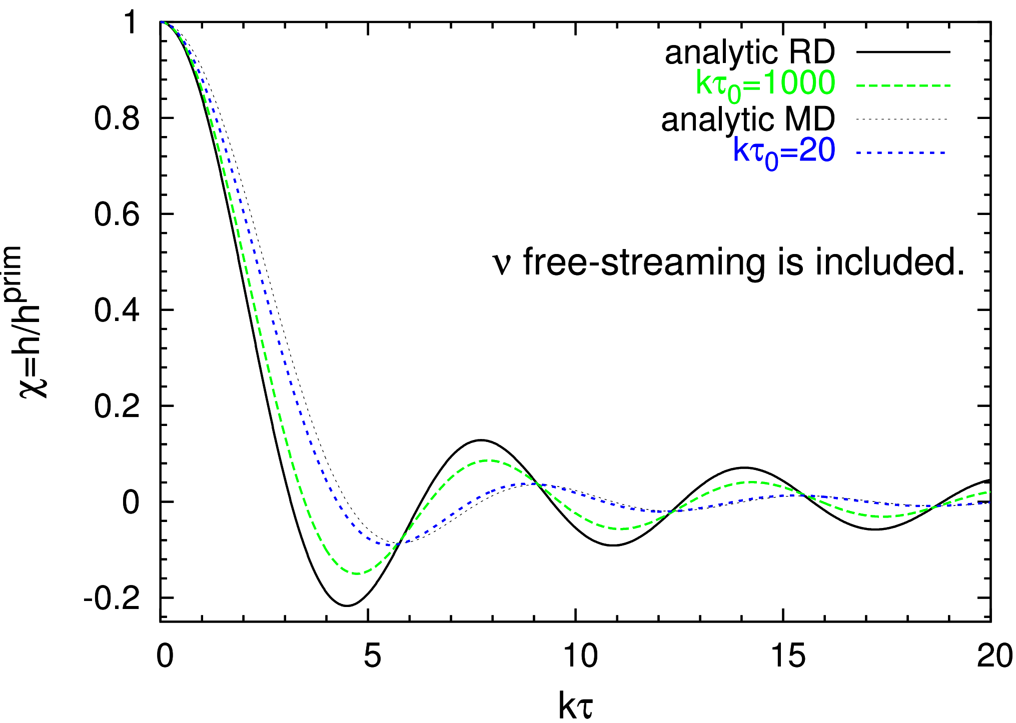

Figure 2.4: Comparison between numerical solutions and analytical solutions of tensor perturbations. The effect of neutrino free-streaming is included for numerical solutions, but not for analytical solutions. The dashed and short-dashed lines show numerical solutions of the high and low frequency modes, respectively. The higher k-modes enter the horizon during the radiation era after neutrino decoupling, and thus the numerical solution is damped by neutrino free-streaming compared to the analytical solution, $\chi(k\tau) = j_0(k\tau)$ (solid line). On the other hand, the lower k-modes enter the horizon much later, and thus the numerical solution is closer to the analytical solution during the matter era, $\chi(k\tau) = 3j_1(k\tau)/k\tau$ (dotted line).

2.3 The effective relativistic degrees of freedom: g_*

It is often taken for granted that energy density of the universe evolves as $\rho \propto a^{-4}$ during the radiation era. This is exactly what caused a scale invariant spectrum of $\Omega_h(k)$ at $k > k_{\rm eq}$. However, $\rho \propto a^{-4}$ does not always hold even during the radiation era, as some particles would become non-relativistic before the others and stop contributing to the radiation energy density.

During the radiation era many kinds of particles interacted with photons frequently so that they were in thermal equilibrium. In an adiabatic system, the entropy per unit comoving volume must be conserved [53];

$$S(T) = s(T)a^3(T) = constant, \tag{2.81}$$

where

$$s(T) = \frac{2\pi^2}{45} g_{*s}(T)T^3.$$

The entropy density, $s(T)$, is given by the energy density and pressure; $s = (\rho+p)/T$. The energy density and pressure in such a plasma-dominant universe are given by

$$\rho(T) = \frac{\pi^2}{30} g_*(T)T^4, \tag{2.82}$$

$$p(T) = \frac{1}{3}\rho(T), \tag{2.83}$$

respectively, where we have defined the "effective number of relativistic degrees of freedom", g_* and g_{*s}, following [53]. These quantities, g_* and g_{*s}, count the (effective) number of relativistic species contributing to the radiation energy density and entropy, respectively. One may call either (or both) of the two the effective number of relativistic degrees of freedom. Equation (2.81) and (2.82) immediately imply that energy density of the universe during the radiation era should evolve as

$$\rho \propto g_* g_{*s}^{-4/3} a^{-4}. \tag{2.84}$$

Therefore, unless g_* and g_{*s} are independent of time, the evolution of ρ would deviate from $\rho \propto a^{-4}$. In other words, the evolution of ρ during the radiation era is sensitive to how many relativistic species the universe had at a given epoch. As the wave equation of gravitational waves contains $(a'/a)h'_{\lambda,k}$, the solution of $h_{\lambda,k}$ would be affected by g_* and g_{*s} via the Friedman equation:

$$\frac{a'(\tau)}{a^2} = H_0 \sqrt{\left(\frac{g_*}{g_{*0}}\right)\left(\frac{g_{*s}}{g_{*s0}}\right)^{-4/3} \Omega_r \left(\frac{a}{a_0}\right)^{-4} + \Omega_m \left(\frac{a}{a_0}\right)^{-3}}. \tag{2.85}$$

Although the interaction rate among particles and antiparticles is assumed to be fast enough (compared with the expansion rate) to keep them in thermal equilibrium, the interaction is assumed to be weak enough for them to be treated as ideal gases. In the case of an ideal gas at temperature T, each particle species of a given mass, $m_i = x_i T$, would contribute to g_* and g_{*s} the amount given by

$$g_{*,i}(T) = g_i \frac{15}{\pi^4} \int_{x_i}^{\infty} \frac{(u^2 - x_i^2)^{1/2}}{e^u \pm 1} u^2 du, \tag{2.86}$$

$$g_{*s,i}(T) = g_i \frac{15}{\pi^4} \int_{x_i}^{\infty} \frac{(u^2 - x_i^2)^{1/2}}{e^u \pm 1} (u^2 - \frac{x_i^2}{4}) du, \tag{2.87}$$

where the sign is $-$ for bosons and $+$ for fermions.

Here, g_i is the number of helicity states of the particle and antiparticle. Note that an integral variable is defined as $u \equiv E/T$, where $E = \sqrt{|\mathbf{p}|^2 + m^2}$. We assume that the chemical potential, μ_i, is negligible. One might also define a similar quantity for the number density,

$$n(T) = \frac{\zeta(3)}{\pi^2} g_{*n} T^3, \tag{2.88}$$

Table 2.1: Particles in the Standard Model and their mass and helicity states

particle	rest mass [MeV]	the number of helicity states: g_i
γ	0	2
ν,$\bar{\nu}$	0	6
e^+,e^-	0.51	4
μ^+,μ^-	106	4
π^+,π^-	135	2
π^0	140	1
$gluons$	0	16
u,$\bar{u}$	5	12
d,$\bar{d}$	9	12
s,$\bar{s}$	115	12
c,$\bar{c}$	1.3×10^3	12
τ^+,τ^-	1.8×10^3	4
b,$\bar{b}$	4.4×10^3	12
W^+,W^-	80×10^3	6
Z	91×10^3	3
H	114×10^3	1
t,$\bar{t}$	174×10^3	12
SUSY particles	$\sim 1 \times 10^6$	~ 110

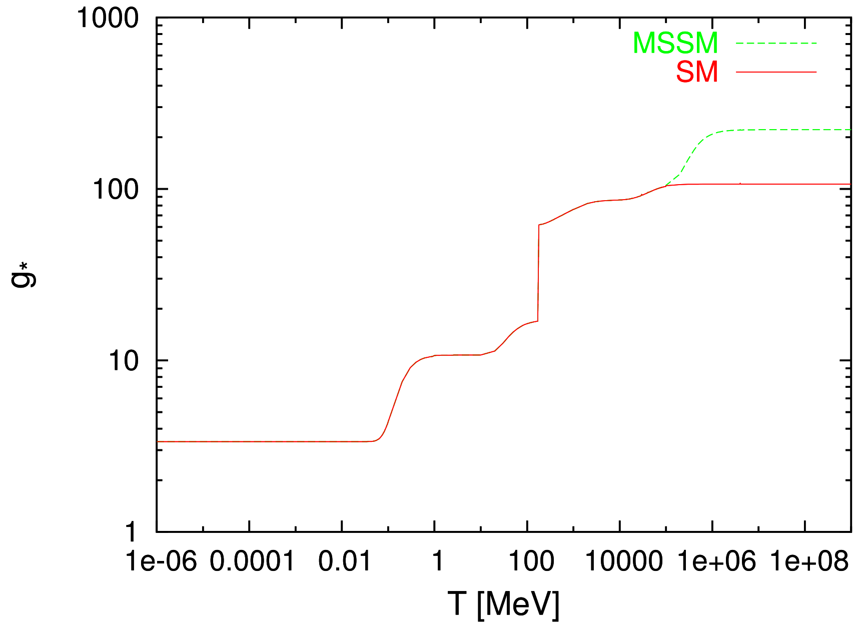

Figure 2.5: Evolution of the effective number of relativistic degrees of freedom contributing to energy density, g_*, as a function of temperature. The solid and dashed lines represent g_* in the Standard Model and in the minimal extension of Standard Model, respectively. At the energy scales above ~ 1 TeV, $g_*^{\rm SM} = 106.75$ and $g_*^{\rm MSSM} \simeq 220$. At the energy scales below ~ 0.1 MeV, $g_* = 3.3626$ and $g_{*s} = 3.9091$; $g_* = g_{*s}$ otherwise.

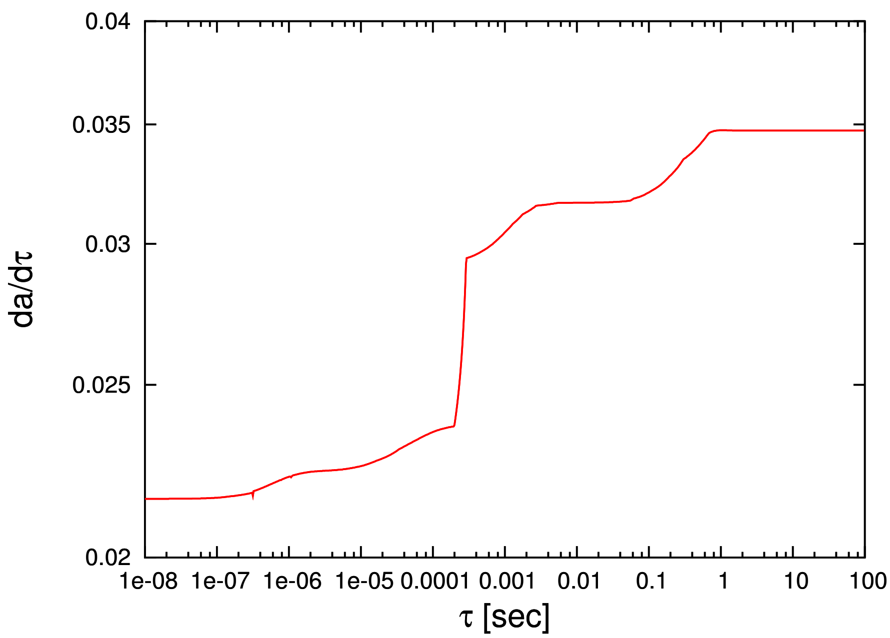

Figure 2.6: Evolution of a' as a function of the conformal time. If g_* and g_{*s} were constant, $\rho \propto a^{-4}$ and a' would also be constant.

where $\zeta(3) \simeq 1.20206$ is the Riemann zeta function of 3. Each species would contribute to g_{*n} by

$$g_{*n,i}(T) = g_i \frac{1}{2\zeta(3)} \int_{x_i}^{\infty} \frac{(u^2 - x_i^2)^{1/2}}{e^u \pm 1} u du. \tag{2.89}$$

The effective number relativistic degrees of freedom is then given by the temperature-weighted sum of all particle contributions:

$$\begin{aligned} g_*(T) &= \sum_i g_{*,i}(T) \left(\frac{T_i}{T}\right)^4, \\ g_{*s}(T) &= \sum_i g_{*s,i}(T) \left(\frac{T_i}{T}\right)^3, \\ g_{*n}(T) &= \sum_i g_{*n,i}(T) \left(\frac{T_i}{T}\right)^3, \end{aligned} \tag{2.90}$$

where we have taken into account the possibility that each species i may have a thermal distribution with a different temperature from that of photons. The most famous example is neutrinos: $T_\nu = \left(\frac{4}{11}\right)^{1/3} T_\gamma$. Neutrinos are cooler than photons at temperatures below MeV scale due to photon heating from electron-positron annihilation.

Fig. 2.5 shows the evolution of g_* as a function of temperature. We have included all the particles in the Standard Model of elementary particles, as listed in table 2.1. (Note that we assume that the mass of Higgs bosons is 114 GeV, which is the current lower bound from experiments.) We neglected hadrons whose mass is heavier than pions. In addition to the particles in the Standard Model, one may also include particles in supersymmetric models. Superpartners in the minimal extension of supersymmetric Standard Model (MSSM) would carry almost the same g_* as that carried by particles within the Standard Model. Fig. 2.6 shows the evolution of a'. If g_* and g_{*s} were constant, a' would also be constant during the radiation era; however, the evolution of a' reveals a series of jumps due to the change in g_* and g_{*s}.

Interactions between particles would change the ideal gas result obtained above, and one cannot use equation (2.86), (2.87) and (2.90) to calculate g_* or g_{*s}. Instead, one needs to extract g_* and g_{*s} directly from energy density and entropy which would be calculated using detailed numerical simulations of particle interactions. For example, above the critical temperature of Quark Gluon Plasma (QGP) phase transition, most of g_* is carried by color degrees of freedom. The dominant correction therefore comes from the colored sector of the Standard Model, whereas corrections from the weak charged sector are suppressed by the masses of weak gauge bosons. Since physics of QCD correction is still uncertain and beyond the scope of this chapter, we shall ignore this effect and treat it as an ideal gas case. The effects of particle interactions on g_* have been investigated by [27, 54, 55].

2.3.1 Heuristic argument based on background density

Before presenting the full numerical results, let us briefly describe how g_* and g_{*s} would affect the shape of $\Omega_h(\tau_0, k)$. In Sec. 2.2, we discussed how the expansion of the universe would affect $\Omega_h(\tau_0, k)$. While energy density of the universe during the radiation era is affected by g_* and g_{*s} as $\rho_{\rm cr} \propto g_* g_{*s}^{-4/3} a^{-4}$, energy density of gravitational waves always evolves as $\tilde{\rho}_h(\tau, k) \propto a^{-4}$ inside the horizon, $k \gg aH$, regardless of g_* or g_{*s}. (Gravitons are not in thermal equilibrium with other particles.) This difference in the evolution of $\tilde{\rho}_h$ and $\rho_{\rm cr}$ significantly modifies a scale-invariant spectrum of $\Omega_h(\tau_0, k)$ at $k > k_{\rm eq}$.

Let us consider a gravitational wave mode with k which entered the horizon at a given time, $\tau_{\rm hc} < \tau_{\rm eq}$ and temperature, $T = T_{\rm hc}$, during the radiation era. After the mode entered the horizon the amplitude of this mode would be suppressed by the cosmological redshift. The relative spectral density at present would then be given by

$$\Omega_h(\tau_0, k > k_{\rm eq}) \quad = \quad \Omega_h(\tau_{\rm hc}, k)\Omega_{r0}\left[\frac{g_{*s}(T_{\rm hc})}{g_{*s0}}\right]^{-4/3}\left[\frac{g_*(T_{\rm hc})}{g_{*0}}\right], \tag{2.91}$$

where Ω_r denotes the relative energy density of radiation and the subscript "0" denotes the present-day value. This equation helps us understand how g_* and g_{*s} would affect $\Omega_h(\tau_0, k)$. For a given wavenumber, k, there would be one horizon-crossing epoch, $\tau_{\rm hc}$. The amount by which the relative spectral energy density of that mode would be suppressed depends on g_* and g_{*s} at $\tau_{\rm hc}$. The mode that entered the horizon earlier should experience larger suppression, as g_* and g_{*s} would be larger than those for the mode that entered the horizon later. (The effective number of relativistic degrees of freedom is larger at earlier times — see Figure 2.5.) As g_* and g_{*s} are equal for $T \gtrsim 0.1$ MeV and nearly the same otherwise ($g_* = 3.3626$ and $g_{*s} = 3.9091$ for $T \lesssim 0.1$ MeV), we expect that suppression factor is given by $(g_*/g_{*0})^{-1/3}$ to a good approximation. The modes that entered the horizon during the matter era should not be affected by g_* or g_{*s}, as they do not change during the matter era.

2.3.2 More rigorous argument using analytical solutions

In this subsection we derive equation (2.91) using a more rigorous approach. Let us go back to the wave equation [Eq. (2.9)], and rewrite it using a new field variable, $\mu_k \equiv ah_k$:

$$\mu_k'' + \left(k^2 - \frac{a''}{a}\right)\mu_k = 16\pi G a^3 \Pi_k. \tag{2.92}$$

Note that we have suppressed the subscript for polarization, λ. To find a solution for μ_k, we must solve the Friedman equation as well:

$$\begin{aligned}\left(\frac{a'}{a^2}\right)^2 &= \frac{8\pi G}{3}\rho_r = H_0^2\frac{g_*}{g_{*0}}\left(\frac{g_{*s}}{g_{*s0}}\right)^{-4/3}\left(\frac{a}{a_0}\right)^{-4} \\ \frac{a'}{a^2} &= H_0\left(\frac{g_*}{g_{*0}}\right)^{1/2}\left(\frac{g_{*s}}{g_{*s0}}\right)^{-2/3}\left(\frac{a}{a_0}\right)^{-2} \\ \frac{a-a_0}{a_0} &= a_0H_0\int_{\tau_0}^{\tau}d\tau'\left(\frac{g_*}{g_{*0}}\right)^{1/2}\left(\frac{g_*}{g_{*0}}\right)^{-2/3},\end{aligned} \tag{2.93}$$

where the subscript "0" denotes some reference epoch during the radiation era. (While "0" means the present epoch in the other sections, we use it to mean some epoch during the radiation era in this section only.) To proceed further, we need to specify the evolution of g_* and g_{*s}. While we have numerical data for the evolution of these quantities, we make an approximation here to make the problem analytically solvable. Since $g_*(\tau)$ decreases monotonically as the universe expands, one may try a reasonable *ansatz*, $g_* \propto \tau^{-6n}$, to obtain analytical solutions. We shall also assume $g_* = g_{*s}$ and $\Pi_k = 0$ for simplicity in this section. (At temperatures below 2 MeV, free-streaming of neutrinos generates anisotropic stress, $\Pi_k \neq 0$. Also, the temperature of neutrinos is different from that of photons below electron-positron annihilation temperature, and thus $g_* \neq g_{*s}$ below ~ 0.51 MeV.) This model gives

$$\frac{a''}{a} \simeq \frac{g_*^{-7/6}\mid g_*'\mid}{6\int_{\tau_0}^{\tau}d\tau' g_*^{-1/6}} \simeq \frac{n}{\tau^2}\left(1+n\right), \tag{2.94}$$

where the primes denote derivatives with respect to τ, and the term $\frac{n}{\tau_0^2}(1+n)$ has been neglected in the last line, assuming $\tau \ll \tau_0$. This form of a''/a allows us to find an analytical solution to equation (2.92):

$$h_k(\tau) = \frac{\mu_k(\tau)}{a} = A(k)\frac{j_n(k\tau)}{(k\tau)^n} + B(k)\frac{y_n(k\tau)}{(k\tau)^n}, \tag{2.95}$$

where $A(k)$ and $B(k)$ are the normalization constants that should be determined by the appropriate boundary conditions. Note that $n = 0$ and $n = 1$ correspond to the solutions for the radiation era and the matter era, respectively.

Let us consider a model of the radiation-dominated universe in which there was a brief period of time during which g_* suddenly decreased as a power-law in time, $g_* \propto \tau^{-6n}$. Outside of this period g_* is a constant. Suppose that g_* changed between $\tau = \tau_2$ and $\tau_1 > \tau_2$. (The change in g_* began at $\tau = \tau_2$ and completed at τ_1.) The modes that entered the horizon after τ_1 do not know anything about the change in g_*. The solution for such modes is therefore given by the usual solution during the radiation era,

$$h_k^{\rm out}(\tau) \quad = \quad h_k^{prim} j_0(k\tau). \tag{2.96}$$

How about the modes that entered the horizon before τ_2? The solution for such modes is given by

$$\begin{aligned}
h_k^{\rm in}(\tau) &= h_k^{prim} j_0(k\tau) & (\tau < \tau_2), \quad & (2.97)\\
h_k^{\rm in}(\tau) &= \frac{h_k^{prim}}{(k\tau)^n}[A(k)j_n(k\tau) + B(k)y_n(k\tau)] & (\tau_2 < \tau < \tau_1), \quad & (2.98)\\
h_k^{\rm in}(\tau) &= h_k^{prim}\left(\frac{\tau_2}{\tau_1}\right)^n [C(k)j_0(k\tau) + D(k)y_0(k\tau)] & (\tau_1 < \tau). \quad & (2.99)
\end{aligned}$$

It is convenient to define $\tau_* \equiv (\tau_1 + \tau_2)/2$ and $\Delta\tau \equiv \tau_1 - \tau_2$ to characterize the time of transition and its duration, respectively. Here, the superscript "in" denotes the modes that have already been *inside* the horizon at τ_*, while "out" denotes the modes that are still *outside* the horizon at τ_*. The coefficients, $A(k)$, $B(k)$, $C(k)$, and $D(k)$, are given by Eqs. (2.105) – (2.108) in subsection 2.4.1. By taking a ratio of equation (2.99) and (2.96), we can find the amount of suppression in $h_k^{\rm in}(\tau > \tau_1)$

relative to $h_k^{\rm out}(\tau > \tau_1)$:

$$
\begin{aligned}
\frac{h_k^{\rm in}(\tau > \tau_1)}{h_k^{\rm out}(\tau > \tau_1)} &= \left(\frac{\tau_2}{\tau_1}\right)^n [C(k) + D(k) y_0(k\tau)/j_0(k\tau)] \\
&\approx \left(\frac{\tau_2}{\tau_1}\right)^n [C(k) + D(k)], \qquad (2.100)
\end{aligned}
$$

where we have ignored the oscillatory part of $y_0(k\tau)/j_0(k\tau)$. While $C(k)$ and $D(k)$ have fairly cumbersome expressions, the sum of the two has a simple limit, $[C(k) + D(k)]^2 \to 1$, for $\Delta\tau \to 0$, regardless of the value of n (see subsection 2.4.1). The energy density in gravitational waves then reflects the effect from the change of g_* as

$$
\frac{\Omega_h^{\rm in}(\tau > \tau_1, k)}{\Omega_h^{\rm out}(\tau > \tau_1, k)} \approx \left[\frac{h_k^{\rm in}(\tau > \tau_1)}{h_k^{\rm out}(\tau > \tau_1)}\right]^2 \approx 1 - 2n\frac{\Delta\tau}{\tau_1}, \qquad (2.101)
$$

where we have used the sub-horizon limit for $\Omega_h(k)$ and $\Delta\tau \ll \tau_2 < \tau_* < \tau_1$. On the other hand, $g_* \propto \tau^{-6n}$ gives

$$
\frac{g_*^{\rm in}}{g_*^{\rm out}} \equiv \frac{g_*(\tau_2)}{g_*(\tau_1)} = \left(\frac{\tau_* - \Delta\tau/2}{\tau_* + \Delta\tau/2}\right)^{-6n} \approx 1 + 6n\frac{\Delta\tau}{\tau_*}. \qquad (2.102)
$$

Hence, combining Eqs.(2.101) and (2.102), we finally obtain the desired result

$$
\frac{\Omega_h^{\rm in}(k)}{\Omega_h^{\rm out}(k)} \approx \left(\frac{g_*^{\rm in}}{g_*^{\rm out}}\right)^{-1/3}, \qquad (2.103)
$$

for $\Delta\tau \ll \tau_*$. This result agrees with equation (2.91), which was obtained in the previous section (Sec. 2.3.1) using a more heuristic argument. (Note that we have assumed $g_* = g_{*s}$ in this section). In Eq. (2.91) there is an extra factor Ω_{r0}, which represents the time evolution of Ω_h from matter-radiation equality to the present epoch. We do not have this factor in equation (2.103), as both $\Omega_h^{\rm in}$ and $\Omega_h^{\rm out}$ are evaluated during the radiation era.

2.4 Prediction for Energy Density of Gravitational Waves from the Standard Model and beyond

In Sec. 2.3 we have described how the evolution of the effective number of relativistic degrees of freedom would affect the shape of relative spectral energy density of primordial gravitational waves at present, $\Omega_h(\tau_0, k)$. In this section we present the full calculation of $\Omega_h(\tau_0, k)$, numerically integrating the wave equation together with the numerical data of g_* and g_{*s} (see Figure 2.5).

Before we do this, there is another effect that one must take into account. While we have ignored anisotropic stress on the right hand side of the wave equation (2.9) so far, free-streaming of relativistic neutrinos which have decoupled from thermal equilibrium at $T \lesssim 2$ MeV significantly contributes to anisotropic stress, damping the amplitude of primordial gravitational waves [30, 44]. Calculations given in subsection 2.2.3 show that neutrino anisotropic stress damps $\Omega_h(\tau_0, k)$ by 35.5% in the frequency region between $\simeq 10^{-16}$ and $\simeq 2 \times 10^{-10}$ Hz. The damping effect is much less significant below 10^{-16} Hz, as this frequency region probes the universe that is dominated by matter. One may understand this by looking at the right hand side of Eq. (2.74). Anisotropic stress is proportional to the fraction of the total energy density in neutrinos, $f_\nu(\tau)$, which is very small when the universe is matter dominated.

We show the results of full numerical integration in Figs. 2.7 and 2.8. The latter figure is just a zoom-up of interesting features in the former one. We find that $\Omega_h(\tau_0, k)$ oscillates very rapidly as $\sin^2(k\tau + \varphi)$, where φ is a phase constant. The cross term, $\sin k\tau \cos k\tau$, appeared as a beat in Fig. 2.1, while they are too small to see in Fig 2.7. From observational point of view these oscillations will not be detectable, as observations are only sensitive to the average power over a few decades in frequency.

The damping effect due to neutrino free-streaming is evident below $2 \times$

10^{-10} Hz. We implicitly assumed an instantaneous decoupling of neutrinos from the thermal plasma at $T_{\nu\,\rm dec} = 2$ MeV, which resulted in the *surface* of decoupling that is extremely thin. Physically speaking, however, the last scattering surface of neutrinos is very thick, unlike for photons. (There is no "recombination" for neutrinos.) In principle, one would need to solve the Boltzmann equation for neutrinos separately, including the effect of neutrino decoupling. Note that there was a minor wiggly feature at around 5×10^{-10} Hz in [1]. Carefully evaluating the anisotropic stress term, this wiggly feature does not exist.[4] We have correctly reevaluated the source term in Figs. 2.7 and 2.8.

The effect of evolution of g_* and g_{*s} is also quite prominent. For example, big changes in g_* would occur at the electron-positron annihilation epoch, ~ 0.51 MeV ($\sim 2 \times 10^{-11}$ Hz), as well as at the QGP to hadron gas phase transition epoch, $\sim$ 180 MeV ($\sim 10^{-7}$ Hz) within the Standard Model. The gravitational wave spectrum is suppressed by roughly 20% and 30% above the electron-positron annihilation and QGP phase transition scale, respectively. If supersymmetry existed above a certain energy scale, e.g., $\sim$ 1 TeV ($\sim 1 \times 10^{-4}$Hz), the spectrum would be suppressed by at least $\sim$ 20% (for N=1 supersymmetry) above that frequency. We also find additional features at the QGP phase transition scale, $\sim 10^{-7}$ Hz, similar to the features at $\sim 5\times10^{-10}$ Hz caused by our assumption about instantaneous decoupling of neutrinos. The feature at the QGP phase transition is nevertheless not artificial — as the QGP phase transition is expected to have happened in a short time period, the instantaneous transition would be a good approximation, unlike for neutrinos.

One may approximately relate the horizon crossing temperature of the universe to the frequency of the gravitational waves [24, 57]. The horizon crossing mode, $k_{\rm hc} = a_{\rm hc}H_{\rm hc}$, is related to the temperature at that time by $H^2_{\rm hc} = \frac{8\pi^3 G}{90} g_{*,\rm hc} T^4_{\rm hc}$. Then using entropy conservation, $g_{*s,\rm hc} a^3_{\rm hc} T^3_{\rm hc} = g_{*s0} a^3_0 T^3_0$, one obtains the following

[4] We thank S. Kuroyanagi for pointing this out. See Appendix C in the published version of [56].

conversion factor from the temperature of the universe to the frequency of gravitational waves observed today:

$$f_0 = 1.65 \times 2\pi \times 10^{-7} \left(\frac{T_{\rm hc}}{1\rm GeV}\right) \left[\frac{g_{*s}(T_{\rm hc})}{100}\right]^{-1/3} \left[\frac{g_*(T_{\rm hc})}{100}\right]^{1/2} \rm Hz, \tag{2.104}$$

which was derived in [24, 57]. (If we take $\epsilon \equiv \frac{1}{2\pi}$ in [57], their equation (156) agrees with the one above.) Throughout this chapter we have been using the comoving wavenumber, k (or kc in units of Hertz), which is related to the conventional frequency by $2\pi f_0 = kc/a_0$, where a_0 is the present-day scale factor and c is the speed of light. We use k in this chapter, rather than f_0, as k is what enters into the wave equation that we solve numerically.

2.4.1 Oscillation due to drastic change of $g_*(\tau)$

In this subsection we explain the effect on the gravitational wave spectrum from a sudden change in the number of relativistic species, g_*. To do this, we need to calculate $\Omega_h^{\rm out}(k_2)/\Omega_h^{\rm in}(k_1)$, where $k_2 \neq k_1$. In Sec. 2.4 we have already seen the numerical prediction of the gravitational wave spectrum. In subsection 2.3.2 we provided the way to understand the relative suppression of gravitational waves at a given k $(= k_1 = k_2)$ with and without changes in g_*. We shall discuss in a similar way what would happen to different Fourier modes, in order to fully understand imprints of g_* on the spectrum, such as oscillations, which are from cosmological events that change g_* instantaneously or drastically.

In Fig. 2.8 we find an oscillatory feature at around 10^{-7} Hz, which corresponds to the mode entering the horizon at the QGP phase transition. At this energy scale, $\sim$ 180 MeV, the effective number of relativistic species changes drastically, giving a sharp feature and oscillation in Ω_h. To understand this, let us consider the simple analytical model employed in subsection 2.3.2. Eq. (2.99) is the mode which

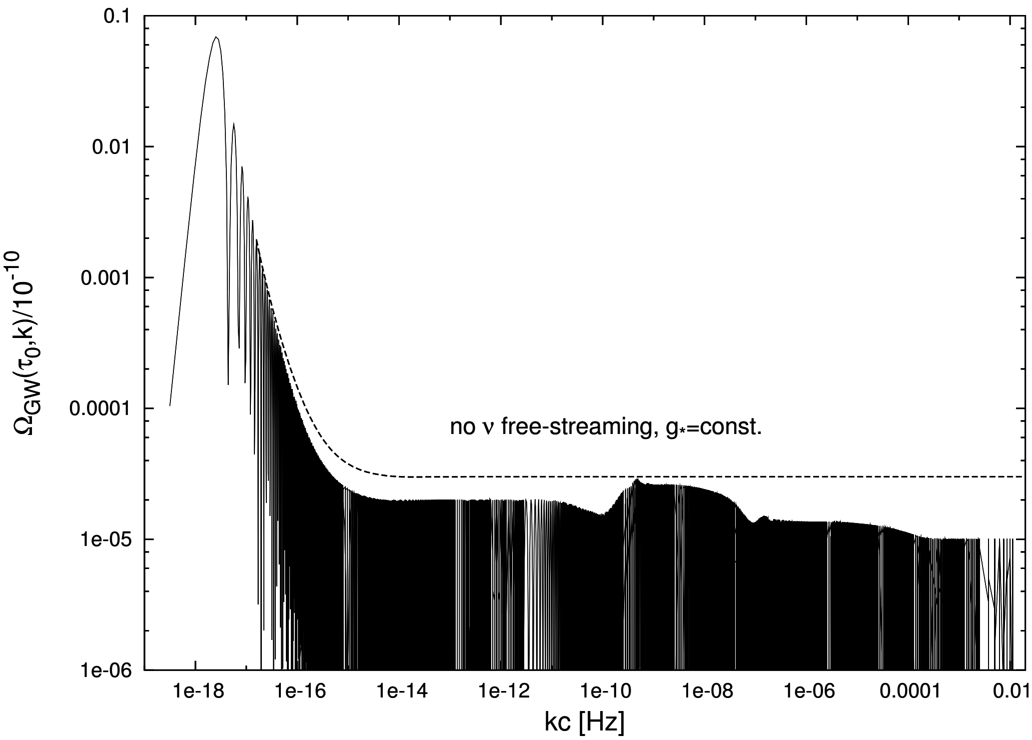

Figure 2.7: The primordial gravitational wave spectrum at present, $\Omega_h(\tau_0, k)/10^{-10}$, as a function of the comoving wavenumber, k (or kc in units of Hertz). The frequency of gravitational waves observed today is related to k by $f_0 = kc/2\pi$. We have assumed a scale-invariant primordial spectrum and $\Omega_m = 1 - \Omega_r$, $\Omega_r = 4.15 \times 10^{-5}h^{-2}$, $h = 0.7$, and $E_{\rm inf} = 10^{16}$ GeV. We have included the effects of the effective number of relativistic degrees of freedom and neutrino free-streaming. The dashed line shows the envelope of the previous calculations which ignored the change in the number of relativistic degrees of freedom and neutrino free-streaming (Fig. 2.1).

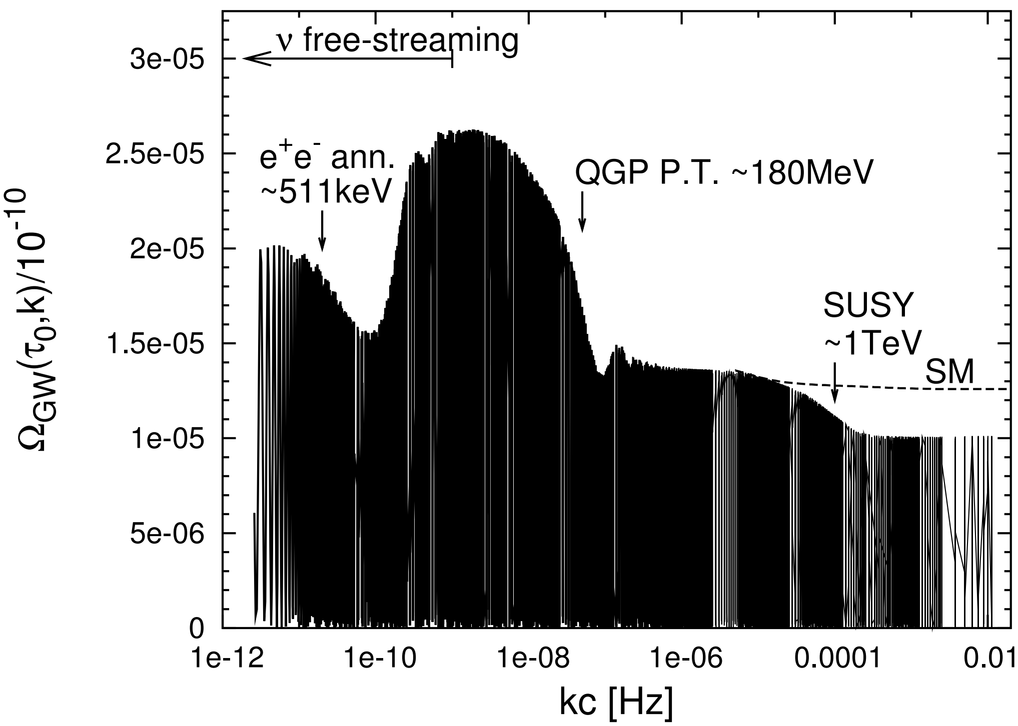

Figure 2.8: A blow-up of Fig. 2.7. Note that density of vertical lines shows density of sampling points at which we evaluate $\Omega_h(\tau_0, k)$. The dashed line shows the envelope of the spectrum in the Standard Model of elementary particles.

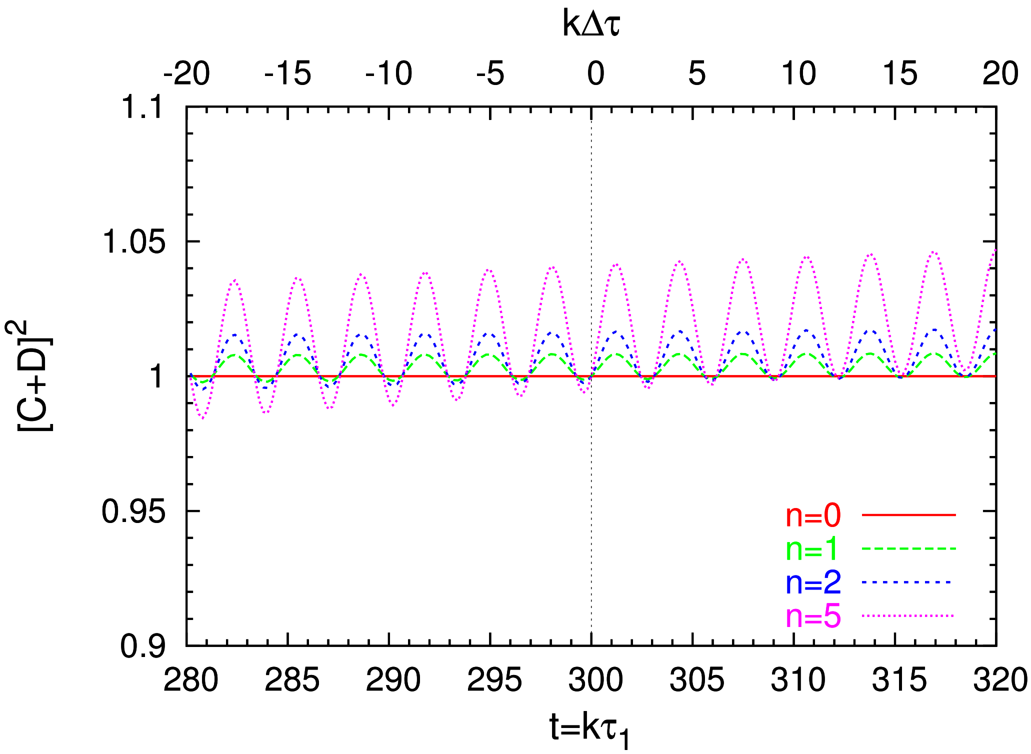

Figure 2.9: The oscillatory factor $[C+D]^2$ with respect to $t \equiv k\tau_1$. The vertical line indicates $s \equiv k\tau_2 = 300 \leq t$ and $\Delta\tau \equiv \tau_1 - \tau_2 = 0$. The solid, dashed, short-dashed, and dotted lines show $n = 0, 1, 2$, and 5 respectively. The factor, $[C+D]^2$, takes on unity at $\Delta\tau \to 0$ regardless of n.

experienced such a change of g_* and its coefficients A, B, C, and D are

$$A(s,n) = \frac{\pi}{4s^{3/2}}\Big[-2sY_{1+\sqrt{1+4n}/2}(s)\sin s + Y_{\sqrt{1+4n}/2}(s)\left(-2s\cos s + (3+\sqrt{1+4n})\sin s\right)\Big], \tag{2.105}$$

$$B(s,n) = -\frac{\pi}{4s^{3/2}}\Big[-2sJ_{1+\sqrt{1+4n}/2}(s)\sin s + J_{\sqrt{1+4n}/2}(s)\left(-2s\cos s + (3+\sqrt{1+4n})\sin s\right)\Big], \tag{2.106}$$

$$\begin{aligned} C(s,t,n) = {} & \\ & \frac{\pi}{4\sqrt{st}}\sec n\pi\Big[-2tJ_{-n-3/2}(t)\cos t\left(J_{n+1/2}(s)(s\cos s - \sin s) + sJ_{n+3/2}(s)\sin s\right) \\ & -2J_{-n-1/2}(t)\left(J_{n+1/2}(s)(s\cos s - \sin s) + sJ_{n+3/2}(s)\sin s\right)(\cos t + t\sin t) \\ & +2\left(J_{-n-1/2}(s)(s\cos s - \sin s) - sJ_{-n-3/2}(s)\sin s\right) \\ & \left(-tJ_{n+3/2}(t)\cos t + J_{n+1/2}(t)(\cos t + t\sin t)\right)\Big], \end{aligned} \tag{2.107}$$

$$\begin{aligned} D(s,t,n) = {} & \\ & \frac{\pi}{4\sqrt{st}}\sec n\pi\Big[2tJ_{n+1/2}(t)\cos t\left(J_{-n-1/2}(s)(-s\cos s + \sin s) + sJ_{-n-3/2}(s)\sin s\right) \\ & -2J_{-n-1/2}(t)\left(J_{n+1/2}(s)(s\cos s - \sin s) + sJ_{n+3/2}(s)\sin s\right)(t\cos t - \sin t) \\ & -2\sin t\Big(tJ_{-n-3/2}(t)\left(J_{n+1/2}(s)(s\cos s - \sin s) + sJ_{n+3/2}(s)\sin s\right) \\ & + \left(-tJ_{n+3/2}(t)\cos t + J_{n+1/2}(t)\right)\left(sJ_{-n-3/2}(s)\sin s + J_{-n-1/2}(s)(-s\cos s + \sin s)\right)\Big)\Big], \end{aligned} \tag{2.108}$$

where $s \equiv k\tau_2$, $t \equiv k\tau_1$ and $s \leq t$. Here, $J_n(x)$ and $Y_n(x)$ are the Bessel function and Neumann function, respectively. At this time, we are interested in different

k-modes, $k_1 < k_2$. (However we evaluate $\Omega_h(k)$ at the same time, τ.) We obtain

$$
\begin{aligned}
\frac{\Omega^{\rm in}(k_2)}{\Omega^{\rm out}(k_1)} &\simeq \frac{k_2^2 h^2(k_2\tau)}{k_1^2 h^2(k_1\tau)} \\
&= \left(\frac{k_2}{k_1}\right)^2 \left(\frac{\tau_2}{\tau_1}\right)^{2n} \left[C(k_2)\frac{j_0(k_2\tau)}{j_0(k_1\tau)} + D(k_2)\frac{y_0(k_2\tau)}{j_0(k_1\tau)}\right]^2 \\
&\approx \left(\frac{k_2}{k_1}\right)^2 \left(\frac{\tau_2}{\tau_1}\right)^{2n} \left[C(k_2)\frac{k_1}{k_2} + D(k_2)\frac{k_1}{k_2}\right]^2 \\
&= \left(\frac{\tau_2}{\tau_1}\right)^{2n} [C(k_2) + D(k_2)]^2 \qquad (2.109) \\
&\to \left(\frac{\tau_2}{\tau_1}\right)^{2n} = \left(\frac{s}{t}\right)^{2n}, \qquad (2.110)
\end{aligned}
$$

where $\simeq$ denotes the subhorizon limit, $\approx$ denotes the asymptotic limit as $k\tau \to$large, and $\to$ denotes the limit in $\Delta k \equiv k_2 - k_1 \to 0$. Eq. (2.109) tells us the exact ratio between different k-modes. While we obtained only the suppression factor, $(\tau_2/\tau_1)^{2n}$, in subsection 2.3.2, we now also obtain the oscillatory factor, $[C + D]^2$. Fig. 2.9 shows that the factor, $[C + D]^2$, oscillates and takes on unity at $\Delta\tau \to 0$ regardless of n. Here, $n = 5$ represents $g_* \propto \tau^{-30}$, which is an extremely drastic change. This gives us a complete analytical account of the shape of Fig. 2.8.

2.5 Discussion and Conclusion

We have calculated the primordial gravitational wave spectrum, fully taking into account the evolution of the effective relativistic degrees of freedom and neutrino free-streaming, which were ignored in the previous calculations. The formalism and results given in this chapter are based on solid physics and can be extended to primordial gravitational waves produced in any inflationary models and high energy particle physics models. As is seen in Figs. 2.7 and 2.8, the spectrum is no longer scale invariant, but has complex features in it. Whatever physics during inflation is, one must include the evolution of the effective relativistic degrees of freedom and neutrino free-streaming.

Schwarz [25, 26] studied the gravitational wave spectrum at the QGP phase transition assuming the first order instantaneous model as well as the second order cross-over model, and found 30% suppression of the energy density spectrum, which is consistent with our calculation. Seto and Yokoyama [58] studied the effect of entropy production from e.g., decay of massive particles in the early universe on the energy density spectrum. We have not included this effect in our calculations, as the late-time entropy production is not predicted within the Standard Model. Boyle and Steinhardt [59] studied the effect of changes in the equation of state of the universe on the energy density spectrum. While they included the effect of neutrino free-streaming, they did not include the evolution of g_*. Instead, they explored general possibilities that the equation of state might be modified by trace anomaly or interactions among particles. They also considered damping of gravitational waves due to anisotropic stress of some hypothetical particles. Our calculations are different from theirs, as we took into account explicitly all the particles in the Standard Model and the minimal extension of the Standard Model, but did not include any exotic physics beyond that.

Let us mention a few points that would merit further studies. At the energy scales where supersymmetry is unbroken (if it exists), say TeV scales and above, the number of relativistic degrees of freedom, g_*, should be at least doubled, and would cause suppression of the primordial gravitational waves (Fig. 2.8 for $N = 1$ supersymmetry). If, for instance, $N = 8$ is the number of internal supersymmetric charges, ~ 250 copies of standard model particles would appear in this theory. This would suppress the spectrum by 85% at the high frequency region (above $\sim 10^{-4}$ Hz) compare to the Standard Model, though the details depend on models. Since we still do not have much idea about a *true* supersymmetric model and its particle rest mass, the search for the primordial gravitational waves would help to constrain the effective number of relativistic degrees of freedom $g_*(T)$ above the TeV scales.

In an extremely high frequency region, $k_{\rm rh}$, the gravitational wave spectrum should provide us with unique information about the reheating of the universe after inflation. If the inflaton potential during reheating is monomial, $V(\phi) \propto \phi^n$, the equation of state during reheating is given by $p_\phi = \alpha(n)\rho_\phi$, where $\alpha(n) = \frac{n-2}{n+2}$. Since the equation of state determines the expansion law of that epoch, one obtains the frequency dependence of the gravitational wave spectrum as $\Omega_h \propto k^{(n-4)/(n-1)}$. In an extremely low frequency region (below $\sim 10^{-18}$ Hz), on the other hand, dark energy dominates the universe and affects the spectrum [60]. Acceleration of the universe reduces the amplitude of gravitational waves that enter the horizon at this epoch; however, we will not be able to observe modes as big as the size of the horizon today.

The signatures of the primordial gravitational waves may be detected only by the CMB polarization in the low frequency region, $\lesssim 10^{-16}$ Hz. For the higher frequency region, however, direct detection of the gravitational waves would be necessary, and it should allow us to search for a particular cosmological event by arranging an appropriate instrument, as the events during the radiation era are imprinted on the spectrum of the primordial gravitational waves.

Chapter 3

Reheating after Inflation with $f(\phi)R$ Gravity

3.1 Introduction

Inflation is an indispensable building-block of the standard model of cosmology [61, 53, 62], and has passed a number of stringent observational tests [63, 64]. Any inflation models must contain a mechanism by which the universe reheats after inflation [65, 66, 67]. The reheating mechanism requires detailed knowledge of interactions (e.g., Yukawa coupling) between inflaton fields and their decay products. Since the physics behind inflation is beyond the standard model of elementary particles, the precise nature of inflaton fields is currently undetermined, and the coupling between inflaton and matter fields is often put in by hand. On the other hand, inflaton and matter fields are coupled through gravity. Of course the gravitational coupling is suppressed by the Planck mass and thus too weak to yield interesting effects [61]; however, we shall show that the reheating occurs spontaneously if inflaton is coupled to gravity non-minimally, i.e., the gravitational action is given not by the Einstein-Hilbert form, R, but by $f(\phi)R$, where ϕ is an inflaton field. Even if matter fields do not interact with ϕ directly, they ought to interact via gravitation whose perturbations lead to Yukawa-type interactions. A similar idea was put forward by [68], who considered *preheating* with a non-minimal coupling between matter and gravity. Here, we do not consider preheating, but focus only on the perturbative reheating arising from $f(\phi)R$ gravity. Therefore, we can analytically calculate the resulting reheating temperature after inflation.

Why study $f(\phi)R$ gravity? There are a number of motivations [69, 70]. The strongest motivation comes from the fact that almost any candidate theories of fundamental physics which involve compactification of extra dimensions yield $f(\phi)R$ with the form of $f(\phi)$ depending on models. One illuminating example would be string moduli with $f(\phi) \propto e^{-\alpha\phi}$. Zee's induced gravity theory [71] has $f(\phi) = \xi\phi^2$, and renormalization in the curved spacetime yields other more complicated higher derivative terms [48]. Classic scalar-tensor theories, originally motivated by Mach's principle [72], also fall into this category. It has been shown that inflation occurs naturally in these generalized gravity models [73, 74, 75, 76, 77, 78, 79, 80, 81, 82], and the spectrum of scalar curvature perturbations [83, 84, 85] as well as of tensor gravity wave perturbations [86, 87, 88, 89, 90] can be affected by the presence of $f(\phi)R$, thereby allowing us to constrain $f(\phi)$ from the cosmological data. We show that limits on the reheating temperature (e.g., gravitino problem) provide additional, totally independent constraints on $f(\phi)$. This argument opens up new possibilities that one can constrain a broad class of inflation models from the reheating temperature. Reheating in Starobinsky's R^2 inflation has been considered by [91, 92, 82].

3.2 Reheating by non-minimal gravitational decay

Interactions between ϕ and matter stem from a mixing between metric and scalar field perturbations through $f(\phi)R$ [69]. It is this "gravitational decay channel" from

ϕ to matter that makes the universe reheat after inflation. We realize this in a simple Lagrangian given by

$$\mathcal{L} = \sqrt{-g}\left[\frac{1}{2}f(\phi)R - \frac{1}{2}g^{\mu\nu}\partial_\mu\phi\partial_\nu\phi - V(\phi)\right] + \mathcal{L}_{\rm m}, \tag{3.1}$$

where $\mathcal{L}_{\rm m}$ is the matter Lagrangian. Note that there is no explicit coupling between ϕ (inflaton) and $\mathcal{L}_{\rm m}$. To guarantee the ordinary Einstein gravity at low energy, we must have $f(v) = M_{\rm Pl}^2$, where v is the vacuum expectation value (vev) of ϕ at the end of inflation and $M_{\rm Pl} = (8\pi G)^{-1/2} = 2.436 \times 10^{18}$ GeV is the reduced Planck mass. This Lagrangian satisfies the weak equivalence principle: ϕ does not couple to matter directly, $\nabla_\mu T_{\rm m}^{\mu\nu} = 0$. This, however, does not imply that inflaton *quanta*, i.e., fluctuations around the vev, cannot decay into matter. The gravitational field equation from Eq. (3.1) is

$$\begin{aligned} f(\phi)G_{\mu\nu} &= T_{\mu\nu}^{\rm m} + \partial_\mu\phi\partial_\nu\phi - \frac{1}{2}g_{\mu\nu}(\partial\phi)^2 - g_{\mu\nu}V(\phi) \\ &\quad -(g_{\mu\nu}\Box - \nabla_\mu\nabla_\nu)f(\phi). \end{aligned} \tag{3.2}$$

Before reheating completes the energy density of the universe was dominated by ϕ; thus, we treat $T_{\mu\nu}^{\rm m}$ as perturbations. As usual we decompose $g_{\mu\nu}$ into the background, $\bar{g}_{\mu\nu}$, and perturbations, $h_{\mu\nu}$, as $g_{\mu\nu} = \bar{g}_{\mu\nu} + h_{\mu\nu}$. The first-order perturbation in $G_{\mu\nu}$ is given by

$$\begin{aligned} \delta G_{\mu\nu} = \frac{1}{2}[&-\Box h_{\mu\nu} + \nabla_\lambda\nabla_\mu h^\lambda{}_\nu + \nabla_\lambda\nabla_\nu h^\lambda{}_\mu - \nabla_\mu\nabla_\nu h \\ &-\bar{g}_{\mu\nu}(\nabla_\rho\nabla_\sigma h^{\rho\sigma} - \Box h - \bar{R}_{\rho\sigma}h^{\rho\sigma}) - \bar{R}h_{\mu\nu}], \end{aligned} \tag{3.3}$$

where $h^\mu{}_\nu \equiv \bar{g}^{\mu\lambda}h_{\lambda\nu}$ and $h \equiv \bar{g}^{\mu\nu}h_{\mu\nu}$.

Reheating occurs at the potential minimum of ϕ where ϕ oscillates about v. We thus expand ϕ as $\phi = v + \sigma$, where σ represents inflaton quanta which decay into matter fields. Treating σ as perturbations, one obtains the linearized field equation:

$$\frac{M_{\rm Pl}^2}{2}\left[-\Box h_{\mu\nu}+\cdots\right]+f'(v)(\bar{g}_{\mu\nu}\Box-\nabla_\mu\nabla_\nu)\sigma=T^{\rm m}_{\mu\nu}, \tag{3.4}$$

where $f'(v)$ means $\partial f/\partial\phi|_{\phi=v}$. This equation contains both $\Box h_{\mu\nu}$ and $\Box\sigma$, and thus wave modes are mixed up together. To diagonalize the wave mode we define a new field as [69]

$$\tilde{h}_{\mu\nu} \equiv h_{\mu\nu}-\frac{1}{2}\bar{g}_{\mu\nu}h-\frac{f'(v)}{M_{\rm Pl}^2}\bar{g}_{\mu\nu}\sigma, \tag{3.5}$$

where the tilde denotes the operation defined by this equation, which essentially corresponds to the infinitesimal conformal transformation. The inverse operation is

$$h_{\mu\nu}=\tilde{h}_{\mu\nu}-\frac{1}{2}\bar{g}_{\mu\nu}\tilde{h}-\frac{f'(v)}{M_{\rm Pl}^2}\bar{g}_{\mu\nu}\sigma. \tag{3.6}$$

Using the harmonic gauge (analog of the Lorenz gauge) conditions, $\nabla_\lambda\tilde{h}^\lambda{}_\nu=0$, one can show that $\tilde{h}_{\mu\nu}$ indeed obeys the linearized field equation for the wave mode (see, e.g., Eq. (35.64) in [52]; Eq. (10.9.4) in [41])

$$\begin{aligned}\Box\tilde{h}_{\mu\nu}-2\bar{R}_{\mu\lambda\rho\nu}\tilde{h}^{\lambda\rho}-2\bar{R}_{\rho(\mu}\tilde{h}^\rho{}_{\nu)}-\bar{g}_{\mu\nu}\bar{R}_{\lambda\rho}\tilde{h}^{\lambda\rho}+\bar{R}\tilde{h}_{\mu\nu}&\\ =-\frac{2}{M_{\rm Pl}^2}T^{\rm m}_{\mu\nu}.&\end{aligned} \tag{3.7}$$

One may also impose the traceless condition on $\tilde{h}_{\mu\nu}$ to make sure that $\tilde{h}_{\mu\nu}$ describes tensor (spin two) gravity waves, $\tilde{h}=-h-4f'(v)\sigma/M_{\rm Pl}^2=0$, which relates a trace part of the original metric perturbations to σ as $h=-4f'(v)\sigma/M_{\rm Pl}^2$. In this sense σ describes the "scalar (spin zero) gravity waves", which are common in scalar-tensor theories of gravity. For generality we keep $\tilde{h}$ explicitly throughout the chapter.

We consider both fermionic, ψ, and bosonic, χ, fields as matter: $\mathcal{L}_{\rm m}=$

$\mathcal{L}_\psi + \mathcal{L}_\chi + \mathcal{L}_{\rm int}$. First, let us write $\mathcal{L}_\psi$ as

$$\mathcal{L}_\psi \;\; = \;\; -\sqrt{-g}\bar{\psi}\left[\not{D} + m_\psi\right]\psi, \tag{3.8}$$

where $\not{D} \equiv e^{\mu\alpha}\gamma_\alpha D_\mu$, $e^{\mu\alpha}$ is a tetrad (vierbein) field, and $D_\mu \equiv \partial_\mu - \Gamma_\mu$ is the covariant derivative for spinor fields [41, 48]. Γ_μ is a spinor connection and $\Sigma^{\alpha\beta}$ are generators of the Lorentz group given by $\Gamma_\mu(x) \equiv -\frac{1}{2}\Sigma^{\alpha\beta}e_\alpha{}^\lambda\nabla_\mu e_{\beta\lambda}$ and $\Sigma^{\alpha\beta} = -\Sigma^{\beta\alpha} = \frac{1}{4}[\gamma^\alpha, \gamma^\beta]$, respectively. Here $\alpha, \beta, \ldots$ denote Lorentz indices while $\mu, \nu, \ldots$ denote general coordinate indices. Note that we have not antisymmetrized the first term in Eq. (3.8) to make the expression simpler. The antisymmetrized term yields the same result. Note also that we shall ignore the existence of torsion.

We expand the tetrad and metric into the background and perturbations as $e^{\mu\alpha} \simeq \bar{e}^{\mu\alpha} - \bar{e}^{\lambda\alpha}h^\mu{}_\lambda/2$, and $\sqrt{-g} = \bar{e} + \delta e \simeq \bar{e}\left(1 + \bar{g}^{\mu\nu}h_{\mu\nu}/2\right)$, respectively. The Lagrangian becomes (with Eq. (3.6))

$$\begin{aligned}\mathcal{L}_\psi \;\; \simeq \;\; & -\bar{e}\bar{\psi}\left[\bar{e}^{\mu\alpha}\gamma_\alpha D_\mu + m_\psi\right]\psi \\ & +\frac{1}{2}\bar{e}\bar{\psi}\big[\bar{e}^{\nu\alpha}\gamma_\alpha(\tilde{h}^\mu{}_\nu + \frac{1}{2}\tilde{h}\delta^\mu{}_\nu)D_\mu + \tilde{h}m_\psi\big]\psi \\ & +\bar{e}g_\psi\sigma\bar{\psi}\psi. \end{aligned}\tag{3.9}$$

The terms that are proportional to $\tilde{h}$ may be set to vanish by gauge transformation. Here we have used the background Dirac equation, $\bar{e}^{\mu\alpha}\gamma_\alpha D_\mu\psi = -m_\psi\psi$, to obtain the last term and ignored the second order terms as well as thermal mass induced by quantum corrections in thermal bath [93, 94]. The last term in Eq. (3.9) is a Yukawa interaction term with a coupling constant given by

$$g_\psi \equiv \frac{f'(v)m_\psi}{2M_{\rm Pl}^2}. \tag{3.10}$$

Therefore, σ can decay into ψ and $\bar{\psi}$. Note that the Yukawa interaction vanishes when $f'(v) = 0$ or $m_\psi = 0$, which is consistent with previous work [77]: as massless fermions are conformally invariant, no peculiar effects can be caused by $f(\phi)R$ gravity at the tree level. Quantum corrections such as a conformal, or trace, anomaly might open additional decay channels.

Next, let us consider the bosonic matter, χ, given by

$$\mathcal{L}_\chi = \sqrt{-g}\left[-\frac{1}{2}g^{\mu\nu}\partial_\mu\chi\partial_\nu\chi - U(\chi)\right], \tag{3.11}$$

which may be expanded as

$$\begin{aligned}\mathcal{L}_\chi \simeq \sqrt{-\bar{g}}\Big[&-\frac{1}{2}\bar{g}^{\mu\nu}\partial_\mu\chi\partial_\nu\chi - U(\chi) + \frac{1}{2}\tilde{h}^{\mu\nu}\partial_\mu\chi\partial_\nu\chi \\ &+\frac{1}{2}\tilde{h}U(\chi) + \frac{f'(v)}{2M_{\rm Pl}^2}\left(4\sigma U(\chi) + \sigma\bar{g}^{\mu\nu}\partial_\mu\chi\partial_\nu\chi\right)\Big],\end{aligned} \tag{3.12}$$

where we have used $\sqrt{-g} \simeq \sqrt{-\bar{g}}(1 - \tilde{h}/2 - 2\sigma f'(v)/M_{\rm Pl}^2)$ and $g^{\mu\nu} \simeq \bar{g}^{\mu\nu} - \tilde{h}^{\mu\nu} + \bar{g}^{\mu\nu}\tilde{h}/2 + \bar{g}^{\mu\nu}\sigma f'(v)/M_{\rm Pl}^2$. Again, the terms that are proportional to $\tilde{h}$ may be set to vanish by gauge transformation. For simplicity we assume that χ is a massive field with self-interaction, $U(\chi) = m_\chi^2\chi^2/2 + \lambda\chi^4/4$. The last term in Eq. (3.12) then yields the following interactions: $\sqrt{-\bar{g}}[\sigma f'(v)/2M_{\rm Pl}^2](2m_\chi^2\chi^2 + \lambda\chi^4 + \bar{g}^{\mu\nu}\partial_\mu\chi\partial_\nu\chi)$. We rewrite these interactions as

$$\sqrt{-\bar{g}}\frac{\sigma f'(v)}{2M_{\rm Pl}^2}\left(m_\chi^2\chi^2 + \bar{g}^{\mu\nu}\bar{\nabla}_\mu(\chi\partial_\nu\chi)\right) \approx \sqrt{-\bar{g}}g_\chi\sigma\chi^2, \tag{3.13}$$

where we have defined a coupling constant,

$$g_\chi \equiv \frac{f'(v)}{2M_{\rm Pl}^2}\left(m_\chi^2 + \frac{m_\sigma^2}{2}\right), \tag{3.14}$$

which will give a rate of σ decaying into two χs. To derive Eq. (3.13) we used $\bar{g}^{\mu\nu}\partial_\mu\chi\partial_\nu\chi = -\chi U'(\chi) + \bar{g}^{\mu\nu}\bar{\nabla}_\mu(\chi\partial_\nu\chi)$, where $\bar{\nabla}_\mu$ is the covariant derivative on the background metric, and estimated as $\sigma\bar{\nabla}_\mu(\chi\partial^\mu\chi) \approx \sigma m_\sigma^2\chi^2/2$. This estimation is valid in the zero temperature limit (see [95] for the high temperature limit). While the first term in Eq. (3.14) is absent when $m_\chi = 0$, σ can still decay through the second term as minimally coupled massless scalar fields are not conformally invariant.

What is the physical interpretation of these couplings? Through the field mixing that can be seen in Eq. (3.5) the inflaton quanta are coupled to the trace (spin zero) part of $h_{\mu\nu}$, which describes the scalar gravity waves. The scalar waves are then coupled to the matter fields. If inflaton quanta are at least twice as heavy as ψ or χ, they decay into $\psi\bar{\psi}$ or two χs.

In order to compute decay rates, one must canonically normalize fields.[1] The kinetic term of σ is given by $\mathcal{L}_\sigma^{\rm kin}/\sqrt{-\bar{g}} = -\frac{1}{2}(\partial\sigma)^2\left[1+\frac{3}{2}(f'(v)/M_{\rm Pl})^2\right]$ to the leading order, and thus $\hat{\sigma} \equiv \sigma\sqrt{1+\frac{3}{2}(f'(v)/M_{\rm Pl})^2}$ is the canonically normalized inflaton field. Therefore, coupling constants should be replaced accordingly by $\hat{g}_\psi = g_\psi\left[1+\frac{3}{2}(f'(v)/M_{\rm Pl})^2\right]^{-1/2}$ and $\hat{g}_\chi = g_\chi\left[1+\frac{3}{2}(f'(v)/M_{\rm Pl})^2\right]^{-1/2}$.

The decay rates of $\sigma \to \psi\bar{\psi}$ from the last term in Eq.(3.9) and $\sigma \to \chi\chi$ from Eq.(3.13), $\Gamma_{\rm tot} = \Gamma_{\sigma\bar{\psi}\psi} + \Gamma_{\sigma\chi\chi} + \ldots$, are given by [96]

$$\Gamma_{\sigma\bar{\psi}\psi} = \frac{\hat{g}_\psi^2 m_\sigma}{8\pi}\left(1-\frac{4m_\psi^2}{m_\sigma^2}\right)^{3/2}\tanh\left(\frac{m_\sigma}{4T}\right)C_\psi, \tag{3.15}$$

$$\Gamma_{\sigma\chi\chi} = \frac{\hat{g}_\chi^2}{8\pi m_\sigma}\left(1-\frac{4m_\chi^2}{m_\sigma^2}\right)^{1/2}\coth\left(\frac{m_\sigma}{4T}\right)C_\chi, \tag{3.16}$$

where $m_\sigma^2 \equiv V''(v)$ and we have included suppression of decay rates due to thermal mass, C_ψ and C_χ, which are unity in the low temperature limit ($T \ll m_\sigma$) in which thermal mass is small, but can be quite small otherwise. The exact form of C depends on how decay products are thermalized. Yokoyama has calculated

[1] We are grateful to N. Kaloper for pointing out importance of the normalization of σ fields.

C_χ from thermalization due to $\Delta U = \lambda\chi^4/4$: for $T \gg m_\sigma/\sqrt{\lambda}$ he finds $C_\chi = \lambda/(8\pi^2)$ for decay via $\sigma\chi^2$ interaction [94] and $C_\chi = \lambda/(1024\pi^2)$ for $\sigma(\partial\chi)^2$ (which corresponds to the last term in Eq. (3.12); if this term dominates g_χ is given by $g_\chi = f'(v)\lambda T^2/(2M_{\rm Pl}^2)$ because of dominance of thermal mass, $\sqrt{\lambda}T$, over the intrinsic mass of χ) [95], while C_ψ has not been calculated explicitly yet.

As usual we use the condition, $3H(t^*) = \Gamma_{\rm tot}$, to define the reheating time, t^*, at which radiation begins to dominate the energy density of the universe. From the Friedmann equation, $H^2 = \rho/(3M_{\rm Pl}^2)$, we get $\rho(t^*) = \Gamma_{\rm tot}^2 M_{\rm Pl}^2/3 = \frac{\pi^2}{30} g_*(T_{\rm rh}) T_{\rm rh}^4$, where the last equality holds if all the decay products interact with each other rapidly enough to achieve thermodynamical equilibrium [93]. If some fraction of inflaton energy density is converted into the species that never interact with the visible sector, the reheating temperature may be lowered. $g_*(T_{\rm rh})$ is the effective number of relativistic degrees of freedom at the reheating time. Since $\Gamma_{\rm tot} > \Gamma_{\sigma\bar{\psi}\psi} + \Gamma_{\sigma\chi\chi}$, the reheating temperature is bounded from below:

$$\begin{aligned} T_{\rm rh} &= \frac{\sqrt{\Gamma_{\rm tot} M_{\rm Pl}}}{(10\pi^2)^{1/4}} \left(\frac{g_*(T_{\rm rh})}{100}\right)^{-1/4} \\ &> \sqrt{\hat{g}_\psi^2 + \frac{\hat{g}_\chi^2}{m_\sigma^2}} \frac{\sqrt{m_\sigma M_{\rm Pl}}}{4\pi(40)^{1/4}} \left(\frac{g_*(T_{\rm rh})}{100}\right)^{-1/4}, \end{aligned} \tag{3.17}$$

where we have used Eq. (3.15) and (3.16) assuming for simplicity that decay products are much lighter than σ (m_ψ, $m_\chi \ll m_\sigma$), the reheating temperature is much smaller than m_σ ($T \ll m_\sigma$), and therefore suppression due to thermal mass is unimportant ($C_\psi = 1 = C_\chi$). Generalization to the other limits is straightforward. One may reverse the argument and set a limit on $f'(v)$ as

$$\frac{|f'(v)|}{\sqrt{1 + \frac{3}{2}\left(\frac{f'(v)}{M_{\rm Pl}}\right)^2}} < 8\pi(40)^{1/4} T_{\rm rh} \left(\frac{M_{\rm Pl}}{m_\sigma}\right)^{3/2} \left(\frac{g_*(T_{\rm rh})}{100}\right)^{1/4}, \tag{3.18}$$

which provides non-trivial constraints on inflation models with $f(\phi)R$ gravity. Let us consider a non-minimal coupling model, $f(\phi) = M^2 + \xi\phi^2$, for instance ($M^2$ is given by the condition $f(v) = M_{\rm Pl}^2$). We obtain $|\xi|(1 + 6\xi^2 v^2/M_{\rm Pl}^2)^{-1/2} < 4\pi(40)^{1/4}(T_{\rm rh}/v)(M_{\rm Pl}/m_\sigma)^{3/2}(g_*(T_{\rm rh})/100)^{1/4}$, which provides a new constraint on ξ, independent of the existing constraints from homogeneity and isotropy [76] and curvature as well as tensor perturbations [86, 87, 88, 89, 90].

One may repeat the same argument by including other channels, e.g., decay into two Abelian gauge fields via conformal anomaly and pair annihilation of inflatons into two scalar fields. The decay rates are estimated in Appendix C and Sec. 4.4, respectively.

Finally, let us show that one can obtain the same results by performing the following conformal transformation, $\hat{g}_{\mu\nu} = \Omega^2 g_{\mu\nu}$, with

$$\Omega^2 = \frac{f(\phi)}{M_{\rm Pl}^2} = 1 + \frac{f'(v)\sigma}{M_{\rm Pl}^2} + \frac{f''(v)\sigma^2}{2M_{\rm Pl}^2} + \mathcal{O}(\sigma^3). \tag{3.19}$$

Hereafter we put hats on variables in the Einstein frame (E frame). We use Maeda's transformation formula [97] to obtain the Lagrangian in the E frame,

$$\mathcal{L} = \sqrt{-\hat{g}}\left[\frac{M_{\rm Pl}^2}{2}\hat{R} - \frac{1}{2}\hat{g}^{\mu\nu}\partial_\mu\hat{\phi}\partial_\nu\hat{\phi} - \hat{V}(\hat{\phi})\right] + \mathcal{L}_{\rm m}, \tag{3.20}$$

where $\hat{R}$ is calculated from $\hat{g}_{\mu\nu}$, a transformed potential is given by $\hat{V}(\hat{\phi}) \equiv \Omega^{-4}V(\phi)$, and a new scalar field, $\hat{\phi}$, is defined such that it has the canonical kinetic term. It is related to the original field by $d\hat{\phi}/d\phi = M_{\rm Pl}\sqrt{1/f(\phi) + \frac{3}{2}\left(f'(\phi)/f(\phi)\right)^2}$. As $\hat{\phi}$ is minimally coupled to $\hat{R}$, there is no mixing between $\hat{g}_{\mu\nu}$ and $\hat{\phi}$.

A transformed Lagrangian for ψ in the E frame is

$$\mathcal{L}_\psi = -\hat{e}\hat{\bar{\psi}}[(\hat{\not{D}} - \overleftarrow{\hat{\not{D}}})/2 + \Omega^{-1}m_\psi]\hat{\psi}, \tag{3.21}$$

where $\hat{\psi} = \Omega^{-3/2}\psi$, $\hat{\bar{\psi}} = \Omega^{-3/2}\bar{\psi}$, $\hat{e}^{\mu\alpha} = \Omega^{-1}e^{\mu\alpha}$, and $\hat{e} = \Omega^4 e$. While no Yukawa interaction arises from the kinetic term, the mass term yields a Yukawa interaction:

$$-\hat{e}\frac{m_\psi}{\Omega}\hat{\bar{\psi}}\hat{\psi} \simeq -\hat{e}m_\psi\hat{\bar{\psi}}\hat{\psi} + \hat{e}\frac{f'(v)m_\psi}{2M_{\rm Pl}^2}\sigma\hat{\bar{\psi}}\hat{\psi}. \tag{3.22}$$

Thus, Yukawa coupling constants agree precisely.

A transformed Lagrangian for χ in the E frame is

$$\mathcal{L}_\chi = -\frac{1}{2}\sqrt{-\hat{g}}\hat{g}^{\mu\nu}\mathcal{D}_\mu\hat{\chi}\mathcal{D}_\nu\hat{\chi} - \sqrt{-\hat{g}}\hat{U}(\hat{\chi}), \tag{3.23}$$

where $\hat{\chi} \equiv \Omega^{-1}\chi$ and we have followed the procedure in [69] to define a "covariant derivative" and potential in the E frame as $\mathcal{D}_\mu \equiv \partial_\mu + \partial_\mu(\ln\Omega)$, and $\hat{U}(\hat{\chi}) \equiv \Omega^{-4}U(\chi)$, respectively. In the case of $U(\chi) = m_\chi^2\chi^2/2 + \lambda\chi^4/4$, the second term of Eq. (3.23) becomes

$$-\sqrt{-\hat{g}}\left[\frac{1}{2}m_\chi^2\hat{\chi}^2 + \frac{\lambda}{4}\hat{\chi}^4 - \frac{f'(v)m_\chi^2}{2M_{\rm Pl}^2}\sigma\hat{\chi}^2\right], \tag{3.24}$$

to the linear order in σ; the last term agrees with the first term in Eq. (3.13). The covariant derivative yields a coupling, $-\sqrt{-\hat{g}}\hat{\chi}\hat{g}^{\mu\nu}(\partial_\mu\hat{\chi})(\partial_\nu\ln\Omega)$. After integration by parts and $\ln\Omega \simeq [f'(v)/(2M_{\rm Pl}^2)]\sigma$ this term yields

$$\frac{f'(v)}{2M_{\rm Pl}^2}\sigma\partial_\nu(\sqrt{-\hat{g}}\hat{\chi}\hat{g}^{\mu\nu}\partial_\mu\hat{\chi}) = \sqrt{-\hat{g}}\frac{f'(v)}{2M_{\rm Pl}^2}\sigma\hat{g}^{\mu\nu}\hat{\nabla}_\mu(\hat{\chi}\partial_\nu\hat{\chi}), \tag{3.25}$$

which agrees with the second term in Eq. (3.13) precisely.

One can calculate the other interaction terms such as $\sigma^2\chi^2$, $\sigma^2\bar{\psi}\psi$, $\sigma^2(\partial\chi)^2$, etc., with known coupling constants in the E frame easily. These interactions, whose coupling constants are proportional to the higher order derivatives such as $f''(v)$, $f'''(v)$, etc., actually dominate if $f(\phi)$ also has a minimum at the vev, $f'(v) = 0$. We must canonically normalize *quanta* as $\hat{\sigma} = \sigma\sqrt{1 + \frac{3}{2}(f'(v)/M_{\rm Pl})^2}$ when calculating their interaction rates. While we have ignored a parametric resonance (preheating)

[7, 98, 99] entirely, it would be interesting to study how preheating might occur in the present context.

3.3 Conclusion

In summary, we have presented a natural mechanism for reheating of the universe after inflation without introducing any explicit couplings between inflaton and fermionic or bosonic matter fields. This mechanism allows inflaton quanta to decay into *any fields* which are present at the end of inflation and are not conformally invariant, when inflaton settles in the vacuum expectation value and oscillates. Reheating therefore occurs spontaneously in *any theories* of $f(\phi)R$ gravity.

We have calculated the reheating temperature from this mechanism. We argue that one must always check that the reheating temperature in any $f(\phi)R$ inflation models is reasonable, e.g., the reheating temperature does not exceed the critical temperature above which too many gravitinos would be produced thermally. This mechanism might also allow ϕ to decay into gravitinos. How our mechanism is related to an inflaton decay through supergravity effects [100, 101, 102] merits further investigation. Both of these effects should provide non-trivial constraints on $f(\phi)$ from the cosmological data.

Chapter 4

Gravitational Inflaton Decay and the Hierarchy Problem

4.1 Introduction

Gravity is 10^{33} times weaker than the weak force. Both forces involve seemingly fundamental constants: Fermi's constant, $G_{\rm F} = 1.17 \times 10^{-5}$ GeV^{-2} = (293 GeV)$^{-2} \equiv M_{\rm w}^{-2}$, for the weak force, and Newton's constant, $G = 0.671 \times 10^{-38}$ GeV^{-2} = (1.22×10^{19} GeV)$^{-2} \equiv (\sqrt{8\pi} M_{\rm Pl})^{-2}$ for gravity. This inexplicably large separation between the Planck scale, $M_{\rm Pl}$, and the weak scale, $M_{\rm w}$, is the so-called gauge hierarchy problem [103].

Why is it a problem? The radiative corrections to the Higgs boson mass are quadratically divergent and sensitive to the ultraviolet cutoff scale of the particle physics theory, $M_{\rm UV}$, and thus drive the bare Higgs mass to a very large value, unless $M_{\rm UV}$ is closer to $M_{\rm w}$. However, if $M_{\rm UV}$ is not much higher than $M_{\rm w}$, one may wonder why $M_{\rm Pl}$ is much higher than $M_{\rm UV}$, i.e., gravity is so weak.[1]

[1] In supersymmetric theory, radiative corrections are only logarithmically divergent. If the supersymmetry breaking scale is close to $M_{\rm w}$, e.g., ~ 1 TeV, it solves the gauge hierarchy problem; however, one still needs to understand the reason why $M_{\rm Pl}$ and the symmetry breaking scale are

Dvali recently proposed a simple but radical solution to the hierarchy problem [4, 105]. He does not use technicolor or supersymmetry, but uses the black hole physics to show that any consistent theory that includes NZ_2-conserved species of the quantum fields with mass Λ must have a value of the Planck mass, which is bounded from below:

$$M_{\rm Pl}^2 \gtrsim N\Lambda^2, \tag{4.1}$$

in a large-N limit.[2]

Therefore, according to Dvali's solution (see also [106]), gravity is weak because there are N species of the quantum fields beyond the Standard Model with mass $\Lambda = O(\text{TeV})$, as well as a discrete Z_2^N-symmetry, with $N \sim 10^{32}$. An example of this scenario is the celebrated large-extra-dimensions solution to the hierarchy problem [107, 108, 109] (see also [110, 111] in the context of String Theory), in which $N \sim 10^{32}$ Kaluza-Klein particles of mass ~ 1 TeV would appear.

Can we construct a cosmological model that is consistent with Dvali's solution to the hierarchy problem? In particular, can we still construct a successful inflationary scenario, in the presence of such an extremely large number of extra species at the TeV scale?

In this chapter, we show that Dvali's proposal is consistent with inflation only when at least one of the followings is tightly fine-tuned: the inflaton mass, m_σ, vacuum expectation value, $\langle\phi\rangle \equiv v$, or non-minimal coupling parameter, ξ. While we consider only single field inflation models, our argument can be extended to a multi-field case in a straightforward manner. Here, ϕ denotes the inflaton field and its mass is given by the shape of the inflaton potential at the *minimum*; $\partial^2 V(\phi)/\partial\phi^2|_{\phi=v} \equiv m_\sigma^2$.

---

so different, i.e., the μ-problem [104].

[2] The reference [4, 105] uses the Planck mass, $m_{\rm Pl} \sim 10^{19}$ GeV, while we shall use the reduced Planck mass, $M_{\rm Pl} \sim 10^{18}$ GeV.

Our argument is based exclusively on reheating of the universe after inflation. Even if we do not know details of interactions between the inflaton and matter sector, we do know that there must be decay channels via gravitational interactions, which give the lower bound of the inflaton decay rate.

The existence of a large number of quantum fields with mass, $\Lambda \sim 1$ TeV, will enhance the decay rate of the inflaton field by $N \sim 10^{32}$. Such a drastic enhancement of the decay rate ought to affect reheating after inflation.

We shall take a particular point of view when we study implications of Dvali's proposal. In general, one may consider two cut-off scales: one for the particle physics, $M_{\rm UV}$, and the other for gravity, $M_{\rm grav}$, which may or may not be the same. In our analysis, we shall assume $M_{\rm UV} \sim \Lambda$ and $M_{\rm grav} \gg \Lambda$. This assumption allows us to analyze the gravitational inflaton decay in the semi-classical limit, without worrying about quantum gravitational effects.

The chapter is organized as follows. In Sec. 4.2 we discuss generic properties of the enhanced decay of inflaton. We especially consider $f(\phi)R$ gravity as an example. In Sec. 4.3 we discuss specific models with $V(\phi) = \frac{\lambda}{4}(\phi^2 - v^2)^2$. In Sec. 4.4 we study reheating via pair annihilation of inflatons and compare that to the gravitational decay. For concreteness, we shall consider single-field inflation models, and assume $\Lambda \sim 1$ TeV and $N \sim 10^{32}$ throughout this chapter unless stated otherwise. We work with the metric signature $(- + ++)$.

4.2 Enhanced gravitational decay of inflaton

In theories with non-minimal couplings between the Ricci curvature and scalar fields, e.g., supergravity, $\mathcal{R}^2$ gravity, scalar-tensor gravity, and higher dimensional gravity theories, inflaton fields can decay via gravitational effects.

The perturbative decay rate, $\Gamma_{\rm grav}$, is typically given by

$$\Gamma_{\rm grav} \sim NC\frac{m_\sigma^3}{M_{\rm Pl}^2}, \tag{4.2}$$

where C is a model-dependent fudge factor. Although the gravitational decay rate is suppressed by the Planck scale, the large number of species, N, would compensate it. One usually takes $N \sim 10^2 - 10^3$ and $NC \sim \mathcal{O}(1)$.

In Dvali's scenario, $N \sim 10^{32}$, and $M_{\rm Pl}^2$ is bounded from below by Eq. (4.1). The decay rate is therefore bounded from above as

$$\Gamma_{\rm grav} \lesssim C\frac{m_\sigma^3}{\Lambda^2}. \tag{4.3}$$

When Dvali's bound is saturated, the decay proceeds very fast and produces radiation[3] and entropy in the universe efficiently.

But, what if the decay is too efficient, and too much radiation is produced? This is the argument that we shall use throughout this chapter.

The most conservative, and model-independent constraint on Dvali's proposal can be obtained by the following argument: at any epoch during or after inflation, the energy density of the universe must not exceed the Planck energy density.

If the energy density of inflaton during inflation is less than the Planck energy density, $\rho_{\rm inf} < M_{\rm Pl}^4$, energy conservation demands that the energy density of radiation must also satisfy $\rho_{\rm rad} < \rho_{\rm inf} < M_{\rm Pl}^4$.

The expansion rate of the universe during reheating roughly equals the total decay rate of inflaton, $H(t_{\rm rh}) \sim \Gamma_{\rm tot} \gtrsim \Gamma_{\rm grav}$. From the Friedmann equation and Eq. (4.2), we get $(\Gamma_{\rm grav} M_{\rm Pl})^2 \sim \left(NCm_\sigma^3/M_{\rm Pl}\right)^2 \lesssim \rho_{\rm rad} < M_{\rm Pl}^4$. Solving this

[3] The "radiation" may contain both visible and hidden sectors.

inequality for inflaton mass, we get an upper limit on the inflaton mass,

$$m_\sigma < 10^8 \text{ GeV} \left(\frac{10^{30}}{NC}\right)^{1/3}. \tag{4.4}$$

This constraint is not very interesting in the conventional scenario in which $NC \sim \mathcal{O}(1)$, e.g., $m_\sigma < 10^{18}$ GeV.

However, in a large-N limit, say $NC \sim 10^{30}$, the constraint becomes very tight: $m_\sigma < 10^8$ GeV $\sim 10^{-10} M_{\rm Pl}$, which is significantly tighter than the usual fine-tuning of the inflaton mass, $m_\sigma \sim 10^{-6} M_{\rm Pl}$, for a successful chaotic inflation model with $V(\phi) = m_\sigma^2 \phi^2/2$. Therefore, Dvali's proposal is consistent only when the inflaton is very light, significantly lighter than the conventional case. While m_σ is fined-tuned with respect to $M_{\rm Pl}$ (or $M_{\rm grav}$), it would be natural to have $m_\sigma \sim M_{\rm UV} \sim O(\text{TeV})$ whose value is consistent with Eq. (4.4).

A more powerful constraint comes from the expansion rate of the universe during inflation, $H_{\rm inf}$. The energy density of inflaton during inflation is related to $H_{\rm inf}$ via the Friedmann equation, $\rho_{\rm inf} = 3M_{\rm Pl}^2 H_{\rm inf}^2$. Energy conservation then demands that the energy density of radiation must satisfy $\rho_{\rm rad} < \rho_{\rm inf} = 3M_{\rm Pl}^2 H_{\rm inf}^2$, which yields a bound on the gravitational decay rate, $\Gamma_{\rm grav} < \sqrt{3} H_{\rm inf}$.

This bound may also be found as follows: since the expansion rate decreases as inflation ends, the expansion rate during inflation, $H_{\rm inf}$, is greater than that during reheating: $H_{\rm inf} > H(t_{\rm rh}) \sim \Gamma_{\rm tot} \gtrsim \Gamma_{\rm grav}$. We can use this inequality to constrain $\Gamma_{\rm grav}$, if we know what $H_{\rm inf}$ is.

How do we constrain $H_{\rm inf}$ observationally? The amplitude of primordial gravity waves is related to the expansion rate of the universe during inflation as

$$H_{\rm inf}^2 \simeq \frac{\pi^2 M_{\rm Pl}^2 \Delta_h^2(k)}{2} = \frac{\pi^2 M_{\rm Pl}^2 r \Delta_{\mathcal{R}}^2(k)}{2}, \tag{4.5}$$

where $\Delta_h^2(k)$ and $\Delta_{\mathcal{R}}^2(k)$ are the dimensionless power spectrum of tensor and curvature perturbations, respectively [112]. The current observational constraint on the tensor-scalar ratio, $r \equiv \Delta_h^2(k)/\Delta_{\mathcal{R}}^2(k)$, is $r \lesssim 1$, and the curvature perturbation is of order $\Delta_{\mathcal{R}}^2(k) \sim 2 \times 10^{-9}$ [113, 64].

Combining these with Eq. (4.2), we get a tighter constraint,

$$m_\sigma < 10^7 \text{ GeV} \left(\frac{10^{30}}{NC}\right)^{1/3} \left(\frac{r\Delta_{\mathcal{R}}^2}{2 \times 10^{-9}}\right)^{1/6}. \tag{4.6}$$

Note that this limit is also fairly model-independent, and makes the fine-tuning of the inflaton mass even tighter.

As this constraint is insensitive to the precise value of r or $\Delta_{\mathcal{R}}^2$, the future observations of the B-mode polarization of the cosmic microwave background, which would reach $r \sim \mathcal{O}(10^{-2})$, will not improve the constraint significantly.

One can obtain even tighter constraints by considering the following limit on the reheating temperature,

$$1 \text{ MeV} \lesssim T_{\text{rh}} \lesssim 10^8 \text{ GeV},$$

where the lower bound comes from the successful primordial nucleosynthesis and the upper bound comes from the requirement that thermal overproduction of gravitino/moduli be avoided [114, 115, 116]. While the lower bound on the temperature must be satisfied for any models[4], the upper bound is a model-dependent limit. Therefore, this limit is not as generic as the previous two limits. Nevertheless, the resulting constraint on the inflaton mass is the strongest, as we shall show below.

If the gravitational decay is a dominant process ($\Gamma_{\text{tot}} \sim \Gamma_{\text{grav}}$), we get $NT_{\text{rh}}^4 \sim (\Gamma_{\text{tot}} M_{\text{Pl}})^2 \sim \left(NCm_\sigma^3/M_{\text{Pl}}\right)^2$, where we have used the Friedmann equation and

[4]Here, we assume that N-species fields are unharmful and cascade into radiation in the visible sector, or stable dark matter particles, eventually. If N-species fields are long-lived, the reheat temperature is roughly given by $T_{\text{rh}} \sim \sqrt{M_{\text{Pl}}}(\Gamma_\sigma^{-1} + \Gamma_N^{-1})^{-1/2}$, where Γ_σ is the total decay rate of inflaton and Γ_N is that of N-species fields. Long-lived, but unstable, N-species fields might cause problems, in a way similar to the late decay of moduli [115].

Eq.(4.2); thus, the reheat temperature is given by

$$T_{\rm rh} \sim N^{1/4}\sqrt{\frac{Cm_\sigma^3}{M_{\rm Pl}}}, \tag{4.7}$$

and the above limit on $T_{\rm rh}$ from the nucleosynthesis and gravitino/moduli problem yields

$$0.1 \text{ GeV} < m_\sigma \left(\frac{NC^2}{10^{30}}\right)^{1/6} < 10^{6.3} \text{ GeV}, \tag{4.8}$$

which can be tighter than Eqs. (4.4) and (4.6), depending on C.

Even if the decay process is dominated by non-gravitational ones (i.e. direct interactions), the upper bound is still valid, as the gravitational decay channel gives the minimal decay rate. The lower bound is a necessary condition to reheat the universe after inflation mainly by gravitational decay of inflaton.

At the earlier stage of reheating, there may be non-perturbative decay of inflaton via preheating, depending on the magnitude of direct interactions. Our argument is valid even after preheating, if any, as the gravitational decay channel gives the minimal decay rate in any case.

Here, we have used a simple, but rather crude, argument to make the main point of this chapter. There is still one unknown quantity, C, which depends on specific models. How do we determine C? We shall present more concrete models in the following sections.

4.2.1 Decay induced by $f(\phi)R$ gravity

In this section we use C that we have derived in [2].

Almost all candidate theories of fundamental physics that involve some compactification of the extra spatial dimensions are expected to yield $f(\phi)R$ term, instead of the Einstein-Hilbert term, in the action, the form of $f(\phi)$ depending on models.

The gravitational decay rate of inflaton into all the species that could have existed at the reheating epoch is then given by $C = [F_1(v)]^2/(128\pi M_{\rm Pl}^2)$ [2], or

$$\Gamma_{\rm tot} \simeq N \frac{[F_1(v)]^2}{128\pi M_{\rm Pl}^2} \frac{m_\sigma^3}{M_{\rm Pl}^2}, \tag{4.9}$$

where $F_1(v) \equiv |f'(v)| \left[1 + \frac{3}{2}(f'(v)/M_{\rm Pl})^2\right]^{-1/2}$, $f'(v) \equiv \partial f/\partial\phi|_{\phi=v}$, and $v \equiv \langle\phi\rangle$ is the vacuum expectation value of ϕ. Here, N-species fields are scalars that are minimally coupled to gravity with a single mass scale, Λ, and $\Lambda \ll m_\sigma$.[5] Of course, all the fields do not need to have exactly the same mass, and our argument still applies when they have a moderate mass spectrum.

In this model the inequality Eq.(4.4) becomes

$$m_\sigma < 10^8 \text{ GeV} \left(\frac{10^{32}}{N}\right)^{1/3} \left(\frac{M_{\rm Pl}}{F_1(v)}\right)^{2/3}. \tag{4.10}$$

To make the constraint on m_σ slightly more general, let us parametrize N in terms of α as $\alpha \equiv N\Lambda^2/M_{\rm Pl}^2 \lesssim 1$. In order to solve the hierarchy problem with Dvali's argument, $\alpha \sim 1$ is required. Note that the minimum of this parameter is given by $\alpha_{\rm grav} = \Lambda^2/M_{\rm Pl}^2$, which represents weakness of gravity for particles with mass of Λ.

Assuming a typical value of $|f'(v)| \sim M_{\rm Pl}$, we find that the inflaton mass must be tuned to be smaller than $10^8\alpha^{-1/3}$ GeV. This constraint is most stringent when the hierarchy problem is solved (i.e. $\alpha \sim 1$).

One may reverse the argument by taking the inflaton mass to be a typical value of chaotic inflation, $m_\sigma \sim 10^{12}$ GeV, which limits $f'(v)$ as $F_1(v)/M_{\rm Pl} \sim |f'(v)|/M_{\rm Pl} < 10^{-6}\alpha^{-1/2}$, i.e., $f'(v)$ must be fine-tuned.

[5] While we consider scalar matter (bosons) only, one can calculate C for fermions as well. However, the gravitational decay channel to those light (compared to inflaton) fermions is suppressed by their mass, as massless fermions are conformally coupled to gravity[2].

The expansion rate during inflation gives a stronger constraint [Eq. (4.6)]:

$$m_\sigma < 10^7 \text{ GeV} \left(\frac{10^{32}}{N}\right)^{1/3} \left(\frac{M_{\rm Pl}}{F_1(v)}\right)^{2/3} \left(\frac{r\Delta^2_{\mathcal{R}}}{2\times 10^{-9}}\right)^{1/6}.$$

For $|f'(v)| \sim M_{\rm Pl}$, $m_\sigma < 10^7\alpha^{-1/3}$ GeV. For $m_\sigma \sim 10^{12}$ GeV, $F_1(v)/M_{\rm Pl} \sim |f'(v)|/M_{\rm Pl} < 10^{-7.5}\alpha^{-1/2}$.

The limit on the reheating temperature [Eq. (4.7)] yields even stronger constraint [Eq. (4.8)]:

$$0.3 \text{ GeV} < m_\sigma \left(\frac{N}{10^{32}}\right)^{1/6} \left(\frac{F_1(v)}{M_{\rm Pl}}\right)^{2/3} < 10^{6.8} \text{ GeV}.$$

For $|f'(v)| \sim M_{\rm Pl}$, the upper limit on the mass is $m_\sigma < 10^{6.8}\alpha^{-1/6}$ GeV. For $m_\sigma \sim 10^{12}$ GeV, $F_1(v)/M_{\rm Pl} \sim |f'(v)|/M_{\rm Pl} < 10^{-8}\alpha^{-1/4}$.[6]

In summary, we have confirmed that, using a physically motivated form of C, Dvali's large-N species solution to the hierarchy problem demands tight fine-tuning of m_σ or $f'(v)$. But, how bad are these fine-tunings?

4.3 Worked example: Ginzburg-Landau potential

The precise values of m_σ and $f'(v)$ depend on models. We shall study this point in further detail, by using a specific model given by the following action:

$$\begin{aligned}
\mathcal{L} &= \sqrt{-g}\left[\frac{1}{2}f(\phi)R - \frac{1}{2}\partial_\mu\phi\partial^\mu\phi - V(\phi)\right] + \mathcal{L}_{\rm matter}, \\
& \quad f(\phi) = M_{\rm Pl}^2 + \xi(\phi^2 - v^2), \\
& \quad V(\phi) = \frac{\lambda}{4}(\phi^2 - v^2)^2,
\end{aligned} \tag{4.11}$$

[6]The upper limit is identical to Eq. (18) in [2], when $\alpha \sim 10^{-32}$.

where the form of $f(\phi)$ is a popular non-minimal coupling[7] with the condition, $f(v) = M_{\rm Pl}^2$, that recovers General Relativity after inflation [2, 77, 84].

The form of $V(\phi)$ is also a popular Ginzburg-Landau-type potential. Therefore, our example is not exotic or peculiar; on the contrary, this is one of the best studied case, and therefore we hope that this example helps ones understand better how much fine-tuning is required by Dvali's solution to the hierarchy problem.

We now consider what happens when inflaton leaves the slow-roll regime, and begins to oscillate around its potential minimum. The inflaton quanta from the oscillations decay into relativistic N species at least perturbatively and gravitationally. The inflaton mass is given by the curvature of potential around the minimum, $m_\sigma^2 \equiv \partial^2 V(\phi)/\partial\phi^2|_{\phi=v} = 2\lambda v^2$.

We use the most conservative (probably overly conservative) limit on the radiation energy, $\rho_{\rm rad} < M_{\rm Pl}^4$ [Eq. (4.10)], to find a limit on λ and $|\xi|$ as

$$\lambda < \frac{10^{-20}}{|\xi|^{4/3}} \left(\frac{10^{32}}{N}\right)^{2/3} \left(\frac{M_{\rm Pl}}{v}\right)^{10/3} \left(1 + 6\xi^2 \frac{v^2}{M_{\rm Pl}^2}\right)^{2/3}, \tag{4.12}$$

which is extremely tight, compared to the existing constraints from inflation [76, 83, 79, 81, 84, 88, 86, 87, 90]. In fact, this limit excludes most of the parameter space allowed by the WMAP 3-yr data. One can find even stronger constraints by considering the expansion rate during inflation, or the limits on the reheating temperature from the gravitino/moduli problem.

It follows from Eq. (4.12) that it is difficult to avoid fine-tuning of one parameter without fine-tuning the other parameters. Either λ, ξ, or $v/M_{\rm Pl}$, or perhaps all of them, need to be fine-tuned for the large-N species solution to the hierarchy problem to be consistent with inflationary cosmology.

[7] In our notation, the conformal coupling corresponds to $\xi = -1/6$.

4.4 Reheating by pair annihilation of inflatons

So far, we have studied implications of the gravitational decay of inflatons enhanced by the existence of large-N species. In deriving Eq. (4.2), we assume that inflatons decay into N-species fields via an effective trilinear vertex, $\mathcal{L}_{\rm int} \propto \sigma\chi\chi$, which couples inflaton quanta, σ, to a pair of N species, χ. However, what if such a coupling is forbidden by the symmetry of the inflaton field? Are there any other channels to reheat the universe after inflation?

In theories of $f(\phi)R$ gravity, the effective interaction Lagrangian is given by the Taylor series expansion of $f(\phi)$ around the vacuum expectation value of ϕ, $\phi = v + \sigma$, where σ is the inflaton quanta. We find [2]

$$\begin{aligned}
\frac{\mathcal{L}_{\rm int}}{\sqrt{-g}} &= \frac{f'(v)}{M_{\rm Pl}^2}\left[\sigma U(\chi) - (\partial_\mu\sigma)G^\mu(\chi)\right] \\
&+\frac{f''(v)}{2M_{\rm Pl}^2}\left[\sigma^2 U(\chi) - 2\sigma(\partial_\mu\sigma)G^\mu(\chi)\right] \\
&+\frac{[f'(v)]^2}{2M_{\rm Pl}^4}\left[2\sigma(\partial_\mu\sigma)G^\mu(\chi) - (\partial_\mu\sigma)(\partial_\nu\sigma)H^{\mu\nu}(\chi)\right] \\
&+\frac{f'''(v)}{6M_{\rm Pl}^2}\left[\sigma^3 U(\chi) + \dots\right] + \dots,
\end{aligned} \tag{4.13}$$

where $U(\chi)$ is the scalar field potential, e.g., $U(\chi) = m_\chi^2\chi^2/2 + \lambda\chi^4/4 + \dots$, and the other functions are given by

$$G^\mu = \frac{1}{2}g^{\mu\alpha}\chi(\partial_\alpha\chi), \tag{4.14}$$

$$H^{\mu\nu} = \frac{1}{4}g^{\mu\nu}\chi^2. \tag{4.15}$$

Note that one can also derive the interaction Lagrangian for fermions systematically in a similar manner.

The first terms in $\mathcal{L}_{\rm int}$ that are proportional to $f'(v)$ yield the decay of σ with the rate given by Eq. (4.9), whereas those proportional to $f''(v)$ and $[f'(v)]^2$

yield the pair annihilation.

Now, let us imagine that the first derivative of $f(\phi)$ vanishes at the vacuum expectation value, $f'(v) = 0$, which will shut off the decay channel. We also assume that χ are massive free fields, $U(\chi) = m_\chi^2 \chi^2/2$. The interaction Lagrangian at the lowest order in σ for this case is given by

$$\frac{\mathcal{L}_{\rm int}}{\sqrt{-g}} = \frac{f''(v)}{2M_{\rm Pl}^2}\left[\frac{1}{2}m_\chi^2\sigma^2\chi^2 - g^{\mu\nu}\sigma(\partial_\mu\sigma)\chi(\partial_\nu\chi)\right],$$

which may also be written in the form of $\hat{g}^2\hat{\sigma}^2\chi^2$ (after some integration by parts and the use of equation of motion, $\Box\chi = \partial U/\partial\chi$), where $\hat{g}^2 = f''(v)\left[1+\frac{3}{2}(f'(v)/M_{\rm Pl})^2\right]^{-1}(m_\chi^2 + s/2)/(4M_{\rm Pl}^2)$ and $s \equiv -g_{\mu\nu}(q_1^\mu + q_2^\mu)(q_1^\nu + q_2^\nu)$ is the square of the total initial 4-momentum of incoming inflaton quanta. We must cannonically normalize inflaton quanta as $\hat{\sigma} \equiv \sigma\sqrt{1+\frac{3}{2}(f'(v)/M_{\rm Pl})^2}$. We calculate the annihilation cross section from this interaction Lagrangian as

$$\sigma_{\rm ann} = N\frac{[F_2(v)]^2}{32\pi M_{\rm Pl}^4}\frac{1}{s}\left(m_\chi^2 + \frac{s}{2}\right)^2\sqrt{\frac{s-4m_\chi^2}{s-4m_\sigma^2}}, \tag{4.16}$$

where $F_2(v) \equiv |f''(v)|\left[1+\frac{3}{2}(f'(v)/M_{\rm Pl})^2\right]^{-1}$.

The annihilation rate of inflatons is then given by

$$\begin{aligned}\Gamma_{\rm ann} &\equiv n_\sigma\langle\sigma_{\rm ann}v_{\rm rel}\rangle \\ &\simeq N\frac{3[F_2(v)]^2H_{\rm rh}^2\langle s\rangle}{64\pi M_{\rm Pl}^2 m_\sigma} \geq N\frac{3[F_2(v)]^2H_{\rm rh}^2 m_\sigma}{16\pi M_{\rm Pl}^2},\end{aligned} \tag{4.17}$$

where $n_\sigma = \rho_\sigma/m_\sigma \simeq 3M_{\rm Pl}^2H_{\rm rh}^2/m_\sigma$ is the number density of inflaton quanta. In deriving Eq. (4.17) we have assumed $m_\chi \ll m_\sigma$. The relative velocity, $v_{\rm rel}$, is given by $v_{\rm rel} = 2\sqrt{1-4m_\sigma^2/s}$ in the center of mass frame. Finally, the average of s, $\langle s\rangle$, is bounded from below, $\langle s\rangle \geq 4m_\sigma^2$, where the equality is satisfied when the inflaton quanta are at rest. While we expect them to be non-relativistic at the beginning of reheating, $\langle s\rangle \sim 4m_\sigma^2$, we keep the inequality explicitly in the following discussion.

In order for annihilation to be efficient during reheating, the annihilation rate has to be greater than the expansion rate during reheating, $\Gamma_{\rm ann} > H_{\rm rh}$. This is satisfied when

$$\frac{\langle s\rangle}{4m_\sigma} > \frac{10^{-7}{\rm GeV}}{[F_2(v)]^2}\left(\frac{10^{-6}M_{\rm Pl}}{H_{\rm rh}}\right)\left(\frac{10^{32}}{N}\right), \tag{4.18}$$

which is a rather weak lower bound on $\langle s\rangle/4m_\sigma$, which is approximately equal to m_σ in the non-relativistic limit, for $N \sim 10^{32}$. Therefore, the presence of large-N species makes annihilation very efficient.

Let us compare $\Gamma_{\rm ann}$ [Eq. (4.17)] with the decay rate, $\Gamma_{\rm decay}$ [Eq. (4.9)]:

$$\frac{\Gamma_{\rm ann}}{\Gamma_{\rm decay}} \gtrsim 24\left(\frac{F_2(v)M_{\rm Pl}}{F_1(v)}\right)^2\left(\frac{H_{\rm rh}}{m_\sigma}\right)^2, \tag{4.19}$$

where the approximate equality is satisfied when inflaton quanta are non-relativistic. We therefore find that the annihilation channel is not necessarily smaller than the decay channel. It may be more informative to write this result in the following form:

$$\frac{\Gamma_{\rm ann}}{\Gamma_{\rm decay}} \gtrsim 8\left(\frac{F_2(v)M_{\rm Pl}}{F_1(v)}\right)^2\frac{n_\sigma}{M_{\rm Pl}^2 m_\sigma}. \tag{4.20}$$

Thus, there is a critical number density above which the annihilation channel dominates over the decay channel:

$$n_\sigma^{\rm crit} \equiv \frac{M_{\rm Pl}^2 m_\sigma}{8}\left(\frac{F_1(v)}{F_2(v)M_{\rm Pl}}\right)^2. \tag{4.21}$$

For $f(\phi) = M_{\rm Pl}^2 + \xi(\phi^2 - v^2)$, for instance, the critical density is given by $n_\sigma^{\rm crit} = M_{\rm Pl}^2 m_\sigma (v/M_{\rm Pl})^2\left[1 + 6\xi^2(v/M_{\rm Pl})^2\right]/8$.

4.5 Conclusion

We have studied consistency between Dvali's large-N species solution to the gauge hierarchy problem and inflationary cosmology.

If there exist the large-N species, the inflaton quanta decay or annihilate too efficiently, and reheat the universe too much. We have found that, in order for this scenario to produce successful reheating of the universe, either inflaton mass, vacuum expectation value, or non-minimal gravitational coupling, or all of them, must be fine-tuned to suppress the gravitational decay and annihilation of the inflaton quanta.

We have shown that fine-tuning of an extreme magnitude, Eq. (4.12), is required by using a widely-studied example. The constraint we have found indeed excludes most of parameter space of the model. This example demonstrates that one must always check whether reheating is successful, whenever their models contain non-minimal coupling, such as $f(\phi)R$ gravity.

One may repeat the same analysis for supergravity inflation models [102, 3, 117, 118] that contain not only non-minimal gravitational coupling (the Kähler potential determines the function $f(\phi)$), but also direct coupling terms in the supergravity frame. However, as supersymmetry alone is able to solve the gauge hierarchy problem (albeit μ problem still remains), it seems difficult to motivate our having both supersymmetry and large-N species (see, however [119]).

Finally, let us point out the limitation and caveat of our analysis.

The constraints given in this chapter are based exclusively upon non-minimal gravitational couplings of inflaton. Therefore, if the non-minimal coupling is totally absent, $f(\phi) \equiv M_{\rm Pl}^2$, or matter fields are conformally coupled to gravity (e.g., massless scalars with $\xi = -1/6$, massless fermions, etc), both classically and quantum mechanically, reheating of the universe must be achieved by direct couplings between inflaton and matter fields. Our limits on Dvali's scenario do not apply to such cases.

We have assumed that the cut-off scale for gravity is much higher than that for the particle physics, Λ, and thus ignored quantum gravitational effects on the decay rates. It would be interesting to extend our analysis to the case where the cut-off for gravity is also similar to Λ [107, 108, 109] or even lower than Λ [120].

Chapter 5

Non-Gaussianity from Coherent Oscillation Phase after Inflation

5.1 Introduction

What happened right after inflation? Though the inflaton field eventually decays and transfers its energy to thermalize the Universe, the detailed process is still in the secret. If the inflation is driven by massive free or weakly interacting fields, the fields are going to oscillate about a local minimum of the potential. The homogeneously oscillating energy fragmented rapidly or gradually, cascading down to create various particles and quanta. This intermediate period is called the *coherent oscillation phase* and the equation of state of the universe becomes dust-like. The universe *reheats* during this unrevealed period.

In the standard inflation scenario the primordial curvature perturbations were generated during inflation and became the seed for the inhomogeneity seen today. This fluctuation is observed to follow nearly Gaussian statistics. Theoretically all single-field inflation models produce almost Gaussian signals [121, 122, 123]. The primordial curvature perturbations freeze in at the Hubble horizon exit and conserves its amplitude until the subsequent horizon re-entry. This holds whatever happens while adiabatic fluctuations are outside the Hubble radius [124]. The fact that the primordial curvature perturbations conserve their amplitude makes inflation scenario very powerful and predictable; however, a flip side of this is that no one can know what happened after inflation before radiation epoch by analysing large-scale inhomogeneities on the sky.

However, if the fluctuation is generated by some other field than inflaton, then it can be very non-Gaussian [125, 126]. Non-Gaussianity and non-linearity in multi-field inflation models are studied by many authors (see, for instance, [127, 128, 129, 130]). The mechanism on producing large non-Gaussian curvature perturbations always involves the existence of entropy perturbations on large scales.

Previous studies on the non-Gaussianity in the multi-field inflation models have mostly used the so-called δN formalism [131, 132, 124, 127], which is geometrically transparent, but the evolution of curvature perturbations is obscure. We use the nonlinear, covariant, and gauge-invariant formalism for multi-scalar fields [129] to solve the evolution of curvature perturbations on large scales explicitly, and apply it to non-Gaussianity from the two-field inflation and the coherent oscillation phase. An advantage of the covariant formalism is that it is physically transparent and relatively easy to carry out numerical analysis.

We present the first, detailed comparison between the two formalisms in case of a two-field inflation model with a large mass ratio. With this model Vernizzi and Wands [133] and Yokoyama et al. [134] used the δN formalism, while Rigopoulos et al. [135] solved equations of motion for large scale curvature perturbations. Their results seem to actually agree qualitatively but not quantitatively. We show that the two approaches agree exactly, although these two approaches are radically different in the ways that they treat the evolution of fluctuations.

The organization of this chapter is as follows. In Sec. 5.2, we define a non-linear curvature perturbation and explain its time evolution on super-Hubble scales based on a covariant formalism. We briefly review the δN formalism in subsection 5.2.4. Non-Gaussianity is defined and its transfer function is derived in subsection 5.2.5. In Sec. 5.3, we describe our model for two-field inflation and coherent oscillation. Our detailed numerical analysis shows that the δN formalism and an approach to solve evolution equations match precisely. An application to preheating models is discussed in Sec. 5.4. We conclude in Sec. 5.5. We use the unit $\hbar = c = 1$ and $8\pi G = M_{\rm Pl}^{-2} = 1$ unless otherwise stated.

5.2 Non-Gaussianity of Entropically Generated Curvature Perturbations

In this section we review generation and evolution of primordial fluctuations for (scalar) fields and metric perturbations. We will explain how entropy modes convert into the curvature perturbations during and after inflation. We assume that the universe completely thermalizes at the epoch of reheating; no residual entropy perturbation remains in the radiation era.

5.2.1 Non-linear curvature perturbation

The flat FRW metric with linear scalar perturbations is given by

$$ds^2 = -(1+2A)dt^2 + 2e^{\alpha(t)}B_{,i}dtdx^i + e^{2\alpha(t)}[(1-2\psi)\delta_{ij} + 2E_{,ij}]dx^i dx^j, \quad (5.1)$$

where $\alpha(t) = \ln[a(t)]$ in terms of the usual scale factor $a(t)$, and two of the four scalar metric perturbations, A, B, ψ and E, can be eliminated by specific gauge choices. Here ψ is called the curvature perturbation since it follows

$$^{(3)}R = \frac{4}{a^2}\nabla^2\psi, \quad (5.2)$$

where ${}^{(3)}R$ is the spatial intrinsic curvature scalar seen by comoving observers (on comoving hypersurfaces, where $T^0_i \propto \delta\phi = 0$ in single-field models). The value of ψ depends on a choice of observers (spatial hypersurfaces). Under a temporal gauge transformation $t \to t + \delta t$, ψ transforms as $\psi \to \psi + H\delta t$ [136]. Therefore, $\psi_A - \psi_B = H\delta t$ between slices A and B. If one of the slices has uniform ϕ and the other is flat ($\psi = 0$), the linear curvature perturbation on comoving hypersurfaces is given by

$$\mathcal{R} \equiv \psi + \frac{H}{\dot{\phi}}\delta\phi, \tag{5.3}$$

where the right hand side is evaluated on a generic slice. For multi-field models it is more useful to consider the linear curvature perturbation on uniform density hypersurfaces,

$$\zeta \equiv -\psi - \frac{H}{\dot{\rho}}\delta\rho. \tag{5.4}$$

The sign convention of gauge-invariant variables depends on literature (see Appendix A). It is known that on super-Hubble scales three hypersurfaces coincide: uniform density, uniform Hubble, and comoving hypersurface [124]. It is also known that ζ is conserved on large scales if pressure is a unique function of energy density.

On super-Hubble scales one can generalize the spatial part of the metric (5.1) to the form [121, 124]

$$g_{ij}dx^i dx^j = e^{2\alpha(t,\mathbf{x})}\delta_{ij}dx^i dx^j = a^2(t)e^{-2\psi(t,\mathbf{x})}\delta_{ij}dx^i dx^j, \tag{5.5}$$

where all the inhomogeneities are in $\psi(t, \mathbf{x})$. This expression is valid on a generic time-slice. On a uniform energy density time-slice, one may replace this with $-\zeta(t, \mathbf{x})$ [121, 137]. Let us define the *non-linear* curvature perturbation on the uniform density slices as [124, 129]

$$\zeta \equiv -\psi - \int_{\bar{\rho}}^{\rho} \frac{H}{\dot{\tilde{\rho}}} d\tilde{\rho}, \tag{5.6}$$

where $-\psi(t, \mathbf{x}) = \delta\alpha = \alpha(t, \mathbf{x}) - \ln[a(t)]$, and $H = \dot{\alpha}$. A dot denotes a Lie derivative along the 4-velocity u^μ, for instance $\dot{\rho} \equiv u^\mu \nabla_\mu \rho$, which is equivalent to an ordinary derivative for scalar quantity but careful treatments are needed when expanding to perturbations. The right hand side is evaluated on a generic time slicing. We will expand this formula up to the second order perturbation to study the leading order contribution to non-Gaussianity.

5.2.2 Evolution of curvature perturbation on large scales

In the following, all perturbed equations and quantities are valid only on super-Hubble scales, i.e., all gradient terms are ignored. Anisotropic stress of the cosmological fluid is negligible within this approximation. This can be verified in specific cases: if the fluid consists of gases and scalar fields, the anisotropic stress is at the second order in gradient expansion [124]. The time evolution of the non-linear curvature perturbation on all scales in the multiple scalar-fields-dominated universe is given by [129].

Using the non-linear conservation equation, $u^\nu \nabla_\mu T^\mu{}_\nu = 0$, on large scales one gets

$$\dot{\rho} = -3\dot{\alpha}(\rho + p) = -3(H - \dot{\psi})(\rho + p), \tag{5.7}$$

where $H = \bar{H} = \dot{a}/a$. On large scale uniform energy density time-slices, $\rho = \bar{\rho}$, and $-\psi = \zeta$ as defined in Eq. (5.6). Hence one obtains

$$\dot{\zeta} = -H - \frac{\dot{\bar{\rho}}}{3(\bar{\rho} + p)} = -\frac{H\delta p}{\bar{\rho} + \bar{p} + \delta p}, \tag{5.8}$$

where $\dot{\bar{\rho}} = -3H(\bar{\rho} + \bar{p})$ is used. According to the equation above, ζ will be constant if the pressure perturbation δp on uniform energy density hypersurfaces (the non-adiabatic pressure perturbation) is negligible. This expression is valid on non-linear orders in perturbations.

Multiple scalar field dynamics

We consider an N-scalar field model for inflation and the coherent oscillation phase. The action is given by

$$S = \int dx^4 \sqrt{-g} \left[\frac{1}{2} R - \frac{1}{2} \sum_{I=1}^{N} \partial_\mu \varphi_I \partial^\mu \varphi_I - V(\varphi_1, \cdots, \varphi_N) \right], \tag{5.9}$$

where kinetic terms are canonically normalized and the potential may not be separable.

For simplicity, we shall assume a homogeneous flat Friedman-Robertson-Walker background spacetime

$$ds^2 = -dt^2 + a^2(t) dx_i dx^i. \tag{5.10}$$

The scalar field and the averaged Einstein equations govern time-evolution of the universe during inflation, coherent oscillation, and possibly preheating. They are given by

$$\ddot{\varphi}_I + 3H\dot{\varphi}_I - \frac{\Delta}{a^2}\varphi_I + V_{\varphi_I} = 0, \tag{5.11}$$

$$H^2 = \frac{1}{3}\bar{\rho}, \quad \frac{\ddot{a}}{a} = -\frac{1}{6}(\bar{\rho} + 3\bar{p}), \tag{5.12}$$

where $\varphi_1 = \phi, \varphi_2 = \chi$, and $V_{\varphi_I} = \partial V / \partial \varphi_I$. The components of the energy momentum tensor are given by

$$
\begin{aligned}
\rho &= -T^0{}_0 = \sum_I \frac{\dot{\varphi}_I^2}{2} + \sum_I \frac{(\nabla\varphi_I)^2}{2a^2} + V(\varphi_I), &(5.13)\\
p &= \frac{1}{3}T^i{}_i = \sum_I \frac{\dot{\varphi}_I^2}{2} - \sum_I \frac{(\nabla\varphi_I)^2}{6a^2} - V(\varphi_I), &(5.14)\\
q_i &= -T^0{}_i = -\frac{1}{a}\sum_I \varphi_I \nabla_i \varphi_I, &(5.15)\\
\pi_{ij} &= T_{ij} - p\delta_{ij} = \frac{1}{a^2}\sum_I \nabla_i\varphi_I \nabla_j\varphi_I - \frac{1}{3a^2}\delta_{ij}(\nabla\varphi_I)^2, &(5.16)
\end{aligned}
$$

where we have chosen a unit time-like vector field as $\bar{u}^\mu = (-1, 0, 0, 0)$.

Adiabatic and entropic perturbations

In the following sections we will take $N = 2$, i.e., double-field model. The extension to models involving more fields is straightforward and shows no new qualitative feature.

In two-field models one can define linear adiabatic and entropy perturbations as [138]

$$
\begin{aligned}
\delta\sigma^{(1)} &\equiv \cos\theta\delta\phi + \sin\theta\delta\chi, &(5.17)\\
\delta s^{(1)} &\equiv -\sin\theta\delta\phi + \cos\theta\delta\chi. &(5.18)
\end{aligned}
$$

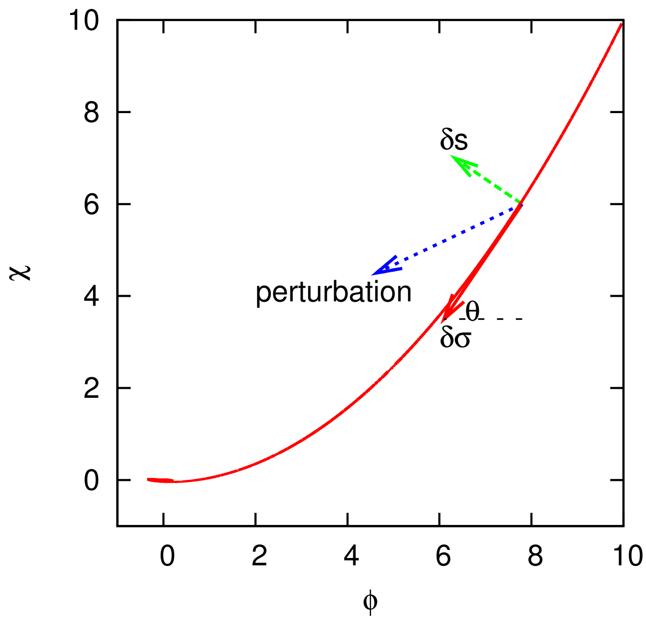

Figure 5.1: The decomposition of a perturbation into adiabatic ($\delta\sigma$) and entropy (δs) directions.

The angle of the background trajectory (see Fig. 5.1) is defined as

$$\tan\theta \equiv \dot{\chi}/\dot{\phi}, \tag{5.19}$$

$$\cos\theta \equiv \dot{\phi}/\dot{\sigma}, \tag{5.20}$$

$$\sin\theta \equiv \dot{\chi}/\dot{\sigma}, \tag{5.21}$$

$$\dot{\sigma} \equiv \sqrt{\dot{\phi}^2 + \dot{\chi}^2} = \sqrt{-2\dot{H}}, \tag{5.22}$$

$$\dot{s} \equiv -\sin\theta\dot{\phi} + \cos\theta\dot{\chi}, \tag{5.23}$$

where we have chosen plus sign for $\dot{\sigma}$. The classical equations of motion with this field redefinition can be written as

$$\ddot{\sigma} + 3H\dot{\sigma} + V_\sigma = 0, \tag{5.24}$$

where we have ignored the spatial gradient term and

$$
\begin{aligned}
V_\sigma &= \frac{1}{\dot\sigma}(\dot\phi V_\phi + \dot\chi V_\chi) \\
&= \cos\theta V_\phi + \sin\theta V_\chi .
\end{aligned}
\tag{5.25}
$$

The *adiabatic field*, σ, represents the path length along the classical trajectory and plays a role of the inflaton field. Its perturbations are along this inflaton direction and thus called adiabatic perturbations. The *entropy field*, s, has fluctuations orthogonal to the background classical trajectory. It is called non-adiabatic perturbations or entropic perturbations. Along the classical trajectory, $s = constant$. Since $\dot s = 0$ by definition (5.23), the equation of motion for the entropy field implies

$$
\begin{aligned}
\ddot s &= -\sin\theta\ddot\phi + \cos\theta\ddot\chi - \dot\theta\dot\sigma \\
&= -3H\dot s - V_s - \dot\theta\dot\sigma .
\end{aligned}
$$

Hence one obtains

$$
\dot\theta = -\frac{V_s}{\dot\sigma}, \tag{5.26}
$$

where we have used the background equations of motion, $\dot s = \ddot s = 0$. The potential gradient orthogonal to the inflaton direction is given by

$$
\begin{aligned}
V_s &= \frac{1}{\dot\sigma}(\dot\phi V_\chi - \dot\chi V_\phi) \\
&= -\sin\theta V_\phi + \cos\theta V_\chi .
\end{aligned}
\tag{5.27}
$$

The classical trajectory is curved in field space if $\dot\theta \neq 0$. When $\dot\theta = 0$, the adiabatic and entropy perturbations decouple.

At the second order, we define [129]

$$\begin{aligned}
\delta\sigma &\equiv \delta\sigma^{(1)} + \delta\sigma^{(2)} \\
&= \cos\theta(\delta\phi^{(1)} + \delta\phi^{(2)}) + \sin\theta(\delta\chi^{(1)} + \delta\chi^{(2)}) + \frac{\delta s \dot{\delta s}}{2\dot{\sigma}}, \qquad (5.28) \\
\delta s &\equiv \delta s^{(1)} + \delta s^{(2)} \\
&= -\sin\theta(\delta\phi^{(1)} + \delta\phi^{(2)}) + \cos\theta(\delta\chi^{(1)} + \delta\chi^{(2)}) - \frac{\delta\sigma}{\dot{\sigma}}\left(\dot{\delta s} + \frac{\dot{\theta}\delta\sigma}{2}\right). \qquad (5.29)
\end{aligned}$$

Note that $\delta s^{(1)}$ and $\delta s^{(2)}$ are gauge invariant, while $\delta\sigma^{(1)}$ and $\delta\sigma^{(2)}$ are not. The second order entropy perturbation, $\delta s^{(2)}$, contains the first order adiabatic perturbation since the adiabatic and entropy fields are defined locally in the covariant formalism [129]. The first order perturbations are decomposed into adiabatic and entropy directions with respect to a background trajectory in the field space that depends only on time. The second order perturbations, on the other hand, are sensitive to the first order fluctuations of the field trajectory that depends also on position. The space dependence is dictated to the combination of the first order adiabatic and entropy perturbations in the last term of Eq. (5.29) in a gauge invariant fashion.

Since the second order adiabatic perturbation, $\delta\sigma^{(2)}$, is not gauge invariant, on contrary to $\delta s^{(2)}$, it is useful to consider an non-linear gauge invariant variable (on large scales), ζ. On large scales uniform energy density and comoving (uniform σ) hypersurfaces coincide, thus from Eq. (5.6) we have

$$\zeta = -\psi - \int_{\bar{\sigma}}^{\sigma} \frac{\alpha'}{\tilde{\sigma}'} d\tilde{\sigma}, \qquad (5.30)$$

where primes have been used for Lie derivatives in order for us to be careful. We will expand this expression up to the second order in later subsections on both spatially flat (subsection 5.2.3) and uniform energy density gauges (subsection 5.2.4).

How does ζ evolve in time with decompositions (5.28) and (5.29)? By using

Eq. (5.8), we can write the second-order evolution equation of ζ in terms of entropy perturbations, $\delta s = \delta s^{(1)} + \delta s^{(2)}$ [129]. Now on uniform energy density gauge, $\delta\rho = \delta(\frac{1}{2}\sigma'^2 + V) = 0$, and hence $\delta p = -2\delta V$. Then one obtains

$$\dot{\zeta} = \frac{2H\delta V}{\dot{\sigma}^2 - 2\delta V}. \tag{5.31}$$

This equation is fully non-linear on large scales and can be expanded up to the desired order. With the definitions of $\delta\sigma$ and δs up to the second order, we expand δV as

$$\begin{aligned} \delta V \;\simeq\;& V_\phi(\delta\phi^{(1)} + \delta\phi^{(2)}) + V_\chi(\delta\chi^{(1)} + \delta\chi^{(2)}) \\ &+\frac{1}{2}V_{\phi\phi}(\delta\phi^{(1)})^2 + V_{\phi\chi}\delta\phi^{(1)}\delta\chi^{(1)} + \frac{1}{2}V_{\chi\chi}(\delta\chi^{(1)})^2 \qquad (5.32)\\ =\;& V_\sigma\left(\delta\sigma^{(1)} + \delta\sigma^{(2)} - \frac{1}{2\dot{\sigma}}\delta s\dot{\delta s}\right) + V_s\left(\delta s^{(1)} + \delta s^{(2)} + \frac{1}{\dot{\sigma}}\delta\sigma\dot{\delta s} + \frac{\dot{\theta}}{2\dot{\sigma}}\delta\sigma^2\right) \\ &+\frac{1}{2}V_{\sigma\sigma}(\delta\sigma^{(1)})^2 + V_{\sigma s}\delta\sigma^{(1)}\delta s^{(1)} + \frac{1}{2}V_{ss}(\delta s^{(1)})^2. \qquad (5.33)\end{aligned}$$

On large scales the comoving gauge ($\delta\sigma^{(1)} = \delta\sigma^{(2)} = 0$) coincides with uniform energy density gauge. Thus we obtain

$$\dot{\zeta}(t) = -\frac{2H}{\dot{\sigma}}\dot{\theta}(\delta s^{(1)} + \delta s^{(2)}) + \frac{H}{\dot{\sigma}^2}(V_{ss} + 4\dot{\theta}^2)\delta s^{(1)2} - \frac{H}{\dot{\sigma}^3}V_\sigma\delta s^{(1)}\dot{\delta s^{(1)}}, \tag{5.34}$$

where dots denote time-derivatives with respect to the physical time. If there is no entropy perturbation on large scales, ζ stays constant after the Hubble-horizon crossing. Note that the last term is missing in the published version of [129] (corrected in version 3).

Entropy perturbations up to the second order on large scales follow

$$\begin{aligned}
\ddot{\delta s} & +3H\dot{\delta s} + (V_{ss} + 3\dot{\theta}^2)\delta s = \qquad (5.35) \\
- & \frac{\dot{\theta}}{\dot{\sigma}}(\dot{\delta s}^{(1)})^2 - \frac{2}{\dot{\sigma}}\left(\ddot{\theta} + \dot{\theta}\frac{V_\sigma}{\dot{\sigma}} - \frac{3}{2}H\dot{\theta}\right)\delta s^{(1)}\dot{\delta s}^{(1)} - \left(\frac{1}{2}V_{sss} - 5\frac{\dot{\theta}}{\dot{\sigma}}V_{ss} - 9\frac{\dot{\theta}^3}{\dot{\sigma}}\right)(\delta s^{(1)})^2,
\end{aligned}$$

where we have ignored gradient terms. Note that

$$\begin{aligned}
V_{ss} &= \frac{1}{\dot{\sigma}^2}(\dot{\phi}^2 V_{\chi\chi} - 2\dot{\phi}\dot{\chi}V_{\phi\chi} + \dot{\chi}^2 V_{\phi\phi}) \qquad (5.36) \\
&= (\sin\theta)^2 V_{\phi\phi} - 2\cos\theta\sin\theta V_{\phi\chi} + (\cos\theta)^2 V_{\chi\chi}, \\
V_{sss} &= \frac{1}{\dot{\sigma}^3}(\dot{\phi}^3 V_{\chi\chi\chi} - 3\dot{\phi}^2\dot{\chi}V_{\phi\chi\chi} + 3\dot{\phi}\dot{\chi}^2 V_{\phi\phi\chi} - \dot{\chi}^3 V_{\phi\phi\phi}) \qquad (5.37) \\
&= -(\sin\theta)^3 V_{\phi\phi\phi} + 3\cos\theta(\sin\theta)^2 V_{\phi\phi\chi} - 3(\cos\theta)^2\sin\theta V_{\phi\chi\chi} + (\cos\theta)^3 V_{\chi\chi\chi}.
\end{aligned}$$

Note also that

$$\begin{aligned}
V_{\sigma\sigma} &= \frac{1}{\dot{\sigma}^2}(\dot{\phi}^2 V_{\phi\phi} + 2\dot{\phi}\dot{\chi}V_{\phi\chi} + \dot{\chi}^2 V_{\chi\chi}) \qquad (5.38) \\
&= (\cos\theta)^2 V_{\phi\phi} + 2\cos\theta\sin\theta V_{\phi\chi} + (\sin\theta)^2 V_{\chi\chi}, \\
V_{\sigma s} &= \sin\theta\cos\theta(V_{\chi\chi} - V_{\phi\phi}) + (\cos^2\theta - \sin^2\theta)V_{\phi\chi}. \qquad (5.39)
\end{aligned}$$

It is convenient to separate random Gaussian variables (initial perturbations) and their time evolutions as

$$\begin{aligned}
\zeta(t,\mathbf{x}) &= \zeta_*(\mathbf{x}) + \delta s_*(\mathbf{x})\mathcal{T}_\zeta^{(1)}(t,\mathbf{x}) + \delta s_*^2(\mathbf{x})\mathcal{T}_\zeta^{(2)}(t,\mathbf{x}), \qquad (5.40) \\
\delta s(t,\mathbf{x}) &= \delta s_*(\mathbf{x})\mathcal{T}_{\delta s}^{(1)}(t,\mathbf{x}) + \delta s_*^2(\mathbf{x})\mathcal{T}_{\delta s}^{(2)}(t,\mathbf{x}), \qquad (5.41)
\end{aligned}$$

where ζ_* and δs_* are the initial values at the Hubble-horizon exit. The subscript $*$ denotes a value evaluated at the Hubble-horizon exit. We will solve transfer functions, $\mathcal{T}_{\zeta,\delta s}$, for ζ and δs from the Hubble-horizon exit to the coherent oscillation phase. During the coherent oscillation phase, scalar fields are distributed homogeneously, and there the synchronicity of time is not broken after inflation. Thus, one may ignore spatial dependence in transfer functions $\mathcal{T}_{\zeta,\delta s}(t,\mathbf{x}) \simeq \mathcal{T}_{\zeta,\delta s}(t)$ on large scales. This is not the case if instability grows exponentially, for instance, preheating happens. (We have confirmed this explicitly by using a lattice simulation.)

5.2.3 Perturbations from slow-roll inflation

Now let us evaluate ζ_* at the Hubble-horizon exit, using slow-roll parameters. Since $V_s \simeq 0$, which follows from slow-roll field equations, there is only one slope parameter, ϵ:

$$\epsilon \equiv -\frac{\dot{H}}{H^2} = \frac{1}{2}\left(\frac{\dot{\sigma}}{H}\right)^2 = 2\left(\frac{H_\sigma}{H}\right)^2 \simeq \frac{1}{2}\left(\frac{V_\sigma}{V}\right)^2. \tag{5.42}$$

On the other hand, there are three $[N(N+1)/2]$ curvature parameters, η_{IJ}:

$$\eta_{IJ} \equiv \frac{V_{IJ}}{V}. \tag{5.43}$$

The background slow-roll solution is described by

$$\frac{1}{2}\dot{\sigma}^2 = -\dot{H} = \epsilon H^2 \simeq \frac{\epsilon}{3}V, \tag{5.44}$$

$$\dot{\theta} \simeq -\eta_{\sigma s}H, \tag{5.45}$$

where $V_s \simeq 0$. Note that $\dot{\theta} = -V_s/\dot{\sigma} \neq 0$ as $\dot{\sigma}$ is slowly rolling. The linear perturbations on large scales obey

$$\dot{\delta\sigma} \simeq (2\epsilon - \eta_{\sigma\sigma})H\delta\sigma - 2\eta_{\sigma s}H\delta s, \tag{5.46}$$

$$\dot{\delta s} \simeq -\eta_{ss}H\delta s, \tag{5.47}$$

where $\delta\sigma$ is evaluated in spatially flat gauge ($\psi = 0$).

How about the second order? Adiabatic curvature perturbations on uniform energy density hypersurfaces, ζ, can be expanded from Eq. (5.30) to the second order as [129, 130]

$$\zeta = -\psi - \frac{H}{\dot{\sigma}}\delta\sigma - \frac{\delta\sigma}{\dot{\sigma}}\left[-\left(\frac{H}{\dot{\sigma}}\delta\sigma\right)^{\cdot} + \frac{1}{2}\left(\frac{H}{\dot{\sigma}}\right)^{\cdot}\delta\sigma + \frac{H}{\dot{\sigma}}\dot{\theta}\delta s\right]. \tag{5.48}$$

Its evolution on large scales is governed by Eq. (5.34). If we employ the flat gauge ($-\psi = 0$ by definition.), and Taylor-expand the second term in Eq. (5.30) with respect to $\delta\sigma$, we get

$$\zeta^{\rm flat} = -\frac{H}{\dot{\sigma}}\delta\sigma - \frac{1}{2\dot{\sigma}}\left(\frac{H}{\dot{\sigma}}\right)^{\cdot}\delta\sigma^2 + \frac{H}{\dot{\sigma}^2}\dot{\theta}\delta s\delta\sigma, \tag{5.49}$$

where the first order Mukhanov-Sasaki equation has been used. Eq. (5.49) can be rewritten in terms of slow-roll parameters as [130]

$$\zeta \simeq -\frac{1}{\sqrt{2\epsilon}}\delta\sigma + \frac{1}{2}\left(1 - \frac{\eta_{\sigma\sigma}}{2\epsilon}\right)\delta\sigma^2 - \frac{\eta_{\sigma s}}{2\epsilon}\delta\sigma\delta s, \tag{5.50}$$

where we have used Eq. (5.47) in Eq. (5.29);

$$\delta\sigma \simeq \delta\sigma^{(1)} - \frac{\eta_{ss}}{2\sqrt{2\epsilon}}\delta s^2. \tag{5.51}$$

5.2.4 The δN formalism

In this subsection we will show the formula that δN is simply expanded as a Taylor series with respect to the initial field fluctuations.

According to the δN formalism [131, 132, 124], ζ on large scales is equivalent to the perturbation of the number of efolds $N(t_f, t_i, \mathbf{x})$ from an initial uniform curvature (flat) hypersurface at at $t = t_i$ to a final uniform energy density (or comoving) hypersurface at $t = t_f$. Hence ζ is given by

$$\zeta(t_f, \mathbf{x}) = \delta N(t_f, t_i, \mathbf{x}) \equiv N(t_f, t_i, \mathbf{x}) - N_0(t_f, t_i), \tag{5.52}$$

where N is the local number of efolds integrated along the comoving observers;

$$N(t_f, t_i, \mathbf{x}) \equiv \int_i^f d\tau \tilde{H} = \ln[\tilde{a}(t_f, \mathbf{x})/\tilde{a}(t_i \mathbf{x})], \tag{5.53}$$

$$N_0(t_f, t_i) \equiv \int_i^f dt H = \ln[a(t_f)/a(t_i)], \tag{5.54}$$

where N_0 is the background value.

To use this formalism we assume the *separate universe*; after the universe has been smoothed on the comoving scale much larger than the horizon, the evolution of local regions (smaller than the smoothing scale) is described by some background universe. Given a content of the universe, this assumption can be checked by the gradient expansion method [139, 132].

In inflationary scenarios, one can take $t_i = t_*$ as the time when the relevant perturbation scales of one or more light scalar fields stretched over more than a few times the Hubble horizon, $H^{-1} = (k/a)^{-1}$. On an initially flat slice, each field $\varphi_I(t_*, \mathbf{x})$ can be split into a background value and its perturbation as $\bar{\varphi}_I(t_*) + \delta\varphi_I(t_*, \mathbf{x})$. One can take t_f as the time during or after inflation. Then ζ is given by [131, 132, 137]

$$\delta N(t_f, t_*, \mathbf{x}) = N[\rho(t_f), \varphi_1(t_*, \mathbf{x}), \varphi_2(t_*, \mathbf{x}), \cdots] - N_0[(\rho(t_f), \bar{\varphi}_1(t_*), \bar{\varphi}_2(t_*), \cdots)] \tag{5.55}$$

Now one can expand δN, which is defined on initial uniform curvature hypersurface and final uniform density hypersurface, up to the second order with respect to field perturbations at horizon crossing as [127]

$$\zeta = \delta N = \sum_I N_I \delta\varphi_{I*} + \frac{1}{2} \sum_{I,J} N_{IJ} \delta\varphi_{I*} \delta\varphi_{J*}, \tag{5.56}$$

where

$$
\begin{aligned}
N_I &\equiv \frac{\partial N}{\partial \varphi_{I*}}, && (5.57)\\
N_{IJ} &\equiv \frac{\partial^2 N}{\partial \varphi_{I*}\partial \varphi_{J*}}. && (5.58)
\end{aligned}
$$

5.2.5 Bispectrum and non-Gaussianity

We define non-Gaussianity of the local type as [140]

$$
\begin{aligned}
\frac{3}{5}f_{NL} &\equiv \frac{B_\zeta(k_1,k_2,k_3)}{2[P_\zeta(k_1)P_\zeta(k_2)+P_\zeta(k_2)P_\zeta(k_3)+P_\zeta(k_3)P_\zeta(k_1)]} && (5.59)\\
&\simeq \frac{\prod_i k_i^3}{\sum_i k_i^3}\frac{B_\zeta}{8\pi^4[\Delta_\zeta^2]^2}, && (5.60)
\end{aligned}
$$

where the factor 3/5 comes from the relation during matter domination before horizon reentry, $\Phi = 3\zeta/5$ [40]. A famous paper by Maldacena [121] defined f_{NL} with opposite sign, $\Phi = -3\zeta_{there}/5$. Note that the model is based on the slow-roll inflation scenario. In evaluating the bispectrum, one has to eliminate uninteresting constant zero-mode, equivalently, to impose a condition, $\langle\zeta(x)\rangle = \langle\zeta_L(x)\rangle = 0$.

How do we recast non-linearity in Eq. (5.34) on the non-linear coupling constant, f_{NL}, in order to compare with observational bispectra? The theory in the previous section tells us that

$$
\begin{aligned}
\zeta^{(1)}(t) &= \zeta_*^{(1)} + \delta s_* \mathcal{T}_\zeta^{(1)}(t),\\
\mathcal{T}_\zeta^{(1)}(t) &= \int_*^t dt' \frac{-2H}{\dot\sigma}\dot\theta \mathcal{T}_{\delta s}^{(1)}(t'), && (5.61)\\
\zeta^{(2)}(t) &= \zeta_*^{(2)} + \delta s_*^2 \mathcal{T}_\zeta^{(2)}(t),\\
\mathcal{T}_\zeta^{(2)}(t) &= \int_*^t dt' \left[\frac{-2H}{\dot\sigma}\dot\theta \mathcal{T}_{\delta s}^{(2)}(t') + \frac{H}{\dot\sigma^2}(V_{ss}+4\dot\theta^2){\mathcal{T}_{\delta s}^{(1)}}^2(t') \right. && (5.62)\\
&\quad \left. -\frac{H}{\dot\sigma^3}V_\sigma \mathcal{T}_{\delta s}^{(1)}(t')\dot{\mathcal{T}}_{\delta s}^{(1)}(t')\right].
\end{aligned}
$$

Given solutions of entropy perturbations in each order, $\mathcal{T}_{\delta s}^{(1)}(t)$ and $\mathcal{T}_{\delta s}^{(2)}(t)$, one obtains ζ by (numerical) integration. Since $\langle\zeta\rangle = 0$, we shift ζ by a constant function in space:

$$\begin{aligned} \zeta &\rightarrow \tilde{\zeta} = \tilde{\zeta}_* + \delta s_* \mathcal{T}_\zeta^{(1)}(t) + \left(\delta s_*^2 - \langle \delta s_*^2 \rangle\right) \mathcal{T}_\zeta^{(2)}(t), \qquad (5.63) \\ \zeta_* &\rightarrow \tilde{\zeta}_*, \end{aligned}$$

where $\langle\tilde{\zeta}_*\rangle = 0$. This shift corresponds to renormalizing a scale factor.

$$a(t) \rightarrow \tilde{a}(t), \qquad (5.64)$$

$$e^{2\zeta} a^2(t) d\mathbf{x}^2 = e^{2\tilde{\zeta}+2C} a^2(t) d\mathbf{x}^2 = e^{2\tilde{\zeta}} \tilde{a}^2(t) d\mathbf{x}^2, \qquad (5.65)$$

where $2C = \langle \delta s_*^{(1)^2} \rangle \mathcal{T}_\zeta^{(2)}(t)$. With this renormalized ζ [Eq. (5.63)], one can find a simple relationship

$$\frac{3}{5} f_{NL}^{\text{horizon}} = \frac{\left(\frac{\eta_{ss}}{4\epsilon}\right)_* \left[\mathcal{T}_\zeta^{(1)}(t)\right]^2 - \left(\frac{\eta_{\sigma s}}{2\epsilon}\right)_* \left(\frac{H}{\dot{\sigma}}\right)_* \mathcal{T}_\zeta^{(1)}(t) + \left(\frac{1}{2} - \frac{\eta_{\sigma\sigma}}{4\epsilon}\right)_* \left(\frac{H}{\dot{\sigma}}\right)_*^2}{\left[\left(\frac{H}{\dot{\sigma}}\right)_*^2 + \left(\mathcal{T}_\zeta^{(1)}(t)\right)^2\right]^2}, \qquad (5.66)$$

$$\frac{3}{5} f_{NL}^{\text{transfer}} = \frac{\left[\mathcal{T}_\zeta^{(1)}(t)\right]^2 \mathcal{T}_\zeta^{(2)}(t)}{\left[\left(\frac{H}{\dot{\sigma}}\right)_*^2 + \left(\mathcal{T}_\zeta^{(1)}(t)\right)^2\right]^2}, \qquad (5.67)$$

where $f_{NL} = f_{NL}^{\text{horizon}} + f_{NL}^{\text{transfer}}$. Here f_{NL}^{horizon} is the non-Gaussianity of ζ_* and expected to be slow-roll suppressed, while f_{NL}^{transfer} represents the non-Gaussianity parameter of curvature perturbations generated from entropy perturbations after the Hubble-horizon exit. In two-field inflation, typically, $(H/\dot{\sigma})_*^2 = 1/(2\epsilon_*) \sim 20$ and $\mathcal{T}_\zeta^{(1)} \sim 5$ at the end of inflation. Hence $f_{NL}^{\text{transfer}} \sim 10^{-2} \mathcal{T}_\zeta^{(2)}$. This f_{NL} is scale independent because we have assumed scale-invariant power spectrum for Δ_ζ^2 and $\Delta_{\delta s}^2$. We ignored higher order correlations and cross correlation, $\Delta_{\zeta\delta s}^2$.

In order to understand f_{NL}^{transfer} in detail, we rewrite it in terms of entropy perturbations as

$$
\begin{aligned}
f_{NL}^{\text{transfer}} &= f_{NL}^{\text{intrinsic}} + f_{NL}^{ss} + f_{NL}^{s\dot{s}}, && (5.68)\\
f_{NL}^{\text{intrinsic}} &\equiv \frac{-5\left[\mathcal{T}_\zeta^{(1)}\right]^2}{3\left[\left(\frac{H}{\dot\sigma}\right)_*^2 + \left(\mathcal{T}_\zeta^{(1)}\right)^2\right]^2}\int_* dt\,\frac{2H}{\dot\sigma}\dot\theta\mathcal{T}_{\delta s}^{(2)}, && (5.69)\\
f_{NL}^{ss} &\equiv \frac{5\left[\mathcal{T}_\zeta^{(1)}\right]^2}{3\left[\left(\frac{H}{\dot\sigma}\right)_*^2 + \left(\mathcal{T}_\zeta^{(1)}\right)^2\right]^2}\int_* dt\,\frac{H}{\dot\sigma^2}(V_{ss}+4\dot\theta^2)\left[\mathcal{T}_{\delta s}^{(1)}\right]^2, && (5.70)\\
f_{NL}^{s\dot{s}} &\equiv \frac{-5\left[\mathcal{T}_\zeta^{(1)}\right]^2}{3\left[\left(\frac{H}{\dot\sigma}\right)_*^2 + \left(\mathcal{T}_\zeta^{(1)}\right)^2\right]^2}\int_* dt\,\frac{H}{\dot\sigma^3}V_\sigma\mathcal{T}_{\delta s}^{(1)}\dot{\mathcal{T}}_{\delta s}^{(1)}. && (5.71)
\end{aligned}
$$

One can easily see that f_{NL}^{ss} always contributes to f_{NL} in a positive way and cumulates over time unless the entropic mode is tachyonic. Indeed, the second term keeps growing and become a dominant source of positive contributions to non-Gaussianity during oscillations of fields. On the other hand, other terms can be both positive and negative.

Based on the δN formalism in the previous subsection 5.2.4, one can derive the corresponding non-Gaussianity parameter as [127]

$$\frac{3}{5}f_{NL} = \frac{\sum_{I,J} N_I N_J N_{IJ}}{2[\sum_K N_K N_K]^2}. \tag{5.72}$$

5.3 Two-field Model for Inflation and Coherent Oscillation: Numerical Analysis

Given the formulation above, we compute non-Gaussianity numerically in both the δN formalism and integrating the evolution of ζ on super-Hubble scales from the

Hubble-horizon exit to the coherent oscillation phase.

Both formalisms can be applied to the physics of interacting scalar fields during and after inflation. We employ simple interactions, such as

$$V(\phi,\chi) = \frac{m_\phi^2}{2}\phi^2 + \frac{m_\chi^2}{2}\chi^2 + \frac{g^2}{2}\phi^2\chi^2. \tag{5.73}$$

We do not consider self-interactions except mass terms. In general there would be other renormalizable interactions like, $\phi\chi^2$, $\phi\chi^3$, derivative couplings, as well as non-renormalizable terms.

With the potential (5.73), the system could undergo single or double inflation, coherent oscillation, and preheating. We consider initial slow-roll inflation to the subsequent coherent oscillations with two *light* or *active* scalar fields whose effective masses are given by $m^{\rm eff} < 3H_*/2$, at the Hubble horizon exit. If one of the scalar fields is *heavy* or *inactive*, $m^{\rm eff} > 3H_*/2$, its vacuum fluctuation does not leave the Hubble horizon. Also, the heavy field quickly rolls down to its instantaneous minimum of the effective potential and becomes decoupled from the dynamics of the rest of active fields.

Although our ultimate goal is to test preheating models by non-Gaussianity, it is worth scrutinizing the case without interaction in order to obtain insights. In the following subsections we scrutinize this model without interaction ($g^2 = 0$). In Sec. 5.4 we comment on the possibility of non-Gaussianity from preheating with $g^2 \neq 0$.

Inflationary attractor initial condition

Inflationary solutions of coupled Eqs. (5.11) and (5.12) are attractor solutions; whatever the field values one chooses as an initial condition, the solution flow of the system quickly approaches to the attractor. We set the initial condition for the background equations by solving slow-roll equations so that the solution immediately reach the attractor. Our simulations last longer than the end of inflation.

Since we are relying on equations valid only on large scales, initial conditions and parameters for fluctuations must be chosen carefully. Information inside the Hubble-horizon is not included in the perturbed equations presented in this chapter.

The solution of the Mukhanov-Sasaki equation, which describes the perturbations of a (effectively) massive scalar field, is given by [141, 142]

$$\Delta^2_{\delta\varphi}(k) \equiv \frac{k^3}{2\pi^2}|\delta\varphi_k(\tau)|^2 = \frac{H^2}{8\pi}(-k\tau)^3|H^{(1)}_\nu(-k\tau)|^2 \tag{5.74}$$

$$\approx \left(\frac{H}{2\pi}\right)^2 2^{2\nu-3}\left[\frac{\Gamma(\nu)}{\Gamma(3/2)}\right]^2\left(\frac{k}{aH}\right)^{3-2\nu}, \tag{5.75}$$

where $\nu^2 = 9/4 - m^2/H^2$ and $H^{(1)}_\nu(x)$ is a Hankel function of the first kind. Here, $H^{(1)}_\nu(x \ll 1) \approx -i\Gamma(\nu)(x/2)^{-2}/\pi$ is used in the last approximation. This approximation corresponds to the super-horizon limit, $k \ll aH$. Note that $\tau \equiv \int dt/a(t)$ is the conformal time and lies in $-\infty < \tau < 0$. Note also that the relation $-k\tau = k/(aH)$ is used above.

Since we assumed light scalar fields, $\nu \to 3/2$, for which the spectrum is independent of k. We also assumed that entropy modes must be light at the Hubble-horizon exit. Therefore, our initial conditions for fluctuations are given by

$$\Delta^2_{\delta\phi*} = \Delta^2_{\delta\chi*} = \Delta^2_{\delta s*} = \left(\frac{H_*}{2\pi}\right)^2 \equiv \Delta^2_*, \tag{5.76}$$

$$\Delta^2_{\zeta*} = \left(\frac{H_*}{\dot\sigma_*}\right)^2\Delta^2_*, \tag{5.77}$$

$$\langle\delta s_*(\mathbf{k}_1)\delta s_*(\mathbf{k}_2)\delta s_*(\mathbf{k}_3)\rangle = 0, \tag{5.78}$$

where the last equation implies $\delta s^{(2)}_* = 0$.

We solve the perturbation equations (5.34) and (5.35) coupled with the background equations (5.11) and (5.12) from $t = t_*$ to some time after inflation. We also solve eight adjacent background trajectories with eight different initial field values, e.g., $(\phi_* + d\phi, \chi_*)$, and then compute the first and second derivatives of the number of efolds with respect to horizon crossing field values, such as

$$N_\phi = \frac{N(\phi + d\phi, \chi) - N(\phi - d\phi, \chi)}{2d\phi}, \tag{5.79}$$

where $d\varphi_I = 10^{-4}$ is chosen. We checked that the results converged with 10^{-4}. For smaller values of $d\varphi_I$, numerical noise tends to increase.

5.3.1 Two-field model with large mass ratios

Two-field inflation with quadratic potential is characterized by a single parameter, a mass ratio $R \equiv m_\phi/m_\chi$. We employ a convention, $m_I < m_{I+1}$, such as $m_\phi < m_\chi$.

In this subsection we re-examine and clarify the primordial non-Gaussianity from a two-field model with large mass ratios that has been studied in the literature. Vernizzi and Wands [133] studied two-massive-field inflation with the mass ratio, $m_\phi/m_\chi = 1/9$, and Yokoyama et al. [134] did with the mass ratio, $m_\phi/m_\chi = 1/20$. Both of them used the δN formalism and concluded that their result seems to agree with another approach by [135] that solved perturbed equations for ζ on large scales with $m_\phi/m_\chi = 1/12$. We will confirm this statement by directly comparing two approaches.

In this model, we can divide the regime into four: (a) slow-roll inflation driven by heavier field χ, (b) a sharp or gradual turn, (c) the second slow-roll inflation driven by lighter field ϕ, and (d) coherent oscillations of ϕ at the minimum of potential. In regimes (a) and (b) both two fields are active, while in regimes (c) and (d) only lighter field play a role in dynamics.

Case 1: double inflation with $m_\phi/m_\chi = 1/9$

We set the same initial condition as [133]. Initial field values are $\phi_i = \chi_i = 13$. We assume that inflation ends at $\epsilon_e = 1$ and the number of efolds at the end of inflation from the Hubble-horizon exit is $N_e = 60$. We found that ($\phi_* = 12.9281, \chi_* = 8.27202$). The perturbed equations are integrated from this time.

The top of Fig. 5.2 shows that a trajectory in the field space. One find a *turn* in the field space. At the turn, entropy perturbations source ζ through Eq. (5.34). Since the entropy mode becomes heavy and decays sufficiently after the turn, it no longer sources ζ. As shown in the bottom of Fig. 5.2 and Fig. 5.3, ζ and its non-Gaussianity are generated during the turn, respectively. Both of them shows very good agreement with two formalisms at the level of $\lesssim 2\%$. The hight of the peak is ~ 0.22 which agrees precisely in both the δN formalism and the one calculated from Eqs. (5.66) and (5.67). Note that f_{NL} computed here corresponds to $f_{NL}^{(4)}$ in [133].

How do we understand the shape of non-Gaussianity appeared during the turn? The cause of the tiny net effect is the precise cancellation between terms in Eq. (5.34). As shown in the top of Fig. 5.3, f_{NL}^{ss} has the sharpest rise due to $4\theta^2$; and then negative contributions from $f_{NL}^{s\dot{s}}$ and $f_{NL}^{\rm intrinsic}$ catch up with it. The value after the turn is given by $f_{NL} \sim 0.007$ that consists of $f_{NL}^{\rm transfer} \sim 0.005$ and $f_{NL}^{\rm horizon} \sim 0.002$. The value before the turn is completely from $f_{NL}^{\rm horizon} \sim 0.021$.

Case 2: double inflation with $m_\phi/m_\chi = 1/20$

We set a similar initial condition as [134]. Initial field values are set to $\phi_i = \chi_i = 10$, and we found ($\phi_* = 9.99920, \chi_* = 9.68230$) by setting $N_e = 50$.

The similar feature as the case 1 can be found in Figs. 5.5 and 5.6. There are a few oscillations in a turn. Each oscillation creates a series of peak and dip. Since the mass ratio is larger, the turn is sharper and leaves imprint on the power spectrum and bispectrum (through non-Gaussianity). Again, the δN formalism and transfer function method agree precisely at the level of $\lesssim 1\%$. The peak value is $f_{NL} \sim 7.5$. The value after the turn is $f_{NL} \sim 0.001$. The value before the turn is

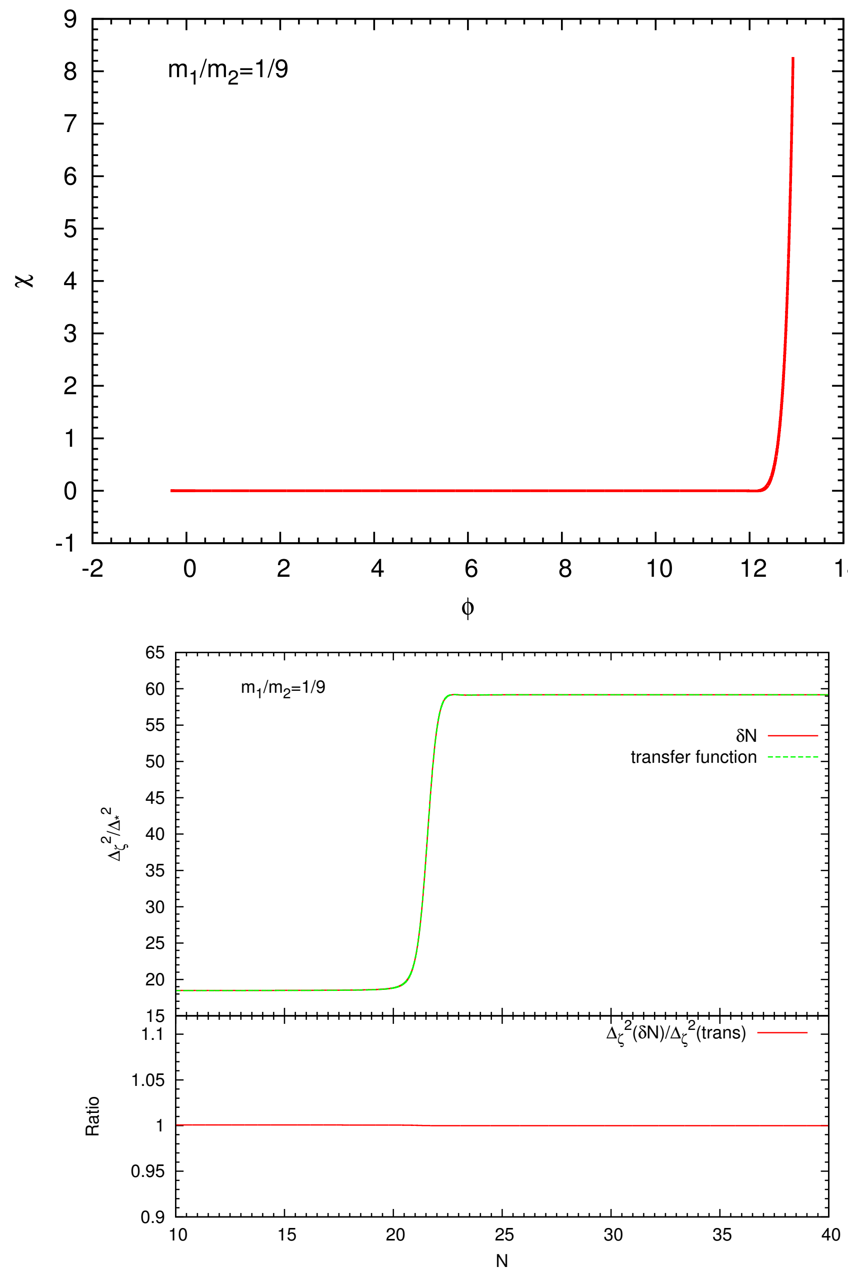

Figure 5.2: [Top] A trajectory of double inflation with a mass ratio 1:9. [Bottom] Evolution of curvature perturbations, ζ.

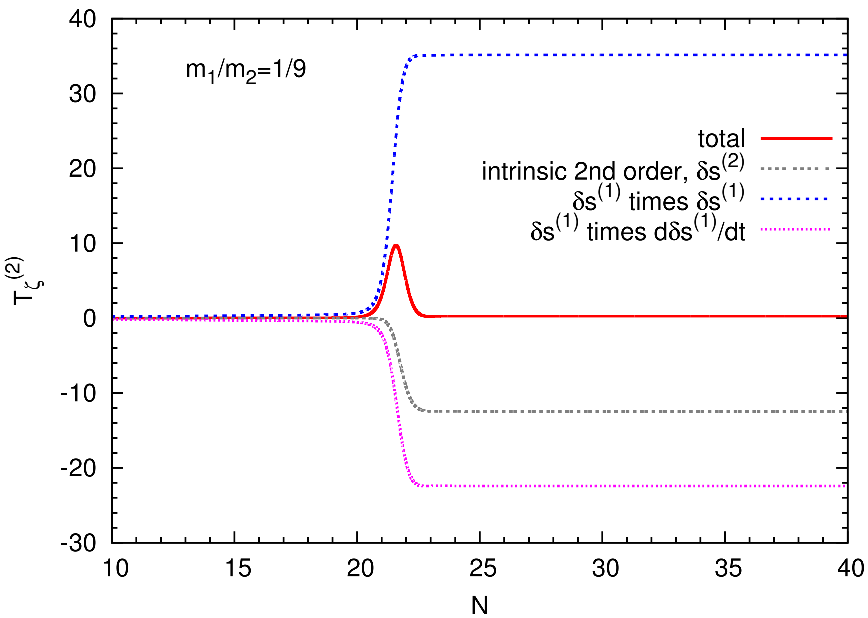

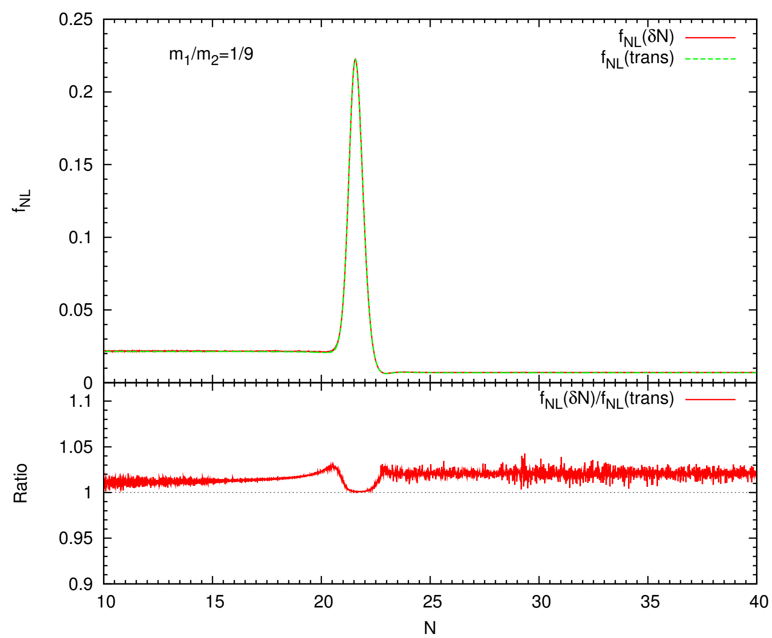

Figure 5.3: [Top] Evolution of the second order transfer function for ζ. [Bottom] Evolution of non-Gaussianity, f_{NL}.

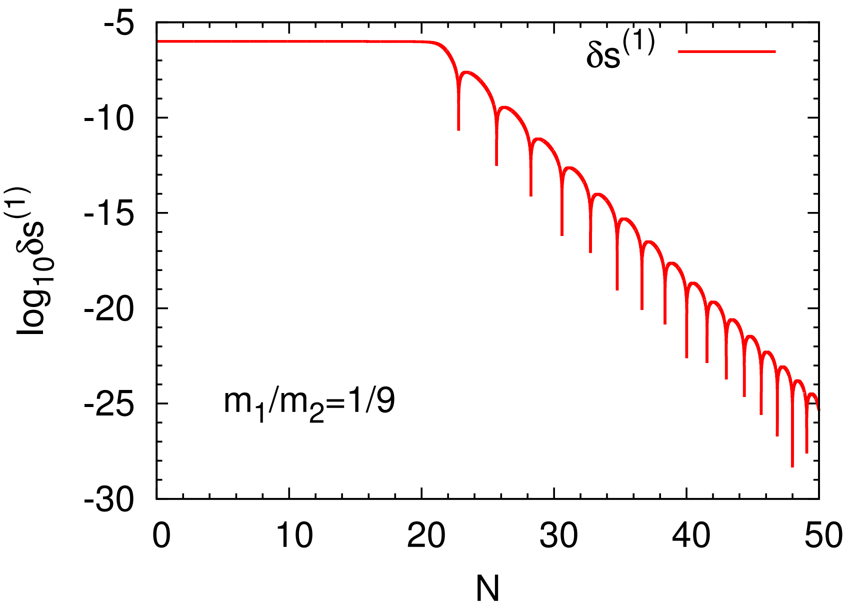

Figure 5.4: Evolution of linear entropy perturbations. $\delta s_* = 10^{-6}$ is chosen.

$f_{NL} \sim 0.002$.

From above two cases, one can gain some insights of the mechanism to generate non-Gaussianity around the turn in the field space. The sharper the turn is, the more non-Gaussianity is peaked. A peak is followed by a dip and erase almost all the traces. The residual non-Gaussianity remains if the turn is slow enough to allow the background quantities, such as the expansion rate, change their vales during the turn.

5.3.2 Two-field model with small mass ratios

Next, we consider the coherent oscillation phase that has two active field. If one of the fields becomes heavy, the entropy direction is shut off and its perturbations decays. The subsequent coherent oscillation phase is described by a single field. In those cases, however many times the adiabatic direction turns, no non-Gaussianity

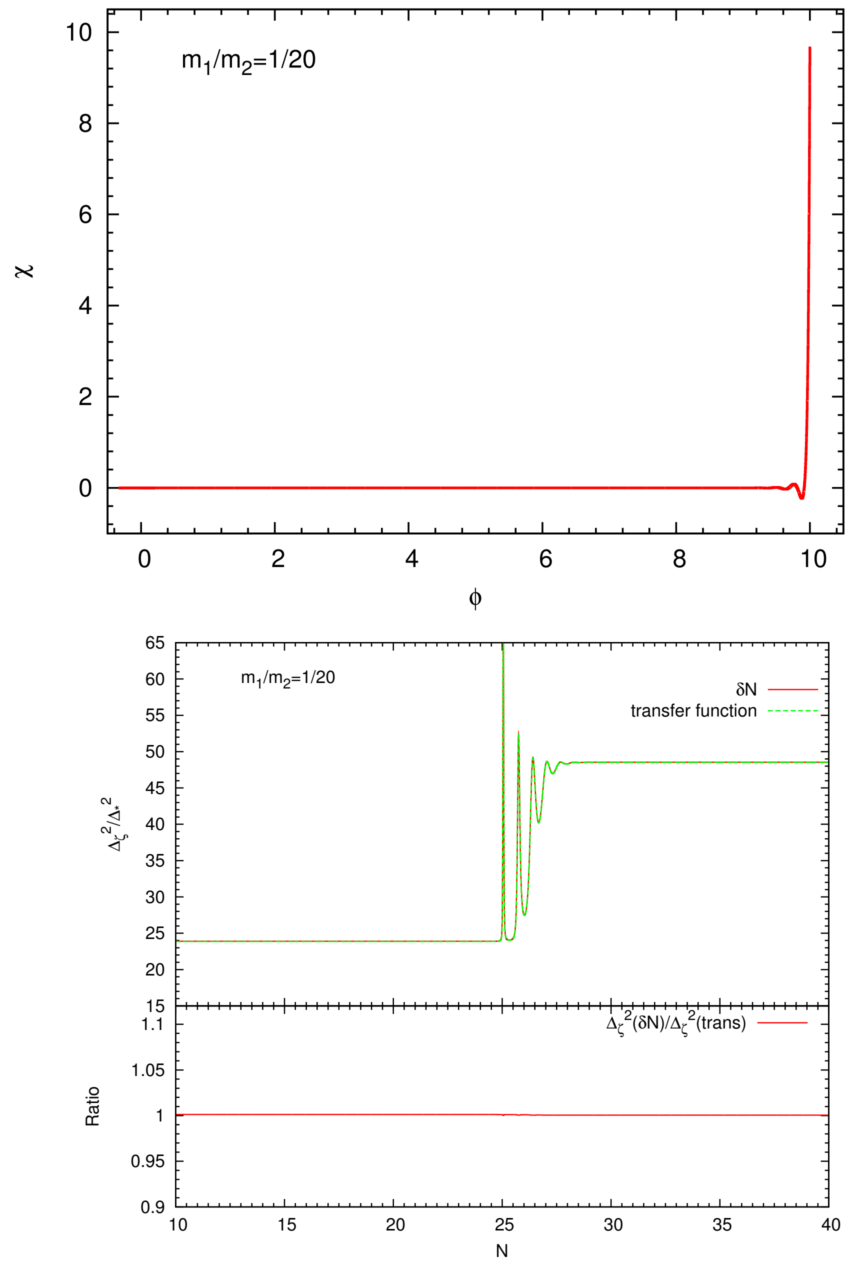

Figure 5.5: [Top] A trajectory of double inflation with a mass ratio 1:20. [Bottom] Evolution of curvature perturbations, ζ.

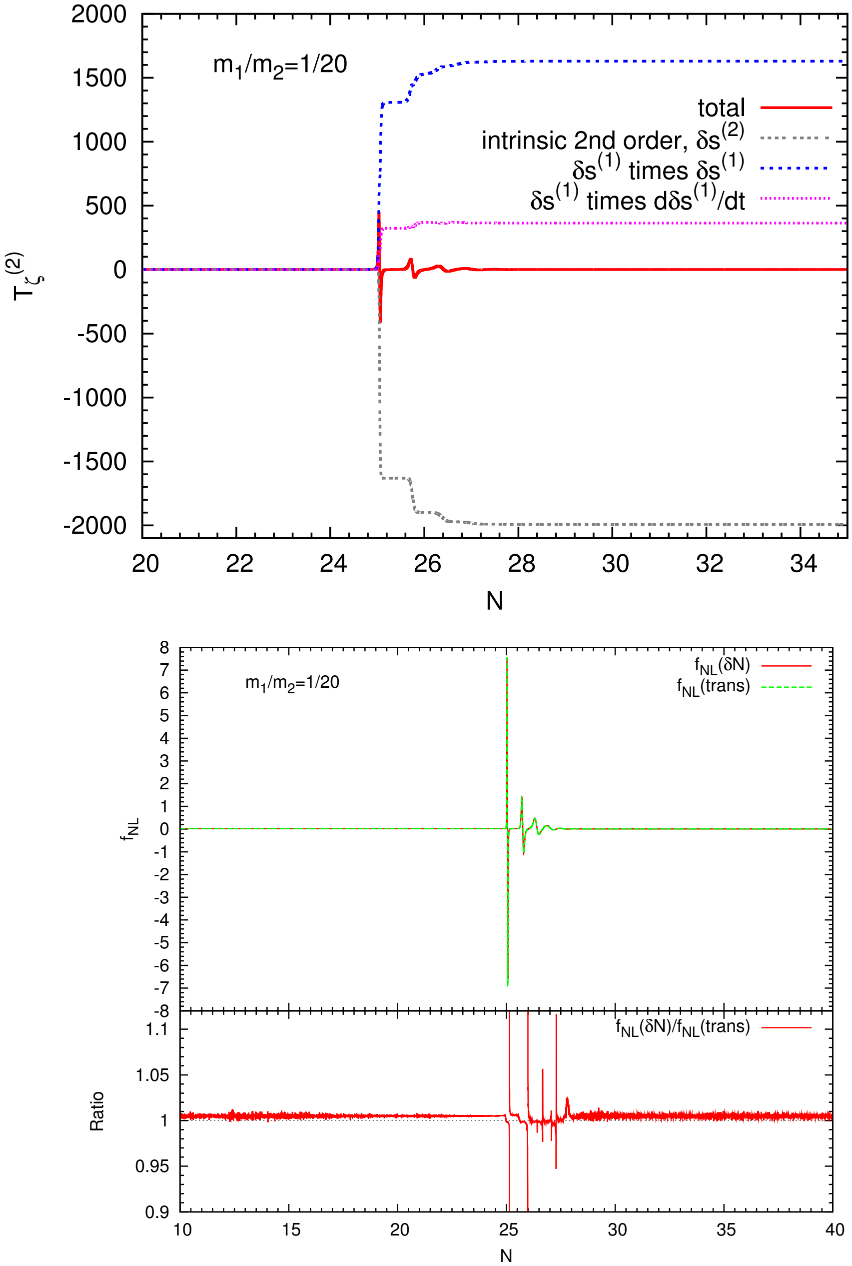

Figure 5.6: [Top] Evolution of the second order transfer function for ζ. [Bottom] Evolution of non-Gaussianity, f_{NL}.

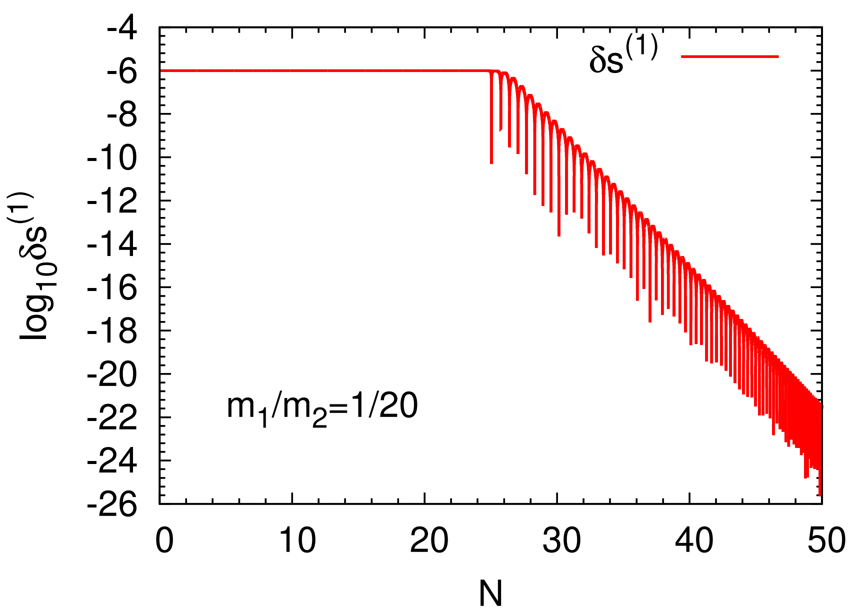

Figure 5.7: Evolution of linear entropy perturbations. $\delta s_* = 10^{-6}$ is chosen.

is generated.

Case 3: inflation and coherent oscillation with $m_\phi/m_\chi = 1/\sqrt{2}$

We set the initial field values $\phi_i = \chi_i = 10$. By setting $N_e = 50$, one finds ($\phi_* = 9.96094, \chi_* = 9.92194$).

In this case, as can be seen from the top of Fig. 5.8, there is no clear turn.until the fields start to oscillate. A small mass ratio implies that the mixing between fields is large.

The linear power spectra computed by two formalisms agrees very good $\lesssim 0.1\%$, while non-Gaussianity shows some discrepancy $\lesssim 18\%$. The value of f_{NL} is very small $\sim 0.007 - 0.009$ and dominated by the contribution from $f_{NL}^{\rm horizon}$. The inaccuracy comes from the leading order slow-roll approximation. If we iterate slow-roll approximation to higher orders, accuracy should be improved.

Where are peaks and dips in f_{NL}? As seen in the top of Fig. 5.9, the terms in the second order ζ are produced and hence a series of peak and dip in total. We cannot see this feature in the bottom of Fig. 5.9 because the number of efolds is chosen as the time variable. Indeed, one can find the peak and dip feature if he/she chooses the characteristic time of oscillation as a time variable (Fig. 5.11).

Case 4: double inflation and coherent oscillation with $m_\phi/m_\chi = 1/4$

Initial field values are set to $\phi_i = \chi_i = 10$. One finds ($\phi_* = 9.98949, \chi_* = 9.83260$) by setting $N_e = 50$.

This case has a turn in the field space, and thus coherent oscillation is almost dominated by the single-field. In top of Fig. 5.9, a huge cancellation in $\zeta^{(2)}$ happens and leaves no signature in f_{NL}. Thus in the single-field limit, there is no net effect on non-Gaussianity during the coherent oscillation phase. This has also happened in cases (a) and (b).

5.4 Preheating and Non-Gaussianity

Entropy mode amplification and suppression

In this section, we turn on the interaction of fields in Eq. (5.73). The importance of preheating in our context is the parametric amplification of entropy perturbations due to the time dependent effective mass,

$$\mu_s^2 \equiv V_{ss} + 3\dot{\theta}^2 = \frac{1}{\dot{\sigma}^2}\left[m_\chi^2\dot{\phi}^2 + m_\phi^2\dot{\chi}^2 + g^2(\phi\dot{\phi} - \chi\dot{\chi})^2\right] + 3\dot{\theta}^2, \tag{5.80}$$

where $\dot{\theta}$ is given by Eq. (5.26). Without resonant interaction, the coherent oscillation phase cannot produce sizable non-Gaussianity because entropy modes are suppressed after inflation as we have seen in the previous section. It is easy to imagine the situation that entropy perturbations are amplified during preheating and sources

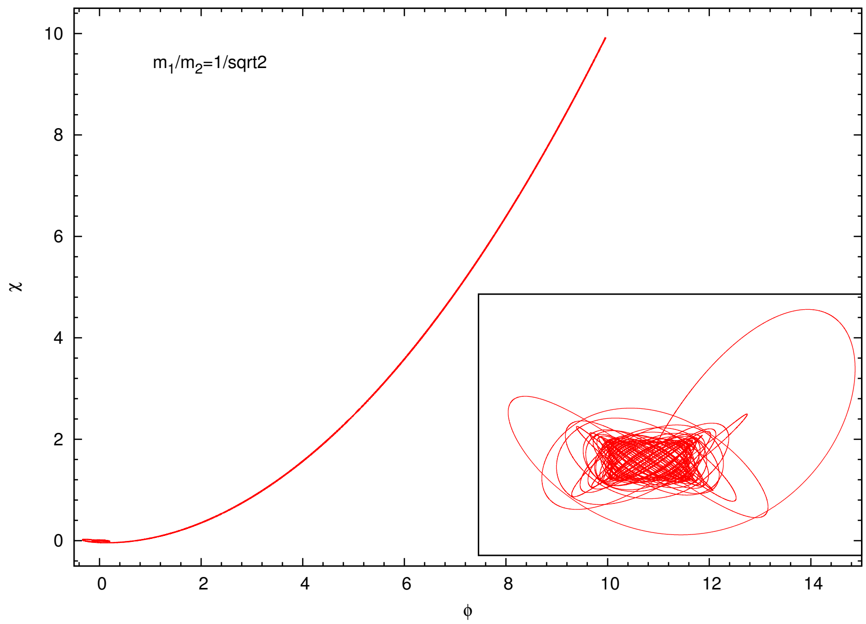

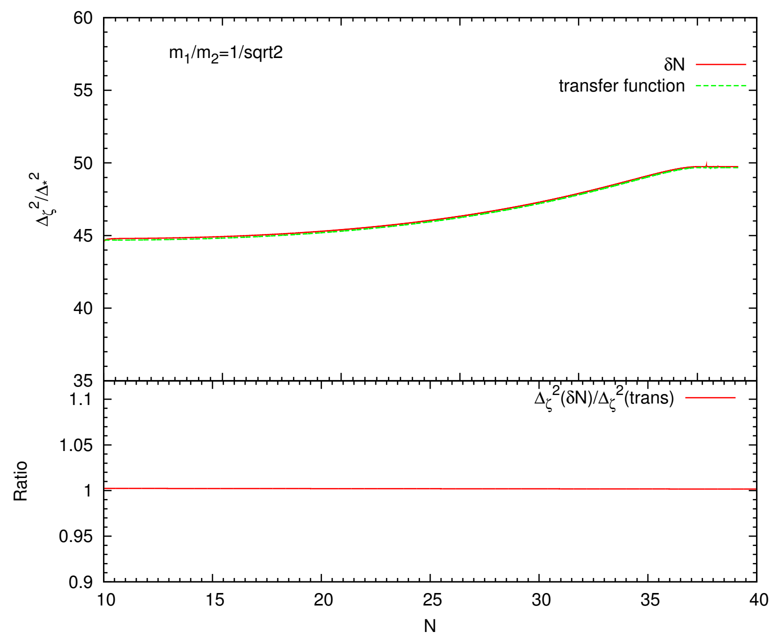

Figure 5.8: [Top] A trajectory of double inflation with a mass ratio 1:$\sqrt{2}$. [Bottom] Evolution of curvature perturbations, ζ.

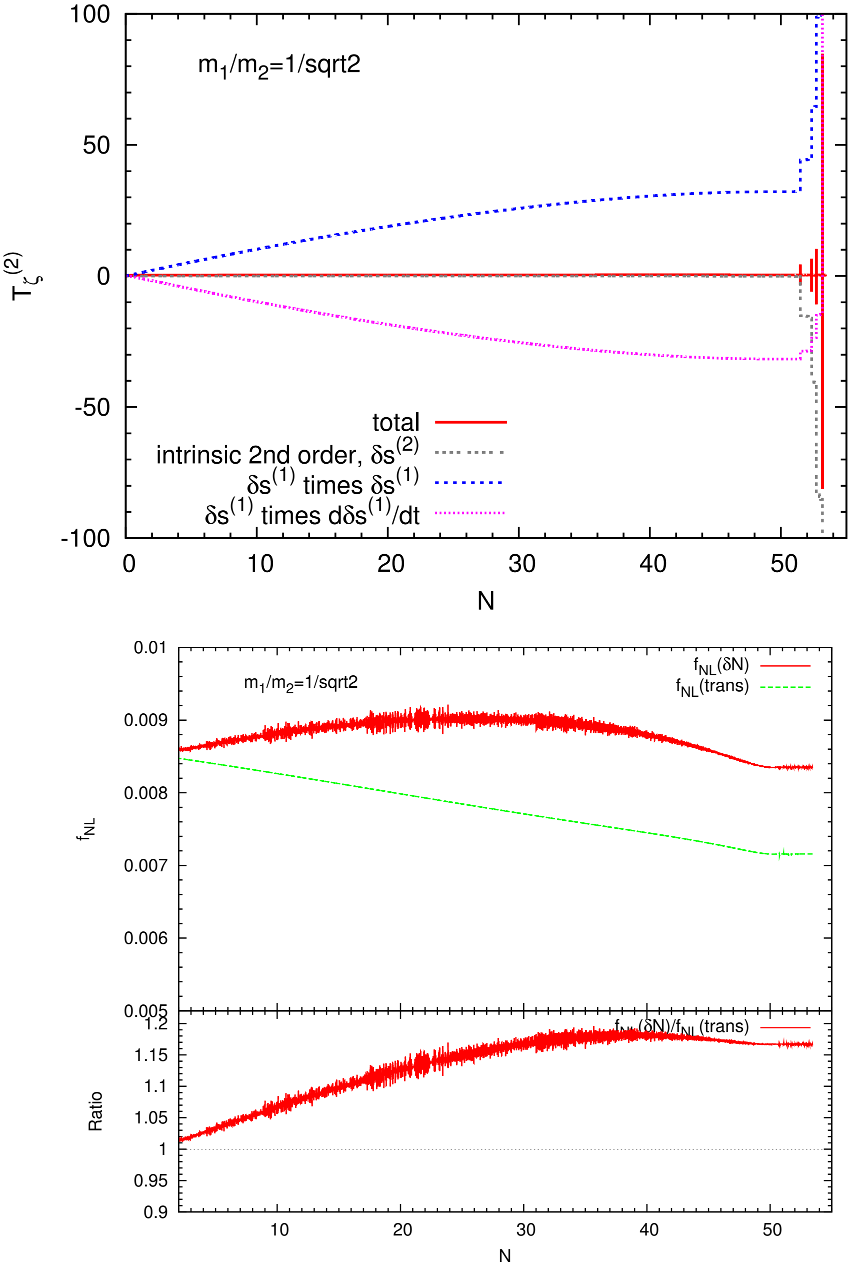

Figure 5.9: [Top] Evolution of the second order transfer function for ζ. [Bottom] Evolution of non-Gaussianity, f_{NL}.

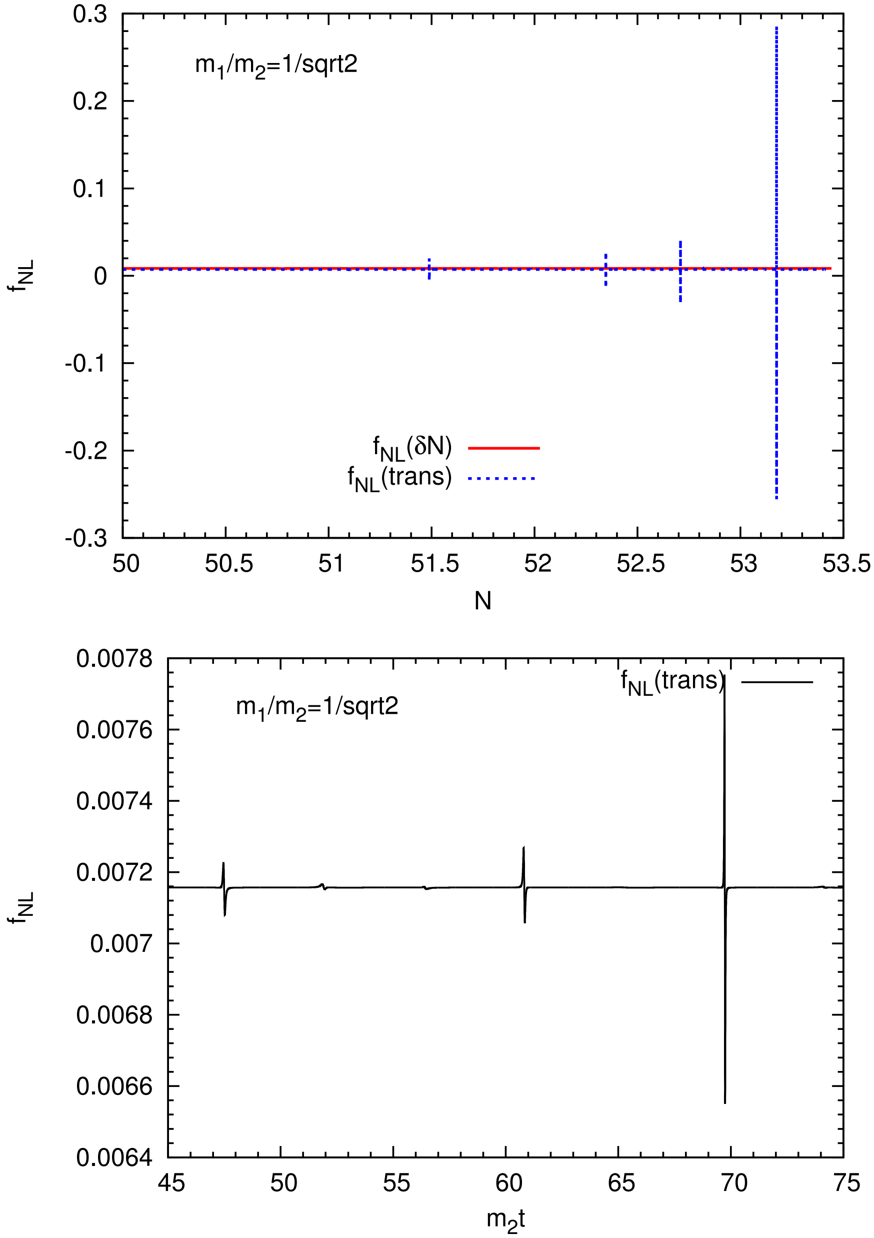

Figure 5.10: Evolution of non-Gaussianity, f_{NL}, as a function of N (top) and the characteristic time, $m_\chi t$ (bottom). The bottom figure focuses on several oscillations.

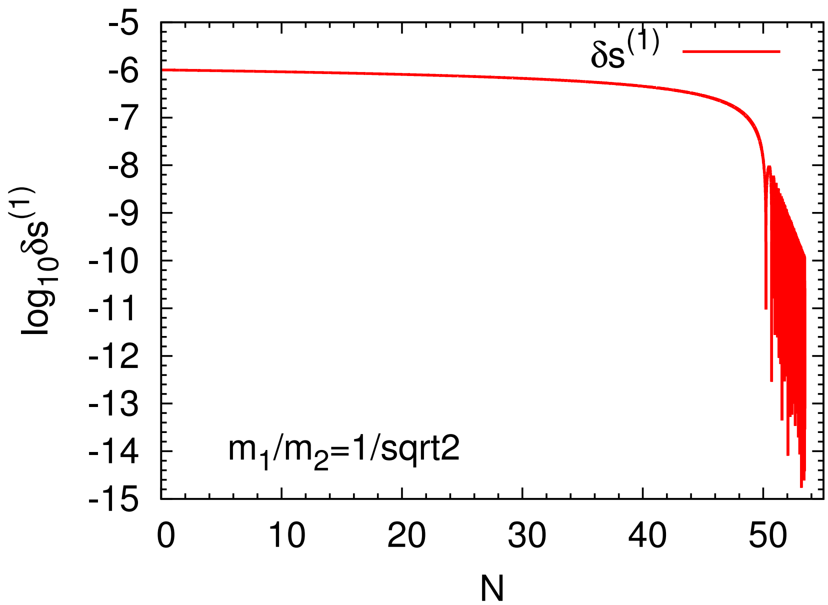

Figure 5.11: Evolution of linear entropy perturbations. $\delta s_* = 10^{-6}$ is chosen.

the curvature perturbations on large scales very efficiently. Will this really happen?

Let us consider the case where $m_\phi = 0$ for simplicity. Now χ field is expected to be the inflaton whose field value during inflation is large. On the other hand, ϕ becomes very massive through the interaction as $\mu_s^2 = g^2\chi_*^2 \sim 100 g^2 M_{\rm Pl}^2$. As a result, the ϕ field is pinned down to the local minimum and decouples from the dynamics until inflation ends. If one ignores the expansion of the universe during the coherent oscillation phase, the evolution equation of the k-mode, $\phi_k = \delta\phi_k = \delta s_k$, can be approximated by the Mathieu equation [7, 98]

$$\phi_k'' + [A - 2q\cos(2m_\chi t)]\phi_k = 0, \tag{5.81}$$

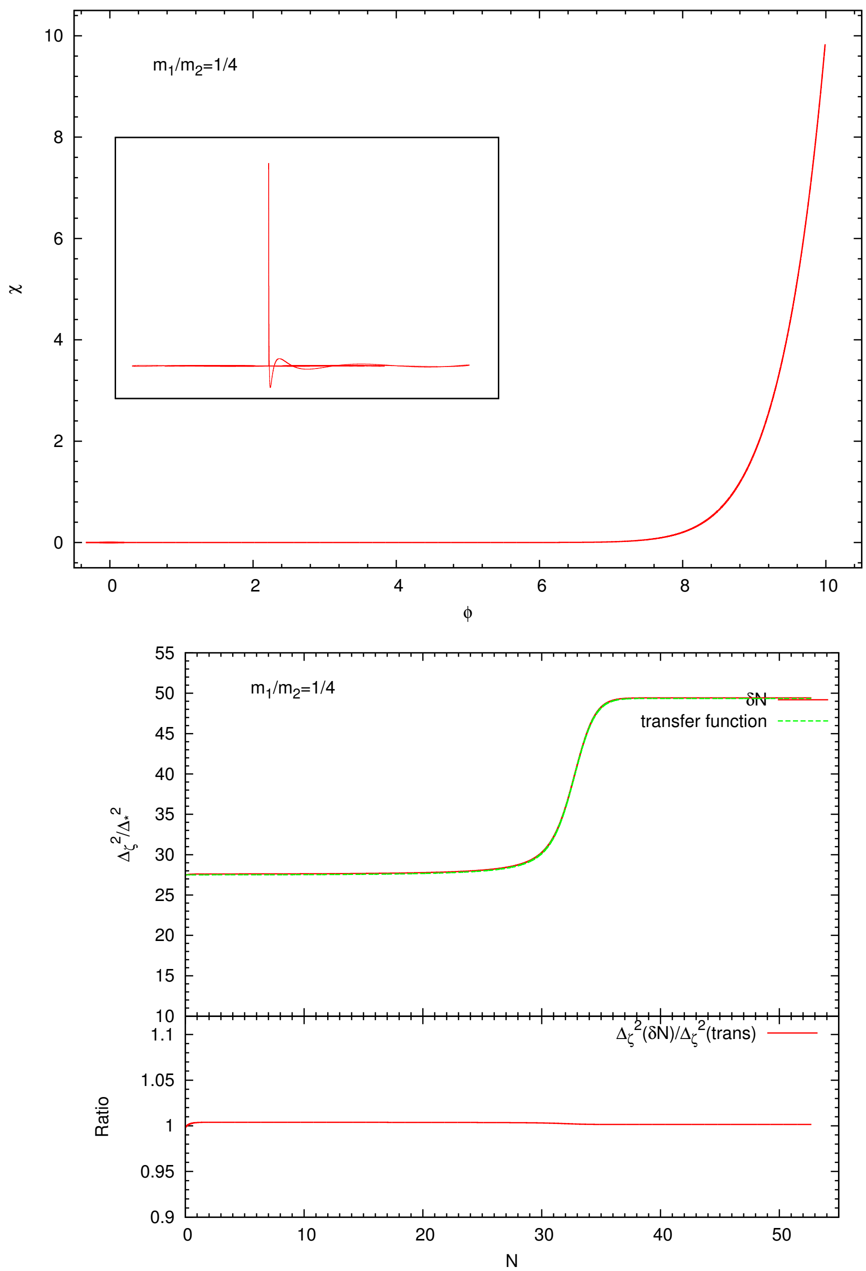

Figure 5.12: [Top] A trajectory of double inflation with a mass ratio 1:4. [Bottom] Evolution of curvature perturbations, ζ.

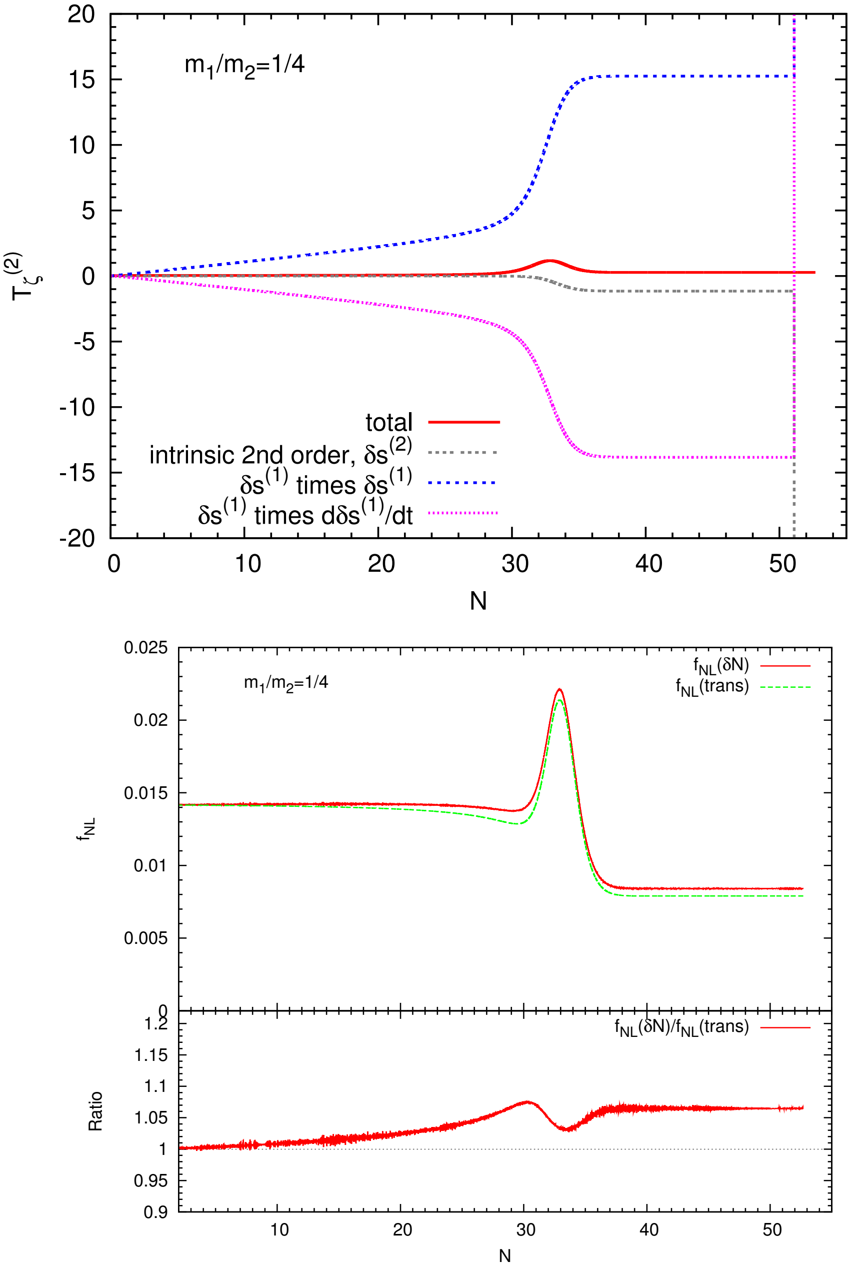

Figure 5.13: [Top] Evolution of the second order transfer function for ζ. [Bottom] Evolution of non-Gaussianity, f_{NL}.

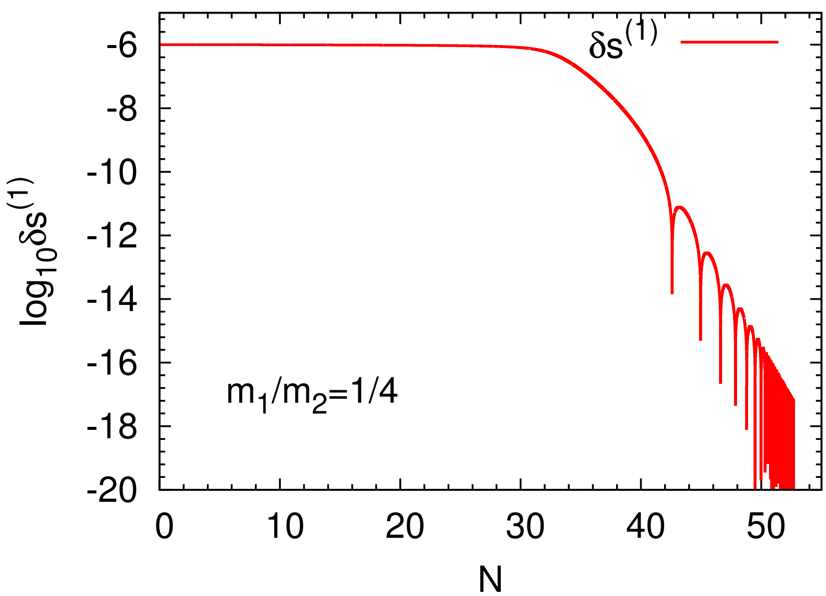

Figure 5.14: Evolution of linear entropy perturbations. $\delta s_* = 10^{-6}$ is chosen.

where

$$A \equiv 2q + \frac{k^2}{m_\chi^2 a^2}, \tag{5.82}$$

$$q \equiv \frac{g^2 \chi_0^2}{4m_\chi^2}, \tag{5.83}$$

and a prime is a derivative with respect to $m_\chi t$. χ_0 is the inflaton field value at the end of inflation or at the beginning of preheating. The q-parameter characterizes the strength of preheating from the resonance bands of the Mathieu chart.

If ϕ field is massive, $m_\phi \neq 0$, and the expansion of the universe is not ignored, modes move through the resonance band. The q-parameter needs to be large, $q \gg 1$, to have efficient parametric resonance [98]. A small coupling constant, $g^2 \ll 1$, and large q are possible as $m_\chi \ll \chi_0 \sim 0.5 M_{\rm Pl}$. However,

$$\mu_s^2 = g^2\chi^2 + m_\phi^2 + 3\dot{\theta}^2 \sim 4m_\chi^2 q \frac{\chi^2}{\chi_0^2} \gg m_\chi^2. \tag{5.84}$$

Thus, ϕ field is effectively heavier than χ field for having efficient preheating, and ultra heavy during inflation. The heavy field's vacuum fluctuation decays very quickly during inflation, leaving no signature on non-Gaussianity if entropy modes are not amplified enormously.

After all, one needs a lattice simulation to tell whether entropy perturbations are amplified or not.

5.5 Conclusion

We have re-examined the primordial non-Gaussianity from multi-field inflation by taking two approaches: the δN formalism and solving perturbed equations of motion for curvature perturbations on large scales. The results agreed exactly in the case of two-field inflation with large mass ratios. The peak feature appears on f_{NL} at the turn in the field space, which can be understood as the precise cancellation between terms in the evolution equation of ζ (5.34). Note, however, that we have made the leading order slow-roll approximation in integrating the evolution of ζ while we have not approximated for the δN approach. Therefore, the agreement has its limitation at the accuracy of the leading order slow-roll approximation at the horizon exit. Our analysis confirms validity of the δN formalism to apply to (almost) any situation. It allows us to interpret non-Gaussianity computed from the δN formalism as a constraint from geometry.

As a result, the net contribution to non-Gaussianity in a two-field model is slow-roll suppressed. Observationally if f_{NL} is detected, a large class of two-field models may be ruled out.

Let us mention the relative merits of integrating the evolution of ζ on large scales. This approach requires only a single realization in the simulation; statistical properties are taken into account in the formulation. It will significantly save a lot of computational time, which requires many realizations with the δN formalism.

The coherent oscillation phase in multi-field inflation shows a qualitatively different feature from that of single-field because of the "kicks" from entropy modes. The kick leaves its imprint on non-Gaussianity as a series of peak and dip. In the single-field limit, these series of peak and dip exactly cancelled out and do not leave any imprint.

When the classical trajectory is bending, the generation of net positive f_{NL} is possible if two conditions are satisfied. (i) A sizable amount of entropy perturbation exists on large scale. (ii) The duration of turns are long enough to change background quantities.

It still remains to be seen a computation of non-Gaussianity by the transfer function approach coupled with a lattice simulation.

Appendix A

Notation and Correspondences

For convenience, we list conventions used in the literature. Note that Komatsu [142] follows convention of Bardeen [39], while this dissertation follows convention of Malik and Wands [143] for the first-order metric perturbations.

Misner et al. [52] (on the end-cover) classified sign conventions in general relativity according to the three signs, (S_1, S_2, S_3), based on

$$\eta_{\mu\nu} = [S_1] \times \mathrm{diag}(-1, 1, 1, 1) \tag{A.1}$$

$$R^{\alpha}{}_{\beta\gamma\delta} = [S_2] \times (\Gamma^{\alpha}{}_{\beta\delta,\gamma} - \Gamma^{\alpha}{}_{\beta\gamma,\delta} + \Gamma^{\alpha}{}_{\lambda\gamma}\Gamma^{\lambda}{}_{\beta\delta} - \Gamma^{\alpha}{}_{\lambda\delta}\Gamma^{\lambda}{}_{\beta\gamma}) \tag{A.2}$$

$$G_{\mu\nu} = [S_3] \times 8\pi G T_{\mu\nu} \tag{A.3}$$

This is the so-called "MTW sign convention". Note that $R_{\mu\nu} = [S_2] \times [S_3] \times R^{\alpha}{}_{\mu\alpha\nu} = [S_2] \times [S_3] \times (\Gamma^{\alpha}{}_{\mu\nu,\alpha} - \Gamma^{\alpha}{}_{\mu\alpha,\nu} + \Gamma^{\alpha}{}_{\lambda\alpha}\Gamma^{\lambda}{}_{\mu\nu} - \Gamma^{\alpha}{}_{\lambda\nu}\Gamma^{\lambda}{}_{\mu\alpha})$. Misner et al. [52] classified themselves as $(+++)$ convention, which we have employed.

A.1 Metric Perturbations

Table A.1: Metric perturbations

Paper	Bardeen [39]	Kodama and Sasaki [40]	Mukhanov et al. [144]
$\eta_{\mu\nu}$	$-+++$	$-+++$	$+---$
MTW	$+++$	$+++$	$-++$
$\bar{N}$	S	a	a
δg_{00}	$-2S^2AQ^{(0)}$	$-2a^2AY$	$2a^2\phi$
δg^S_{0i}	$-S^2B^{(0)}Q^{(0)}_i$	$-a^2BY_i$	$-a^2B_{\vert i}$
δg^S_{ij}	$2S^2(H_LQ^{(0)3}g_{ij}$ $+H^{(0)}_TQ^{(0)}_{ij})$	$2a^2(H_LY\gamma_{ij}$ $+H_TY_{ij})$	$2a^2(\psi\gamma_{ij}-E_{\vert ij})$
δg^V_{0i}	$-S^2B^{(1)}Q^{(1)}_i$	$-a^2B^{(1)}Y^{(1)}_i$	a^2S_i
δg^V_{ij}	$2S^2H^{(1)}_TQ^{(1)}_{ij}$	$2a^2H^{(1)}_TY^{(1)}_{ij}$	$-a^2(F_{i\vert j}+F_{j\vert i})$
δg^T_{ij}	$2S^2H^{(2)}_TQ^{(2)}_{ij}$	$2a^2H^{(2)}_TY^{(2)}_{ij}$	$-a^2h_{ij}$

Book	Weinberg [141]	Liddle and Lyth [62]	Mukhanov [136]
$\eta_{\mu\nu}$	$-+++$	$-+++$	$+---$
MTW	$+--$	$+++$	$-++$
$\bar{N}$	1	a	a
δg_{00}	$-E$	$-2a^2A$	$2a^2\phi$
δg^S_{0i}	$aF_{,i}$	$-a^2B^S_i$	$a^2B_{,i}$
δg^S_{ij}	$a^2(A\delta_{ij}+B_{,ij})$	$2a^2(D\delta_{ij}+E^S_{ij})$	$2a^2(\psi\delta_{ij}+E_{,ij})$
δg^V_{0i}	aG_i	$-a^2B^V_i$	a^2S_i
δg^V_{ij}	$a^2(C_{i,j}+C_{j,i})$	$2a^2E^V_{ij}$	$a^2(F_{i,j}+F_{j,i})$
δg^T_{ij}	a^2D_{ij}	$2a^2E^T_{ij}$	a^2h_{ij}

Paper	This Thesis	Malik and Wands [143]	Bartolo et al. [145]
$\eta_{\mu\nu}$	$-+++$	$-+++$	$-+++$
MTW	$+++$	$+++$	$+++$
$\bar{N}$	1	a	a
δg_{00}	$-2A$	$-2a^2\phi$	$-2a^2\phi$
δg^S_{0i}	$aB_{,i}$	$a^2B_{,i}$	$a^2\omega_{,i}$
δg^S_{ij}	$2a^2(-\psi\delta_{ij}+E_{,ij})$	$2a^2(-\psi\delta_{ij}+E_{,ij})$	$a^2(-2\psi\delta_{ij}+D_{ij}\chi)$
δg^V_{0i}	$-$	$-a^2S_i$	$a^2\omega_i$
δg^V_{ij}	$-$	$a^2(F_{i,j}+F_{j,i})$	$a^2(\chi_{i,j}+\chi_{j,i})$
δg^T_{ij}	a^2h_{ij}	a^2h_{ij}	$a^2\chi_{ij}$
2^{nd} order	$\delta X^{(2)}$	$\frac{1}{2}\delta X^{(2)}$	$\frac{1}{2}\delta^{(2)}X$

Appendix B

Special Functions

B.1 Spherical Bessel type functions

We present some formulae for Bessel type functions used in this paper.

$$\frac{d}{dx}\left[\frac{z_n(x)}{x^n}\right] = -\frac{z_{n+1}(x)}{x^n}, \qquad \frac{d}{dx}\left[x^{n+1}z_n(x)\right] = x^{n+1}z_{n-1}(x), \tag{B.1}$$

where $z_n(x)$ can be spherical Bessel functions, spherical Neumann functions, Bessel functions, and Neumann functions.

Spherical Bessel functions and spherical Neumann functions are related by

$$y_n(x) = (-1)^{n+1} j_{-n-1}(x). \tag{B.2}$$

Their asymptotic forms are

$$j_n(x) \approx \frac{\sin\left(x - n\pi/2\right)}{x}, \qquad y_n(x) \approx -\frac{\cos\left(x - n\pi/2\right)}{x} \tag{B.3}$$

for $x \gg 1$. If n is even, $j_n(x) \approx \pm j_0(x)$ and $y_n(x) \approx \pm y_0(x)$. If n is odd, $j_n(x) \approx \pm y_0(x)$ and $y_n(x) \approx \pm j_0(x)$. The first and second kinds of spherical Hankel functions are defined as

$$h_n^{(1)}(x) = j_n(x) + iy_n(x), \qquad h_n^{(2)}(x) = j_n(x) - iy_n(x). \tag{B.4}$$

Using elementary functions, we have

$$\begin{aligned}
j_0(x) &= \frac{\sin x}{x}, && \text{(B.5)}\\
j_1(x) &= \frac{1}{x}\left[\frac{\sin x}{x} - \cos x\right], && \text{(B.6)}\\
j_2(x) &= \frac{1}{x}\left[\left(\frac{3}{x^2} - 1\right)\sin x - \frac{3}{x}\cos x\right], && \text{(B.7)}\\
y_0(x) &= -\frac{\cos x}{x}, && \text{(B.8)}\\
y_1(x) &= -\frac{1}{x}\left[\frac{1}{x}\cos x + \sin x\right], && \text{(B.9)}\\
y_2(x) &= -\frac{1}{x}\left[\left(\frac{3}{x^2} - 1\right)\cos x + \frac{3}{x}\sin x\right], && \text{(B.10)}\\
h_1^{(1)}(x) &= -\frac{1}{x}\left(1 + \frac{i}{x}\right)e^{-ix}, && \text{(B.11)}\\
h_1^{(2)}(x) &= -\frac{1}{x}\left(1 - \frac{i}{x}\right)e^{-ix}. && \text{(B.12)}
\end{aligned}$$

Appendix C

Gravitational Inflaton Decay via Trace Anomaly

The inflaton field, ϕ, couples to the matter fields via the trace of the energy momentum tensor of matter fields:

$$\mathcal{L}_{\rm int} = -\sqrt{-g}\frac{\phi}{v}T^{\mu}_{{\rm m}\mu}, \tag{C.1}$$

$$T^{\mu}_{{\rm m}\mu} = \sum_f m_f\bar{\psi}_f\psi_f + \sum_s m_s^2\chi_s^2 + \sum_V m_V^2 V_\mu V^\mu + \frac{\beta(g)}{2g}F^a_{\mu\nu}F^{a\mu\nu}, \tag{C.2}$$

where v is the vacuum expectation value of inflaton field.[1] Here indices f, s, and V run through massive fermion, scalar, and vector field species, respectively. $F^a_{\mu\nu} = \partial_\mu A^a_\nu - \partial_\nu A^a_\mu + gf^{abc}A^b_\mu A^c_\nu$ is the SU(n) gauge field strength tensor, and g and $\beta(g)$ are the gauge coupling constant and its Gell-Mann-Low β-function respectively. In this Appendix, we calculate the decay rate of scalar fields into gauge fields, A^a_μ, via the gravitational decay formulated in chapter 3. (We have decays into scalars, χ, and fermions, ψ, in chapter 3.) To calculate the β-function, we include only the

[1]This would be replaced by M which is the energy scale of interest. In our model, $M = 2M_{\rm Pl}^2/f'(v)$.

fermion loops, just for simplicity. The other loops due to s, V, and/or other gauge fields should yield the results of the same order of magnitude. In an SU(n) gauge theory with fermions in the fundamental representation, the β-function is given by

$$\beta(g) = -\frac{g^3}{(4\pi)^2}\left(\frac{11}{3}n - \frac{2}{3}n_f\right), \tag{C.3}$$

where n_f is the internal quantum number of fermion species. This is the fermionic 1-loop correction to the effective action. The higher order loops and charged bosonic loops also modify the coefficients of the β-function.

The transition matrix amplitude for $\phi \to 2A^a_\mu$ via the fermionic 1-loop is

$$\begin{aligned}
\mathcal{M} &\equiv\ < A(k)A(k')|T|\phi(q) >= \mathcal{M}_1 + \mathcal{M}_2 + \mathcal{M}_3 \\
&= \frac{2}{2!} i g^2 g_f n_f \epsilon^*_\mu(k)\epsilon^*_\nu(k') \times \\
&\quad \int \frac{d^4 s}{(2\pi)^4} \frac{\mathrm{Tr}(\not{s} + m)\gamma^\mu t^a(\not{s} + \not{k} + m)\gamma^\nu t^b(\not{s} + \not{q} + m)}{(s^2 - m^2 + i\epsilon)((s+k)^2 - m^2 + i\epsilon)((s+q)^2 - m^2 + i\epsilon)} \\
&\quad +(k \leftrightarrow k') + \mathcal{M}_3 \qquad\qquad\qquad\qquad\qquad\qquad\qquad\qquad\qquad\qquad\qquad\qquad\qquad (\text{C.4}) \\
&= i g^2 g_f n_f [\epsilon^*_\mu(k)\epsilon^*_\nu(k') t^a t^b I^{\mu\nu}(k,k') + \epsilon^*_\mu(k')\epsilon^*_\nu(k) t^b t^a I^{\mu\nu}(k',k)] + \mathcal{M}_3,
\end{aligned}$$

where the factor of 2 represents the triangle diagrams with opposite charge current (or internal momentum) directions, g_f is a (direct or induced) coupling constant between ϕ and an intermediate fermion particle, and $m \equiv m_f$ is the mass of the intermediate particle. We have used the Feynman slash notation for 4-momentum, $\not{q} \equiv \gamma^\mu q_\mu$. Note that the diagram, $\mathcal{M}_3$, is peculiar to non-Abelian gauge fields; it does not exist for Abelian gauge fields. For instance, the pair annihilation process, $\bar{\psi} + \psi \to g + g$, possesses *three* tree-level diagrams because gluons interact with themselves, while photons do not. To carry out loop momentum integration we need to combine propagators. Using the Feynman parameter trick, we rewrite the denominator as

$$
\begin{aligned}
\frac{1}{D} &\equiv \frac{1}{(s^2-m^2+i\epsilon)((s+k)^2-m^2+i\epsilon)((s+q)^2-m^2+i\epsilon)} \\
&= 2\int_0^1 dx \int_0^1 dy x\{(1-x)(s^2-m^2+i\epsilon)+xy((s+k)^2-m^2+i\epsilon) \\
&\qquad\qquad +x(1-y)((s+q)^2-m^2+i\epsilon)\}^{-3} \\
&= 2\int_0^1 dx \int_0^1 dy x\{\ell^2-\Lambda^2+i\epsilon\}^{-3}, \qquad \text{(C.5)}
\end{aligned}
$$

where

$$
\ell^\mu \equiv s^\mu + k^\mu x + k'^\mu x(1-y), \quad \Lambda^2 \equiv m^2 - \mu^2 x(1-x)(1-y). \qquad \text{(C.6)}
$$

Here we have used $q^\mu = k^\mu + k'^\mu$ and on-mass shell conditions; $k^2 = k'^2 = 0$, $q^2 = m_\phi^2 \equiv \mu^2$. The numerator in the loop integral is

$$
\begin{aligned}
N^{ab\mu\nu} &\equiv \mathrm{Tr}(\not{s}+m)\gamma^\mu t^a(\not{s}+\not{k}+m)\gamma^\nu t^b(\not{s}+\not{q}+m) \\
&= 4mt^a t^b[4s^\mu s^\nu + 2(s^\mu k^\nu + k^\mu s^\nu + s^\mu q^\nu) + k^\mu q^\nu + q^\mu k^\nu \\
&\qquad +(-2s\cdot k - k\cdot q - s^2 + m^2)g^{\mu\nu}], \qquad \text{(C.7)}
\end{aligned}
$$

where we have used the γ-matrix algebra;

$$
\begin{aligned}
\mathrm{Tr}(odd\,\#\,\gamma) &= 0, \qquad \text{(C.8)} \\
\mathrm{Tr}(\gamma^\mu\gamma^\nu) &= 4g^{\mu\nu}, \qquad \text{(C.9)} \\
\mathrm{Tr}(\gamma^\mu\gamma^\nu\gamma^\alpha\gamma^\beta) &= 4(g^{\mu\nu}g^{\alpha\beta} - g^{\mu\alpha}g^{\nu\beta} + g^{\mu\beta}g^{\nu\alpha}). \qquad \text{(C.10)}
\end{aligned}
$$

Shifting loop momentum by Eq. (C.6), one can rewrite the numerator as

$$
\begin{aligned}
N^{ab\mu\nu} &= 4mt^a t^b[4\ell^\mu \ell^\nu + 4(k^\mu x + k'^\mu x(1-y))(k^\nu x + k'^\nu x(1-y)) \\
&\quad -2x(3k^\mu k^\nu + k^\mu k'^\nu) - 2x(1-y)(2k'^\mu k^\nu + k^\mu k'^\nu + k'^\mu k'^\nu) \\
&\quad +2k^\mu k^\nu + k^\mu k'^\nu + k'^\mu k^\nu \\
&\quad +(2x(1-y)\mu^2 - \mu^2/2 - \ell^2 - x^2(1-y)\mu^2 + m^2)g^{\mu\nu}] \\
&= 4mt^a t^b[2(1-x)(1-2x)k^\mu k^\nu - 2x(1-y)(1-2x(1-y))k'^\mu k'^\nu \\
&\quad +(1-2x)(1-2x(1-y))k^\mu k'^\nu \\
&\quad +(1-4x(1-x)(1-y))k'^\mu k^\nu \\
&\quad -(1-4x(1-x)(1-y)+2x^2(1-y))\mu^2 g^{\mu\nu}/2 + m^2 g^{\mu\nu}], \qquad \text{(C.11)}
\end{aligned}
$$

where we have used and will use 4-dimensional integrals in Minkowski space;

$$\int \frac{d^4\ell}{(2\pi)^4}\frac{4\ell^\mu\ell^\nu}{\{\ell^2-\Lambda^2+i\epsilon\}^3} = \int \frac{d^4\ell}{(2\pi)^4}\frac{\ell^2 g^{\mu\nu}}{\{\ell^2-\Lambda^2+i\epsilon\}^3}, \qquad \text{(C.12)}$$

$$\int \frac{d^4\ell}{(2\pi)^4}\frac{\ell^\mu}{\{\ell^2-\Lambda^2+i\epsilon\}^3} = 0, \qquad \text{(C.13)}$$

$$\int \frac{d^4\ell}{(2\pi)^4}\frac{1}{\{\ell^2-\Lambda^2+i\epsilon\}^3} = \frac{-i}{2(4\pi)^2\Lambda^2}. \qquad \text{(C.14)}$$

Since the integrals converge, we have evaluated the γ-matrices and loop integrations in 4-dimension.

The matrix amplitude must be gauge invariant in a given order of perturbation theory. Since non-Abelian gauge invariance is not trivial, we first consider Abelian gauge field (i.e. U(1) gauge field). In this case, $\mathcal{M}_3$ in Eq. (C.4) does not exist and the generators of symmetry is simply taken as $t^a = 1$. The Ward-Takahashi identity implies

$$k_\mu \mathcal{M}^{\mu\nu} = k'_\nu \mathcal{M}^{\mu\nu} = 0, \tag{C.15}$$

$$k_\mu \mathcal{M}_1^{\mu\nu} = -k_\mu \mathcal{M}_2^{\mu\nu}, \qquad k'_\nu \mathcal{M}_1^{\mu\nu} = -k'_\nu \mathcal{M}_2^{\mu\nu}. \tag{C.16}$$

In non-Abelian gauge field theory we no longer have the Ward-Takahashi identity, $k_\mu \mathcal{M}^{\mu\nu} \neq 0$. Instead, the weak Ward-Takahashi identity

$$k_\mu \mathcal{M}^{\mu\nu} \epsilon^*_\nu(k') = k'_\nu \mathcal{M}^{\mu\nu} \epsilon^*_\mu(k) = 0 \tag{C.17}$$

holds. Note that $t^a t^b = t^b t^a + igf^{abc}$, where the last term is contained in $\mathcal{M}_3$. The transverse condition for external gauge boson momenta is

$$\epsilon^*_\mu(k) k^\mu = \epsilon^*_\nu(k') k'^\nu = 0. \tag{C.18}$$

The matrix amplitude, therefore, becomes

$$\begin{aligned} \mathcal{M} &= ig^2 g_f n_f \epsilon^*_\mu(k,\lambda)\epsilon^*_\nu(k',\lambda') I^{\mu\nu}, \\ I^{\mu\nu} &= \frac{-i}{(2\pi)^2 m}(k'^\mu k^\nu - \frac{\mu^2}{2} g^{\mu\nu}) I\left(\frac{\mu^2}{m^2}\right), \end{aligned} \tag{C.19}$$

where we have explicitly shown polarization of gauge fields, λ. A function, $I(\mu^2/m^2)$, represents mass or energy dependence of an intermediate particle:

$$\begin{aligned} I(\xi) &\equiv \int_0^1 dx \int_0^1 dyx \frac{1-4x(1-x)(1-y)}{1-\xi x(1-x)(1-y)} \\ &= \int_0^1 dx \int_0^{1-x} dy \frac{1-4xy}{1-\xi xy}. \end{aligned} \tag{C.20}$$

Note that in the heavy intermediate particle limit, we have $I(\xi \to 0) = 1/3$, and in the light intermediate particle limit, $I(\xi \to \infty) = 0$. The decay rate of $\phi \to 2A_\mu$

can be calculated as

$$
\begin{aligned}
\Gamma(\phi \to 2A_\mu) &= \frac{1}{(2\pi)^2}\frac{1}{2\mu}\frac{1}{2}\int\frac{d^3k}{2\omega_k}\int\frac{d^3k'}{2\omega_{k'}}\delta^{(4)}(q-k-k')\sum_{\lambda\lambda'}|\mathcal{M}|^2 \\
&= \frac{1}{32\pi\mu}\sum_{\lambda\lambda'}|\mathcal{M}|^2 \\
&= \frac{1}{32\pi\mu}\frac{g^4 g_f^2 n_f^2 \mu^4}{2(2\pi)^4 m^2}\left|I\left(\frac{\mu^2}{m^2}\right)\right|^2 \\
&= \frac{\alpha^2 g_f^2 n_f^2 \mu^3}{64\pi^3 m^2}\left|I\left(\frac{\mu^2}{m^2}\right)\right|^2, \qquad \text{(C.21)}
\end{aligned}
$$

where $\alpha \equiv g^2/(4\pi)$. One can evaluate scalar and vector loop diagrams similarly: the magnitude of the results should be of the same order as the fermion loop diagrams.

For $f(\phi)R$ gravity, the fermionic matter field, ψ, couples to inflaton by $g_\psi = f'(v)m/(2M_{\rm Pl}^2)/[1+\frac{3}{2}(f'(v)/M_{\rm Pl})^2]^{1/2}$ [Eqs. (3.10) and (3.15)]. Note that the inflaton field ϕ corresponds to $\hat{\sigma}$ in chapter 3. Thus, we obtain

$$
\Gamma(\sigma \to 2A_\mu) = \frac{\alpha^2 n_\psi^2 [f'(v)]^2 m_\sigma^3}{256\pi^3 M_{\rm Pl}^4\sqrt{1+\frac{3}{2}[f'(v)/M_{\rm Pl}]^2}}\left|I\left(\frac{m_\sigma^2}{m_\psi^2}\right)\right|^2, \qquad \text{(C.22)}
$$

where intermediate mass dependence appears only in the function $I(m_\sigma^2/m_\psi^2)$.

Appendix D

Glossary of Symbols

Table D.1: Symbols

symbol	quantity	chapter
a	scale factor	all
A	scalar (Newtonian) potential perturbation	5
A_μ	vector field	3, C
B	shift (scalar metric perturbation)	5
c	speed of light	2
E	scalar spatial metric perturbation	5
f_ν	neutrino energy fraction	2
$F(x, P)$	distribution function	2
h_{ij}	tensor metric perturbation	2
H	Hubble rate	2,4,5
$g_{\mu\nu}$	metric tensor	all
g_*	the effective number of relativistic species	2
G	Newton's gravitational constant	2,4
$G_{\mu\nu}$	Einstein tensor	2,3

Table D.1: Symbols

symbol	quantity	chapter
k	wave number	2,4,5
k^μ	4-momentum	C
$m_{\rm Pl}$	Planck mass	2
p	pressure	2,5
P^μ	4-momentum	2
q^μ	comoving 4-momentum	2
	4-momentum	3,C
Q_{ij}	solution of the Helmholtz equation	2,A
$R_{\mu\nu}$	Ricci tensor	2
s	entropy density	2
	Mandelstam variable	4
s^μ	internal 4-momentum	C
S	action	all
t	physical time	2,5
t^a	generator of SU(n)	C
T	cosmic temperature	all
	T-matrix	C
$T_{\mu\nu}$	energy-momentum tensor	2,3,5,C
$\mathcal{T}$	transfer function	2,5
$\alpha(\mathbf{k})$	stochastic variable	2
γ^i	directional cosine	2
γ^μ	gamma matrix	3,C
$\Gamma^\lambda_{\mu\nu}$	Christoffel symbol	2,3
$\delta_{\alpha,\beta}$	Kronecker delta	all

Table D.1: Symbols

symbol	quantity	chapter
$\delta^{(D)}(x)$	D-dimensional Dirac delta function	all
$\Delta_h^2(k)$	dimensionless power spectrum of tensor modes	2,4
ϵ_{ij}^{λ}	polarization tensor	2
Ω	relative energy density	2
	conformal factor	3
$\Omega_h(k)$	relative spectral energy density of gravitational waves	2
Π_{ij}	anisotropic stress	2
ρ	energy density	2,4,5
τ	conformal time	2
ϕ	inflaton	all
ψ	curvature perturbation	5
	fermion matter field	3,C
∇^2	3-dimensional Laplacian	2
...	...	
...	...	

Bibliography

[1] Y. Watanabe and E. Komatsu, Phys. Rev. **D73**, 123515 (2006), `astro-ph/0604176`.

[2] Y. Watanabe and E. Komatsu, Phys. Rev. **D75**, 061301 (2007), `gr-qc/0612120`.

[3] M. Endo, F. Takahashi, and T. T. Yanagida, Phys. Rev. **D76**, 083509 (2007), `0706.0986`.

[4] G. Dvali (2007), `0706.2050`.

[5] Y. Watanabe and E. Komatsu, Phys. Rev. **D77**, 043514 (2008), `0711.3442`.

[6] J. H. Traschen and R. H. Brandenberger, Phys. Rev. **D42**, 2491 (1990).

[7] L. Kofman, A. D. Linde, and A. A. Starobinsky, Phys. Rev. Lett. **73**, 3195 (1994), `hep-th/9405187`.

[8] K. Enqvist, A. Jokinen, A. Mazumdar, T. Multamaki, and A. Vaihkonen, Phys. Rev. Lett. **94**, 161301 (2005), `astro-ph/0411394`.

[9] A. Chambers and A. Rajantie, Phys. Rev. Lett. **100**, 041302 (2008), `0710.4133`.

[10] J. R. Bond, A. V. Frolov, Z. Huang, and L. Kofman (2009), `0903.3407`.

[11] L. P. Grishchuk, Sov. Phys. JETP **40**, 409 (1975).

[12] A. A. Starobinsky, JETP Lett. **30**, 682 (1979).

[13] V. A. Rubakov, M. V. Sazhin, and A. V. Veryaskin, Phys. Lett. **B115**, 189 (1982).

[14] R. Fabbri and M. d. Pollock, Phys. Lett. **B125**, 445 (1983).

[15] L. F. Abbott and M. B. Wise, Nucl. Phys. **B244**, 541 (1984).

[16] A. A. Starobinsky, Sov. Astron. Lett. **11**, 133 (1985).

[17] L. H. Ford, Phys. Rev. **D35**, 2955 (1987).

[18] B. Allen, Phys. Rev. **D37**, 2078 (1988).

[19] V. Sahni, Phys. Rev. **D42**, 453 (1990).

[20] M. J. White, Phys. Rev. **D46**, 4198 (1992), `hep-ph/9207239`.

[21] M. S. Turner, Phys. Rev. **D48**, 3502 (1993), `astro-ph/9302013`.

[22] M. S. Turner, M. J. White, and J. E. Lidsey, Phys. Rev. **D48**, 4613 (1993), `astro-ph/9306029`.

[23] M. S. Turner, Phys. Rev. **D55**, 435 (1997), `astro-ph/9607066`.

[24] M. Kamionkowski, A. Kosowsky, and M. S. Turner, Phys. Rev. **D49**, 2837 (1994), `astro-ph/9310044`.

[25] D. J. Schwarz, Mod. Phys. Lett. **A13**, 2771 (1998), `gr-qc/9709027`.

[26] D. J. Schwarz, Annalen Phys. **12**, 220 (2003), `astro-ph/0303574`.

[27] D. A. Dicus et al., Phys. Rev. **D26**, 2694 (1982).

[28] E. T. Vishniac, Astrophys. J. **257**, 456 (1982).

[29] A. K. Rebhan and D. J. Schwarz, Phys. Rev. **D50**, 2541 (1994), `gr-qc/9403032`.

[30] S. Weinberg, Phys. Rev. **D69**, 023503 (2004), `astro-ph/0306304`.

[31] A. H. Guth, Phys. Rev. **D23**, 347 (1981).

[32] A. D. Linde, Phys. Lett. **B108**, 389 (1982).

[33] A. J. Albrecht and P. J. Steinhardt, Phys. Rev. Lett. **48**, 1220 (1982).

[34] T. L. Smith, M. Kamionkowski, and A. Cooray, Phys. Rev. **D73**, 023504 (2006), `astro-ph/0506422`.

[35] T. L. Smith, H. V. Peiris, and A. Cooray, Phys. Rev. **D73**, 123503 (2006), `astro-ph/0602137`.

[36] J. Khoury, B. A. Ovrut, P. J. Steinhardt, and N. Turok, Phys. Rev. **D64**, 123522 (2001), `hep-th/0103239`.

[37] G. M. Harry, P. Fritschel, D. A. Shaddock, W. Folkner, and E. S. Phinney, Class. Quant. Grav. **23**, 4887 (2006).

[38] N. Seto, S. Kawamura, and T. Nakamura, Phys. Rev. Lett. **87**, 221103 (2001), `astro-ph/0108011`.

[39] J. M. Bardeen, Phys. Rev. **D22**, 1882 (1980).

[40] H. Kodama and M. Sasaki, Prog. Theor. Phys. Suppl. **78**, 1 (1984).

[41] S. Weinberg, *Gravitation and Cosmology* (Wiley, NY, 1972).

[42] J. R. Bond and A. S. Szalay, Astrophys. J. **274**, 443 (1983).

[43] M. Kasai and K. Tomita, Phys. Rev. **D33**, 1576 (1986).

[44] J. R. Pritchard and M. Kamionkowski, Annals Phys. **318**, 2 (2005), astro-ph/0412581.

[45] D. A. Dicus and W. W. Repko, Phys. Rev. **D72**, 088302 (2005), astro-ph/0509096.

[46] S. Bashinsky (2005), astro-ph/0505502.

[47] E. Hawking, S. W. and E. Israel, W., *300 Years of Gravitation* (Cambridge University Press, Cambridge, UK, 1987), pp. 330-458.

[48] N. D. Birrell and P. C. W. Davies, *Quantum Fields in Curved Space* (Cambridge University Press, Cambridge, UK, 1982).

[49] D. N. Spergel et al. (WMAP), Astrophys. J. Suppl. **148**, 175 (2003), astro-ph/0302209.

[50] K.-w. Ng and A. D. Speliotopoulos, Phys. Rev. **D52**, 2112 (1995), astro-ph/9405043.

[51] K.-W. Ng, Int. J. Mod. Phys. **A11**, 3175 (1996), gr-qc/9311002.

[52] C. W. Misner, K. S. Thorne, and J. A. Wheeler, *Gravitation* (Freeman, NY, 1973).

[53] E. W. Kolb and M. S. Turner, *The Early Universe* (Westview Press, 1990).

[54] G. Mangano, G. Miele, S. Pastor, and M. Peloso, Phys. Lett. **B534**, 8 (2002), astro-ph/0111408.

[55] M. Hindmarsh and O. Philipsen, Phys. Rev. **D71**, 087302 (2005), hep-ph/0501232.

[56] S. Kuroyanagi, T. Chiba, and N. Sugiyama, Phys. Rev. **D79**, 103501 (2009), `0804.3249`.

[57] M. Maggiore, Phys. Rept. **331**, 283 (2000), `gr-qc/9909001`.

[58] N. Seto and J. Yokoyama, J. Phys. Soc. Jap. **72**, 3082 (2003), `gr-qc/0305096`.

[59] L. A. Boyle and P. J. Steinhardt, Phys. Rev. **D77**, 063504 (2008), `astro-ph/0512014`.

[60] Y. Zhang, X. Z. Er, T. Y. Xia, W. Zhao, and H. X. Miao, Class. Quant. Grav. **23**, 3783 (2006), `astro-ph/0604456`.

[61] A. D. Linde (2005), `hep-th/0503203`.

[62] A. R. Liddle and D. H. Lyth, *Cosmological Inflation and Large-Scale Structure* (Cambridge University Press, Cambridge, UK, 2000).

[63] H. V. Peiris et al. (WMAP), Astrophys. J. Suppl. **148**, 213 (2003), `astro-ph/0302225`.

[64] D. N. Spergel et al. (WMAP), Astrophys. J. Suppl. **170**, 377 (2007), `astro-ph/0603449`.

[65] A. D. Dolgov and A. D. Linde, Phys. Lett. **B116**, 329 (1982).

[66] L. F. Abbott, E. Farhi, and M. B. Wise, Phys. Lett. **B117**, 29 (1982).

[67] A. J. Albrecht, P. J. Steinhardt, M. S. Turner, and F. Wilczek, Phys. Rev. Lett. **48**, 1437 (1982).

[68] B. A. Bassett and S. Liberati, Phys. Rev. **D58**, 021302 (1998), `hep-ph/9709417`.

[69] Y. Fujii and K. Maeda, *The Scalar-Tensor Theory of Gravitation* (Cambridge University Press, Cambridge, USA, 2003).

[70] V. Faraoni, *Cosmology in Scalar-Tensor Gravity* (Kluwer Academic Publishers, MA, 2004).

[71] A. Zee, Phys. Rev. Lett. **42**, 417 (1979).

[72] R. H. Dicke, Phys. Rev. **125**, 2163 (1962).

[73] F. S. Accetta, D. J. Zoller, and M. S. Turner, Phys. Rev. **D31**, 3046 (1985).

[74] D. La and P. J. Steinhardt, Phys. Rev. Lett. **62**, 376 (1989).

[75] P. J. Steinhardt and F. S. Accetta, Phys. Rev. Lett. **64**, 2740 (1990).

[76] T. Futamase and K.-i. Maeda, Phys. Rev. **D39**, 399 (1989).

[77] D. S. Salopek, J. R. Bond, and J. M. Bardeen, Phys. Rev. **D40**, 1753 (1989).

[78] A. L. Berkin and K.-I. Maeda, Phys. Rev. **D44**, 1691 (1991).

[79] R. Fakir and W. G. Unruh, Phys. Rev. **D41**, 1783 (1990).

[80] R. Fakir and W. G. Unruh, Phys. Rev. **D41**, 1792 (1990).

[81] R. Fakir, S. Habib, and W. Unruh, Astrophys. J. **394**, 396 (1992).

[82] S. Kalara, N. Kaloper, and K. A. Olive, Nucl. Phys. **B341**, 252 (1990).

[83] N. Makino and M. Sasaki, Prog. Theor. Phys. **86**, 103 (1991).

[84] D. I. Kaiser, Phys. Rev. **D52**, 4295 (1995), `astro-ph/9408044`.

[85] V. Faraoni, Phys. Lett. **A269**, 209 (2000), `gr-qc/0004007`.

[86] E. Komatsu and T. Futamase, Phys. Rev. **D59**, 064029 (1999), `astro-ph/9901127`.

[87] E. Komatsu and T. Futamase, Phys. Rev. **D58**, 023004 (1998), `astro-ph/9711340`.

[88] J. C. Hwang and H. Noh, Phys. Rev. Lett. **81**, 5274 (1998).

[89] H. Noh and J.-c. Hwang, Phys. Lett. **B515**, 231 (2001), `astro-ph/0107069`.

[90] S. Tsujikawa and B. Gumjudpai, Phys. Rev. **D69**, 123523 (2004), `astro-ph/0402185`.

[91] A. Vilenkin, Phys. Rev. **D32**, 2511 (1985).

[92] M. B. Mijic, M. S. Morris, and W.-M. Suen, Phys. Rev. **D34**, 2934 (1986).

[93] E. W. Kolb, A. Notari, and A. Riotto, Phys. Rev. **D68**, 123505 (2003), `hep-ph/0307241`.

[94] J. Yokoyama, Phys. Lett. **B635**, 66 (2006), `hep-ph/0510091`.

[95] J. Yokoyama, Phys. Rev. Lett. **96**, 171301 (2006), `hep-ph/0601067`.

[96] J. Yokoyama, Phys. Rev. **D70**, 103511 (2004), `hep-ph/0406072`.

[97] K.-i. Maeda, Phys. Rev. **D39**, 3159 (1989).

[98] L. Kofman, A. D. Linde, and A. A. Starobinsky, Phys. Rev. **D56**, 3258 (1997), `hep-ph/9704452`.

[99] P. B. Greene and L. Kofman, Phys. Rev. **D62**, 123516 (2000), `hep-ph/0003018`.

[100] S. Weinberg, Phys. Rev. Lett. **48**, 1303 (1982).

[101] W. Fischler, Phys. Lett. **B332**, 277 (1994), `hep-th/9404044`.

[102] M. Endo, M. Kawasaki, F. Takahashi, and T. T. Yanagida, Phys. Lett. **B642**, 518 (2006), `hep-ph/0607170`.

[103] L. Susskind, *1982 Proceedings from the SLAC Summer Institute on Particle Physics: Physics at Very High Energies* (SLAC-R-259, 1982).

[104] S. Weinberg, *The Quantum Theory of Fields, Vol. III: Supersymmetry* (Cambridge University Press, Cambridge, UK, 2000).

[105] G. Dvali and M. Redi, Phys. Rev. **D77**, 045027 (2008), `0710.4344`.

[106] G. Veneziano, JHEP **06**, 051 (2002), `hep-th/0110129`.

[107] N. Arkani-Hamed, S. Dimopoulos, and G. R. Dvali, Phys. Lett. **B429**, 263 (1998), `hep-ph/9803315`.

[108] N. Arkani-Hamed, S. Dimopoulos, and G. R. Dvali, Phys. Rev. **D59**, 086004 (1999), `hep-ph/9807344`.

[109] I. Antoniadis, N. Arkani-Hamed, S. Dimopoulos, and G. R. Dvali, Phys. Lett. **B436**, 257 (1998), `hep-ph/9804398`.

[110] D. Cremades, L. E. Ibanez, and F. Marchesano, Nucl. Phys. **B643**, 93 (2002), `hep-th/0205074`.

[111] C. Kokorelis, Nucl. Phys. **B677**, 115 (2004), `hep-th/0207234`.

[112] L. Verde et al. (WMAP), Astrophys. J. Suppl. **148**, 195 (2003), `astro-ph/0302218`.

[113] L. Page et al. (WMAP), Astrophys. J. Suppl. **170**, 335 (2007), `astro-ph/0603450`.

[114] H. Pagels and J. R. Primack, Phys. Rev. Lett. **48**, 223 (1982).

[115] G. D. Coughlan, W. Fischler, E. W. Kolb, S. Raby, and G. G. Ross, Phys. Lett. **B131**, 59 (1983).

[116] J. R. Ellis, D. V. Nanopoulos, and M. Quiros, Phys. Lett. **B174**, 176 (1986).

[117] M. Endo, F. Takahashi, and T. T. Yanagida, Phys. Lett. **B658**, 236 (2008), `hep-ph/0701042`.

[118] M. Endo, K. Kadota, K. A. Olive, F. Takahashi, and T. T. Yanagida, JCAP **0702**, 018 (2007), `hep-ph/0612263`.

[119] A. Berera and T. W. Kephart, Phys. Lett. **B456**, 135 (1999), `hep-ph/9811295`.

[120] G. R. Dvali, G. Gabadadze, M. Kolanovic, and F. Nitti, Phys. Rev. **D65**, 024031 (2002), `hep-th/0106058`.

[121] J. M. Maldacena, JHEP **05**, 013 (2003), `astro-ph/0210603`.

[122] P. Creminelli and M. Zaldarriaga, JCAP **0410**, 006 (2004), `astro-ph/0407059`.

[123] D. Seery and J. E. Lidsey, JCAP **0506**, 003 (2005), `astro-ph/0503692`.

[124] D. H. Lyth, K. A. Malik, and M. Sasaki, JCAP **0505**, 004 (2005), `astro-ph/0411220`.

[125] D. H. Lyth, C. Ungarelli, and D. Wands, Phys. Rev. **D67**, 023503 (2003), `astro-ph/0208055`.

[126] G. Dvali, A. Gruzinov, and M. Zaldarriaga, Phys. Rev. **D69**, 023505 (2004), `astro-ph/0303591`.

[127] D. H. Lyth and Y. Rodriguez, Phys. Rev. Lett. **95**, 121302 (2005), `astro-ph/0504045`.

[128] D. Seery and J. E. Lidsey, JCAP **0509**, 011 (2005), `astro-ph/0506056`.

[129] D. Langlois and F. Vernizzi, JCAP **0702**, 017 (2007), `astro-ph/0610064`.

[130] D. Langlois, F. Vernizzi, and D. Wands, JCAP **0812**, 004 (2008), `0809.4646`.

[131] M. Sasaki and E. D. Stewart, Prog. Theor. Phys. **95**, 71 (1996), `astro-ph/9507001`.

[132] M. Sasaki and T. Tanaka, Prog. Theor. Phys. **99**, 763 (1998), `gr-qc/9801017`.

[133] F. Vernizzi and D. Wands, JCAP **0605**, 019 (2006), `astro-ph/0603799`.

[134] S. Yokoyama, T. Suyama, and T. Tanaka, Phys. Rev. **D77**, 083511 (2008), `0711.2920`.

[135] G. I. Rigopoulos, E. P. S. Shellard, and B. J. W. van Tent, Phys. Rev. **D76**, 083512 (2007), `astro-ph/0511041`.

[136] V. Mukhanov, *Physical Foundations of Cosmology* (Cambridge University Press, NY, 2005).

[137] D. H. Lyth and Y. Rodriguez, Phys. Rev. **D71**, 123508 (2005), `astro-ph/0502578`.

[138] C. Gordon, D. Wands, B. A. Bassett, and R. Maartens, Phys. Rev. **D63**, 023506 (2001), `astro-ph/0009131`.

[139] D. S. Salopek and J. R. Bond, Phys. Rev. **D42**, 3936 (1990).

[140] E. Komatsu and D. N. Spergel, Phys. Rev. **D63**, 063002 (2001), `astro-ph/0005036`.

[141] S. Weinberg, *Cosmology* (Oxford University Press, NY, 2008).

[142] E. Komatsu (2002), `astro-ph/0206039`.

[143] K. A. Malik and D. Wands, Phys. Rept. **475**, 1 (2009), `0809.4944`.

[144] V. F. Mukhanov, H. A. Feldman, and R. H. Brandenberger, Phys. Rept. **215**, 203 (1992).

[145] N. Bartolo, E. Komatsu, S. Matarrese, and A. Riotto, Phys. Rept. **402**, 103 (2004), `astro-ph/0406398`.

Vita

Yuki Watanabe attended Atsugi High School, Kanagawa, Japan. In 1999 he entered Tokyo University of Science, Tokyo, Japan, where he received the Bachelor of Science degree in Physics in 2003. He started graduate studies in the Physics Department at the University of Texas at Austin from the fall of 2003, where he served as a teaching assistant, an assistant instractor, and a research assistant for Dr. Eiichiro Komatsu.

Permanent Address: 1 University Station, C1400, Austin, TX 78712

This dissertation was typeset with LaTeX 2ε[1] by the author.

[1]LaTeX 2ε is an extension of LaTeX. LaTeX is a collection of macros for TeX. TeX is a trademark of the American Mathematical Society. The macros used in formatting this dissertation were written by Dinesh Das, Department of Computer Sciences, The University of Texas at Austin, and extended by Bert Kay, James A. Bednar, and Ayman El-Khashab.